

Site-selective cation- π -interaction as a way of selective recognition of caesium cation with sumanene-functionalized ferrocenes

Artur Kasprzak^{a*}, Hidehiro Sakurai^b

^a Faculty of Chemistry, Warsaw University of Technology, Noakowskiego Str. 3, 00-664 Warsaw, Poland

^b Division of Applied Chemistry Graduate School of Engineering, Osaka University, 2-1 Yamadaoka, Suita, Osaka 565-0871, Japan

* e-mail: akasprzak@ch.pw.edu.pl

Supplementary Information

Table of contents

S1.	Experimental section	2
S1.1	Materials and methods	2
S1.2	Synthesis	3
S1.3	Florescence spectra titration.....	8
S1.4	¹ H NMR titration	8
S1.5	Cyclic voltammetry	9
S2.	NMR spectra.....	10
S3.	IR spectra	22
S4.	UV-Vis spectra	30
S5.	Fluorescence spectroscopy and titration experiments	33
S6.	The Job's plots	42
S7.	¹ H NMR titration experiments	45
S8.	Cyclic voltammograms	48
S9.	Details on calculation of K_a and LOD	53
S10.	References	55

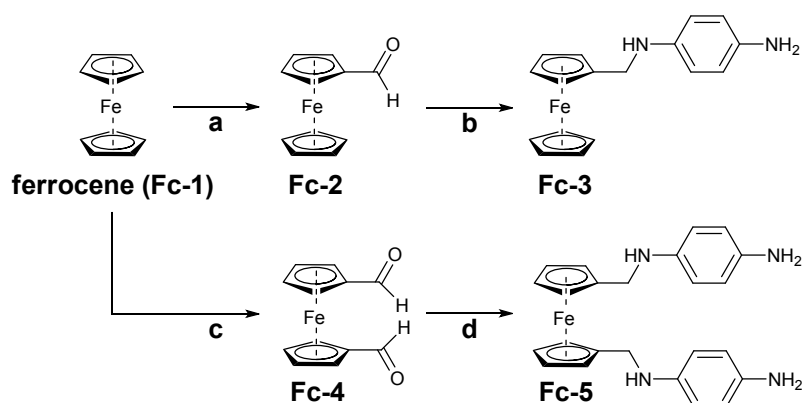
S1. Experimental section

S1.1 Materials and methods

Chemical reagents and solvents were commercially purchased and purified according to the standard methods, if necessary. Air- and moisture-sensitive reactions were carried out using commercially available anhydrous solvents under an inert atmosphere of nitrogen. The NMR experiments were carried out using JEOL JNM-ECZS spectrometer operating at 400 MHz (^1H NMR at 400 MHz or $^{13}\text{C}\{^1\text{H}\}$ NMR at 100 MHz). Unless otherwise stated, the spectra were recorded at 23 °C. Standard 5 mm NMR tubes were used. ^1H and ^{13}C chemical shifts (δ) were reported in parts per million (ppm) relative to the solvent signals: CDCl_3 , δ_{H} (residual CHCl_3) 7.26 ppm, δ_{C} 77.23 ppm, or $(\text{CD}_3)_2\text{CO}$, δ_{H} (residual $(\text{CH}_3)_2\text{CO}$) 2.05 ppm. Melting points were determined on Stanford Research Systems MPA 100 and were uncorrected. Infrared (IR) spectra were recorded on a JASCO FT IR-4100 spectrometer with a spectral resolution of 2 cm^{-1} (80 scans) in the wavelength range of $2000\text{--}600\text{ cm}^{-1}$. UV–visible (UV–Vis) absorption spectra were recorded on a JASCO V-670 spectrometer with the spectral resolution of 1 nm. Fluorescence spectra were recorded on a JASCO FP6500 spectrometer with the spectral resolution of 1 nm. Cyclic voltammetry (CV) was measured with a ALS/CH Instruments Electrochemical Analyzer Model 600A. Elemental analyses were performed using CHNS Elementar Vario EL III apparatus. Each elemental composition was reported as an average of two analyses. APCI-MS spectra were measured with ACQUITY ultra performance LC instrument. Gel permeable chromatography (GPC) was conducted on JAIGEL 2H using a JAI Recycling Preparative HPLC LC-908W with CHCl_3 as eluent. TLC analysis was performed using Merck Silica gel 60 F254 and PTLC was conducted using Wako Wakogel B-5F or with Al_2O_3 (neutral) plates.

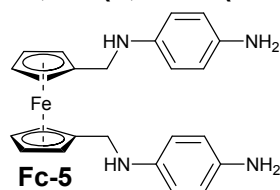
Sumanene (**1**)^[1], formylsumanene (**2**)^[2], nitrosumanene (**6**)^[2], formylferrocene (**Fc-2**)^[3], 1,1'-diformylferrocene (**Fc-4**)^[4], *N*-(ferrocenylmethyl)benzene-1,4-diamine (**Fc-3**)^[5], were synthesized according to the literature procedures.

S1.2 Synthesis



Scheme S1. Synthesis of the ferrocene derivatives: **(a)** ferrocene 100 mol%, DMF 200 mol%, POCl₃ 200 mol%, CHCl₃, 55°C, 24 h, 69% yield; **(b)** formylferrocene 100 mol%, *p*-phenylenediamine 500 mol%, MeOH, reflux, 6 h then NaBH₄ 200 mol%, reflux, 1h, 70% yield; **(c)** ferrocene 100 mol%, TMEDA 200%, ⁿBuLi 220 mol%, hex, 27°C, 24 h then DMF 220 mol% in diethyl ether, -78°C, 2 h, 72% yield; **(d)** 1,1'-diformylferrocene 100 mol%, *p*-phenylenediamine 600 mol%, MeOH, reflux, 6 h then NaBH₄ 800 mol%, reflux, 1h, 73% yield.

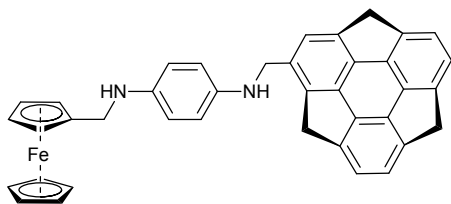
N',N'-(1,1'-bis(methyl)ferrocenyl)bis(benzene-1,4-diamine) (Fc-5)



A solution of 1,1'-diformylferrocene (24.2 mg, 0.1 mmol) and *p*-phenylenediamine (64.9 mg, 0.6 mmol) in methanol^[6] (5 mL) was refluxed for 6 h. Sodium borohydride (30.2 mg, 0.8 mmol) was then added and the mixture was further refluxed for 1 h. The reaction mixture was diluted with CH₂Cl₂ (20 mL), washed with water (5 mL), brine (3 mL), dried over Na₂SO₄, filtered and evaporated in vacuum. The crude product was purified by PTLC (SiO₂; CH₂Cl₂/MeOH, 95:5 v/v) to give compound N',N'-(1,1'-bis(methyl)ferrocenyl)bis(benzene-1,4-diamine) (**Fc-5**; 31.1 mg ; 73% yield) as a dark-orange solid.

Mp: 132 °C (decomp.); ¹H NMR (CDCl₃, 400 MHz, ppm), δ_H 6.64-6.62 (m, 4H), 6.58-6.54 (m, 4H), 4.23-4.22 (t, *J* = 1.8 Hz, 2H), 4.14-4.13 (t, *J* = 1.9 Hz, 2H), 3.92 (s, 4H), 3.29 (bs, 6H); ¹³C{¹H} NMR (CDCl₃, 100 MHz, ppm), δ_C 114.7 (2C), 138.8 (2C), 138.2 (2C), 116.9 (2C), 114.9 (2C), 87.4 (2C), 68.8 (4C), 68.5 (4C), 68.0 (2C), 44.7 (2C); IR (ATR), ν 1565, 1510, 1485, 1300, 1245, 1105, 815 cm⁻¹; Elemental analysis: calculated for C₂₄H₂₆FeN₄: C (67.61%), H (6.15%), N (13.14%); found: C (67.50%), H (6.13%), N (13.28%); APCI-MS calcd. for C₂₄H₂₆FeN₄ [M]⁺ = 426.15, found: *m/z* 426.16; R_f (SiO₂; CH₂Cl₂/MeOH, 95:5 v/v) = 0.55

***N*¹-(ferrocenylmethyl)-*N*⁴-(sumanenylmethyl)benzene-1,4-diamine (**3**)**

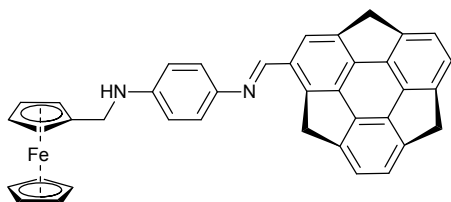


3

A solution of *N*-(ferrocenylmethyl)benzene-1,4-diamine (**Fc-3**; 2.5 mg, 0.0082 mmol) in MeOH^[6] (0.8 mL) was added to a stirred solution of formylsumanene (**2**; 2.4 mg, 0.0082 mmol) in dry THF (1.0 mL). Formic acid (85%; 10 μ L) was added and the mixture was stirred at 27 °C for 24 h. Then, sodium borohydride (1.2 mg, 0.0248 mmol) was added and the mixture was further stirred at 27 °C for 3 h. CH₂Cl₂ (15 mL) was added and the organic layer was washed with saturated NaHCO₃ (2 mL), water (2 mL), brine (2 mL), dried with Na₂SO₄, filtered, and the solvent was removed in vacuum. The resultant residue was purified by column chromatography (Al₂O₃; CH₂Cl₂/MeOH = 99.5:0.5 v/v) to give *N*¹-(ferrocenylmethyl)-*N*⁴-(sumanenylmethyl)benzene-1,4-diamine (**3**; 3.6 mg, 75% yield) as the light-orange solid.

Mp: 195 °C (decomp.); ¹H NMR (CDCl₃, 400 MHz, ppm), δ _H 7.16 (s, 1H), 7.11–7.09 (m, 4H), 6.63–6.62 (m, 4H), 4.35–4.22 (m, 5H), 4.24–4.23 (t, *J* = 1.9 Hz, 2H), 4.17 (s, 5H), 4.13–4.12 (t, *J* = 1.9 Hz, 2H), 3.91 (s, 2H), 3.52 (d, *J* = 19.9 Hz, 1H), 3.44 (d, *J* = 15.0 Hz, 1H), 3.39 (d, *J* = 15.1 Hz, 1H); ¹H NMR ((CD₃)₂CO, 400 MHz, ppm), δ _H 7.25 (s, 1H), 7.16–7.14 (m, 4H), 6.60–6.54 (m, 4H), 4.72–4.64 (m, 4H), 4.40–4.27 (m, 4H), 4.23–4.22 (t, *J* = 1.9 Hz, 2H), 4.16 (s, 5H), 4.12–4.10 (t, *J* = 5.9 Hz, 1H), 4.07–4.05 (t, *J* = 1.9 Hz, 2H), 3.91 (d, *J* = 5.9 Hz, 2H), 3.64 (d, *J* = 20.0 Hz, 1H), 3.48 (d, *J* = 15.1 Hz, 1H), 3.44 (d, *J* = 15.0 Hz, 1H); ¹³C{¹H} NMR (CDCl₃, 100 MHz, ppm), δ _C 150.3, 149.2, 149.2, 149.1, 149.0, 148.9, 148.8 (2C), 148.2, 147.1, 141.3, 141.2, 135.9, 123.6, 123.5 (2C), 123.4 (2C), 115.1 (2C), 115.0 (2C), 87.2, 87.2, 68.7 (5C), 68.3 (2C), 68.0 (2C), 49.0, 45.0, 42.0 (2C), 41.0; IR (ATR), ν 1560, 1510, 1460, 1300, 1225, 1100, 1000, 800, 750 cm⁻¹; UV-Vis, λ _{max} (CHCl₃:MeOH = 1:1 v/v) 250, 280, 360, 395 nm; Elemental analysis: calculated for C₃₉H₃₀FeN₂: C (80.41%), H (5.19%), N (4.81%); found: C (80.07%), H (5.28%), N (4.65%); APCI-MS: calcd. for C₃₉H₃₀FeN₂[M]⁺ = 582.81, found: *m/z* 582.83; R_f (Al₂O₃; CH₂Cl₂/MeOH, 99.5:0.5 v/v) = 0.40

(*E*)-*N*¹-(ferrocenylmethyl)-*N*⁴-(sumenylmethyl)benzene-1,4-diamine (4**)**



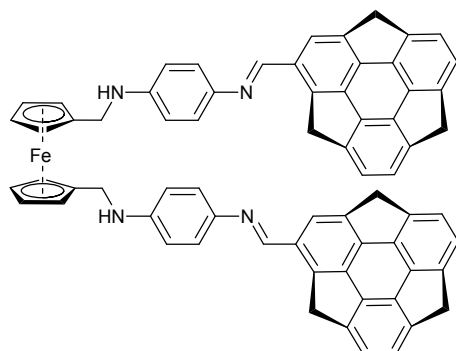
4

A solution of *N*-(ferrocenylmethyl)benzene-1,4-diamine (**Fc-3**; 2.5 mg, 0.0082 mmol) in MeOH^[6] (0.8 mL) was added to a stirred solution of formylsumenene (**2**; 2.4 mg,

0.0082 mmol) in dry THF (1.0 mL). Formic acid (85%; 10 μ L) was added and the mixture was stirred at 27 °C for 24 h. CH₂Cl₂ (15 mL) was added and the organic layer was washed with saturated NaHCO₃ (2 mL), water (2 mL), brine (2 mL), dried with Na₂SO₄, filtered, and the solvent was removed in vacuum. The resultant residue was purified by using a recycling GPC (chloroform as eluting solvent) to give (*E*)-*N*¹-(ferrocenylmethyl)-*N*⁴-(sumenenyilmethyl)benzene-1,4-diamine (**4**; 4.5 mg, 94% yield) as the dark yellow solid.

Mp: 178°C (decomp.); ¹H NMR (CDCl₃, 400 MHz, ppm), 8.60 (s, 1H), 7.61 (s, 1H), 7.25-7.23 (m, 2H), 7.17-7.11 (m, 4H), 6.71-6.69 (m, 2H), 4.98 (d, *J* = 20.6 Hz, 1H), 4.75 (d, *J* = 19.6 Hz, 1H), 4.72 (d, *J* = 19.6 Hz, 1H), 4.27-4.26 (t, *J* = 1.9 Hz, 2H), 4.20 (s, 5H), 4.17-4.16 (t, *J* = 1.9 Hz, 2H), 4.00-3.98 (bm, 3H), 3.66 (d, *J* = 20.6 Hz, 1H), 3.50 (d, *J* = 19.6 Hz, 1H), 3.45 (d, *J* = 19.6 Hz, 1H); ¹³C{¹H} NMR (CDCl₃, 100 MHz, ppm), δ_c 156.1, 150.1, 149.5, 149.4 (2C), 149.1, 149.0, 148.9, 148.8, 148.6, 148.2, 147.5, 147.3, 147.1, 142.6, 133.7, 124.9, 124.1, 124.0, 123.6 (2C), 122.7 (2C), 113.4 (2C), 86.5, 68.7 (5C), 68.4 (2C), 68.2 (2C), 43.8, 43.0, 42.0, 41.8; IR (ATR), ν 1635, 1555, 1510, 1455, 1300, 1250, 1100, 995, 805, 755 cm⁻¹; UV-Vis, λ_{max} (CHCl₃:MeOH = 1:1 v/v) 255, 295, 360, 390 nm; Elemental analysis: calculated for C₃₉H₂₈FeN₂: C (80.69%), H (4.86%), N (4.83%); found: C (80.15%), H (4.59%), N (4.60%); APCI-MS: calcd. for C₃₉H₂₈FeN₂ [M]⁺ = 580.49, found: *m/z* 582.48. R_f (SiO₂; CH₂Cl₂) = 0.56

(*N*⁴*E*,*N*⁴*E*)-*N*¹,*N*^{1'}-(1,1'-bis(methyl)ferrocenyl)bis(*N*⁴-(sumenenyilmethyl)benzene-1,4-diamine) (5**)**



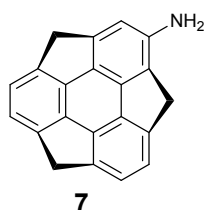
5

A solution of *N*¹,*N*^{1'}-(1,1'-bis(methyl)ferrocenyl)bis(benzene-1,4-diamine) (**Fc-5**; 3.1 mg, 0.0072 mmol) in MeOH^[6] (1.0 mL) was added to a stirred solution of formylsumanene (**2**; 4.2 mg, 0.0144 mmol) in dry THF (2.0 mL). Formic acid (85%; 20 μ L) was added and the mixture was stirred at 27 °C for 24 h. CH₂Cl₂ (20 mL) was added and the organic layer was washed with saturated NaHCO₃ (3 mL), water (2 mL), brine (3 mL), dried with Na₂SO₄, filtered, and the solvent was removed in vacuum. The resultant residue was purified by using a recycling GPC (chloroform as eluting solvent) to give (*N*⁴*E*, *N*⁴*E*)-*N*¹,*N*^{1'}-(1,1'-bis(methyl)ferrocenyl)bis(*N*⁴-(sumenenyilmethyl)benzene-1,4-diamine) (**5**; 5.0 mg, 72% yield) as the yellow solid.^[7]

Mp: 171°C (decomp.); ¹H NMR (CDCl₃, 400 MHz, ppm), δ 8.57 (s, 1H), 8.55 (s, 1H), 7.59 (s, 1H), 7.56 (s, 1H), 7.23-7.20 (m, 4H), 7.11-7.06 (m, 8H), 6.67-6.63 (m, 4H),

4.94-4.84 (m, 2H), 4.72-4.59 (m, 4H), 4.29-4.28 (t, $J = 1.8$ Hz, 2H), 4.21-4.20 (t, $J = 1.8$ Hz, 2H), 4.02-4.00 (bm, 6H), 3.84-3.69 (m, 2H), 3.45-3.29 (m, 4H); $^{13}\text{C}\{^1\text{H}\}$ NMR (CDCl_3 , 100 MHz, ppm), δ_{C} 156.3, 156.1, 149.5 (2C), 149.4 (2C), 149.3 (4C), 149.2 (2C), 149.1 (2C), 149.0 (2C), 148.9 (2C), 148.2 (2C), 148.0 (2C), 147.8 (2C), 147.5 (4C), 147.4 (2C), 147.3 (2C), 135.5 (2C), 124.9 (2C), 124.4 (2C), 124.1 (2C), 123.9 (2C), 123.5 (2C), 122.8 (4C), 113.50 (6C), 87.0 (2C), 68.8 (2C), 68.7 (2C), 43.0 (2C), 42.8 (2C), 42.0 (2C), 41.7 (2C); IR (ATR), ν 1650, 1605, 1510, 1460, 1395, 1255, 1085, 1020, 795 cm^{-1} ; UV-Vis, λ_{max} (CHCl_3 :MeOH = 1:1 v/v) 255, 295, 395 nm; Elemental analysis: calculated for $\text{C}_{68}\text{H}_{46}\text{FeN}_4$: C (83.77%), H (4.76%), N (5.75%); found: C (84.02%), H (4.85%), N (5.60%); APCI-MS: calcd. for $\text{C}_{68}\text{H}_{46}\text{FeN}_4[\text{M}]^+ = 974.97$, found: m/z 974.96. R_f (SiO_2 ; CH_2Cl_2) = 0.75

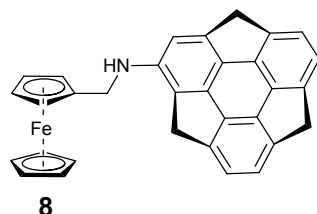
Aminosumanene (7)



A mixture containing nitrosumanene (**6**; 4.0 mg, 0.0121 mmol) and Pd/C (10% Pd; 8.0 mg, 200 w/w%) in the solvent ($\text{EtOH}/\text{AcOEt} = 1:1$ v/v, 4.0 mL)^[8] was stirred at 27 °C for 3 h. The mixture was filtered through celite and washed with CH_2Cl_2 (15 mL). The volatiles were distilled off in vacuum to give aminosumanene (**7**; 3.4 mg, 99% yield) as a yellow-white solid.

Mp: 118 °C (decomp.); ^1H NMR (CDCl_3 , 400 MHz, ppm), δ 7.12-7.10 (m, 3H), 7.03-6.96 (m, 2H), 6.42 (bs, 2H), 4.70-4.49 (m, 3H), 3.41-3.28 (m, 3H); $^{13}\text{C}\{^1\text{H}\}$ NMR (CDCl_3 , 100 MHz, ppm), δ_{C} 153.0, 150.7, 150.1, 149.3, 149.1, 149.0, 148.4, 147.9, 147.4, 143.2, 140.8, 129.4, 123.6, 123.5, 123.3, 121.7, 121.7, 111.7, 41.8, 41.6, 39.7; IR (ATR), ν 1585, 1535, 1320, 1250, 985, 815, 750 cm^{-1} ; Elemental analysis: calculated for $\text{C}_{21}\text{H}_{13}\text{N}$: C (90.29%), H (4.70%), N (5.01%); found: C (90.20%), H (4.59%), N (5.21%); APCI-MS: calcd. for $\text{C}_{21}\text{H}_{13}\text{N}[\text{M}]^+ = 279.33$, found: m/z 279.34. R_f (SiO_2 ; CH_2Cl_2) = 0.67

N-(ferrocenylmethyl)sumanene (8)

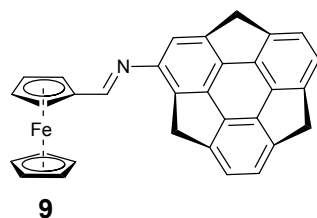


A solution of formylferrocene (3.0 mg, 0.0140 mmol), aminosumanene (3.9 mg, 0.0140 mmol) and formic acid (85%; 20 μL) in THF/methanol solvent system (1:2 v/v)^[8] (2.5 mL) was refluxed for 6 hours at nitrogen atmosphere. Sodium borohydride (1.7 mg, 0.0420 mmol, 3 eq) was then added and the mixture was further refluxed for 1 h. The

reaction mixture was diluted with CH₂Cl₂ (15 mL), washed saturated NaHCO₃ (2 mL), water (2 mL), brine (2 mL), dried over Na₂SO₄, filtered and evaporated in vacuum. The resultant residue was purified by using a recycling GPC (chloroform as eluting solvent) to give *N*-(ferrocenylmethyl)sumanene (**8**; 4.6 mg, 69%) as the light-orange solid.^[9]

Mp: 221 °C (decomp.); ¹H NMR (CDCl₃, 400 MHz, ppm), δ_H 7.10-7.09 (m, 3H), 7.04-6.94 (m, 2H), 6.45 (bs, 1H), 4.68 (d, *J* = 19.2 Hz, 1H), 4.63 (d, *J* = 19.1 Hz, 1H), 4.59 (d, *J* = 19.4 Hz, 1H), 4.27-4.26 (t, *J* = 1.8 Hz, 2H), 4.21 (s, 5H), 4.18-4.17 (t, *J* = 1.8 Hz, 2H), 4.01 (d, *J* = 7.8 Hz, 2H), 3.41 (d, *J* = 19.2 Hz, 1H), 3.36 (d, *J* = 19.1 Hz, 1H), 3.32 (d, *J* = 19.4 Hz, 1H); ¹³C{¹H} NMR (CDCl₃, 100 MHz, ppm), δ_C 153.1, 149.8, 149.5, 149.2, 148.4, 148.3, 148.0, 147.9, 147.5, 147.4 (2C), 147.1, 146.9, 146.6, 136.0, 134.6, 123.4, 108.0, 98.4, 68.73 (5C), 68.33, (2C), 68.2 (2C), 51.2, 42.7, 41.7, 40.6; IR (ATR), ν 1545, 1515, 1465, 1290, 1245, 1130, 1105, 995, 810 cm⁻¹; UV-Vis, λ_{max} (CHCl₃:MeOH = 1:1 v/v) 250, 280, 370 nm; Elemental analysis: calculated for C₃₂H₂₃FeN: C (80.51%), H (4.86%), N (2.93%); found: C (80.71%), H (4.72%), N (3.04%); APCI-MS: calcd. for C₃₂H₂₃FeN [M]⁺ = 477.38, found: *m/z* 477.36. R_f (SiO₂; CH₂Cl₂/hexane, 95:5 v/v) = 0.82

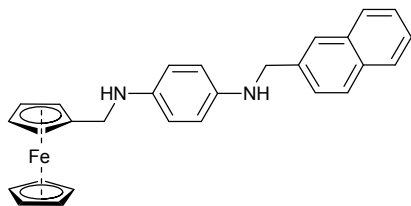
(*E*)-*N*-(ferrocenylmethyl)sumanene (**9**)



A solution of formylferrocene (3.0 mg, 0.0140 mmol), aminosumanene (3.9 mg, 0.0140 mmol) and formic acid (85%; 20 μL) in THF/methanol solvent system (1:2 v/v)^[8] (2.5 mL) was refluxed for 6 h. The reaction mixture was diluted with CH₂Cl₂ (15 mL), washed saturated NaHCO₃ (2 mL), water (2 mL), brine (2 mL), dried over Na₂SO₄, filtered and evaporated in vacuum. The resultant residue was purified by using a recycling GPC (chloroform as eluting solvent) to give (*E*)-*N*-(ferrocenylmethyl)sumanene (**9**; 4.1 mg, 61%) as the orange solid.

Mp: 202 °C (decomp.); ¹H NMR (CDCl₃, 400 MHz, ppm), δ_H 8.56 (s, 1H), 7.13-7.09 (m, 4H), 6.96 (s, 1H), 4.80 (d, *J* = 19.9 Hz, 1H), 4.82-4.81 (t, *J* = 1.9 Hz, 2H), 4.72 (d, *J* = 19.6 Hz, 2H), 4.50 (t, *J* = 1.9 Hz, 2H), 4.25 (s, 5H), 3.56 (d, *J* = 19.9 Hz, 1H), 3.47 (d, *J* = 19.6 Hz, 1H), 3.42 (d, *J* = 19.6 Hz, 1H); ¹³C{¹H} NMR (CDCl₃, 100 MHz, ppm), δ_C 162.1, 151.7, 149.5, 149.3, 149.2, 149.1, 149.0, 148.9, 148.7, 148.6, 148.5, 148.4 (2C), 123.8, 123.6, 123.5 (2C), 123.1, 119.3, 71.5, 69.6 (5C), 69.3 (2C), 69.2 (2C), 41.9, 41.8, 41.5; IR (ATR), ν 1630, 1520, 1465, 1395, 1295, 1255, 1120, 1005, 815 cm⁻¹; UV-Vis, λ_{max} (CHCl₃:MeOH = 1:1 v/v) 240, 280, 375 nm; Elemental analysis: calculated for C₃₂H₂₁FeN: C (80.85%), H (4.45%), N (2.95%); found: C (80.99%), H (4.28%), N (3.09%); APCI-MS: calcd. for C₃₂H₂₁FeN [M]⁺ = 475.36, found: *m/z* 475.35. R_f (SiO₂; CH₂Cl₂/hexane, 90:10 v/v) = 0.85

***N*¹-(ferrocenylmethyl)-*N*⁴-(naphthalen-2-ylmethyl)benzene-1,4-diamine (**10**)**



A solution of *N*-(ferrocenylmethyl)benzene-1,4-diamine (**Fc-3**; 5.6 mg, 0.0082 mmol), 2-naphthaldehyde (2.9 mg, 0.0183 mmol) and formic acid (85%; 30 μ L) in MeOH^[6] (2.0 mL) was stirred at 27 °C for 24 h. Then, sodium borohydride (1.2 mg, 0.0248 mmol) was added and the mixture was further stirred at 27 °C for 3 h. CH₂Cl₂ (20 mL) was added and the organic layer was washed with saturated NaHCO₃ (2 mL), water (2 mL), brine (2 mL), dried with Na₂SO₄, filtered, and the solvent was removed in vacuum. The resultant residue was purified by PTLC (SiO₂; CH₂Cl₂) to give *N*¹-(ferrocenylmethyl)-*N*⁴-(naphthalen-2-ylmethyl)benzene-1,4-diamine (**10**; 5.5 mg, 67% yield) as the light-orange solid.

Mp: 110 °C (decomp.); ¹H NMR (CDCl₃, 400 MHz, ppm), δ_{H} 7.86-7.80 (m, 4H), 7.52-7.45 (m, 3H), 6.66-6.60 (m, 4H), 4.87 (bs, 1H), 4.44-4.455 (bm, 2H), 4.24-4.23 (t, J = 1.9 Hz, 2H), 4.17 (s, 5H), 4.13-4.12 (t, J = 1.9 Hz, 2H), 3.90-3.89 (bm, 2H), 3.64 (bs, 1H); ¹³C{¹H} NMR (CDCl₃, 100 MHz, ppm), δ_{C} 141.2, 141.0, 137.7, 132.9, 128.4, 128.1, 128.0, 127.9, 126.3 (2C), 126.2 (2C), 125.8, 125.4, 115.0 (2C), 87.13, 68.6 (5C), 68.3 (2C), 67.9 (2C), 49.9, 44.9; IR (ATR), ν 1555, 1515, 1460, 1295, 1250, 1130, 1095, 1005, 810, 745 cm⁻¹; UV-Vis, λ_{max} (CHCl₃:MeOH = 1:1 v/v) 260, 265, 270, 380 nm; Elemental analysis: calculated for C₂₈H₂₆FeN₂: C (75.34%), H (5.87%), N (6.28%); found: C (75.83%), H (5.26%), N (6.36%); APCI-MS: calcd. for C₂₈H₂₆FeN₂ [M]⁺ = 446.36, found: m/z 446.35; R_f (SiO₂; CH₂Cl₂) = 0.31.

S1.3 Florescence spectra titration

The 0.5 mM stock solution of the sumanene-ferrocene conjugate and 2 mM stock solution of Cs⁺ (in the form of CsCl) in the solvent system (CHCl₃:MeOH = 1/1 v/v) were prepared. The concentration of sumanene-ferrocene conjugate was kept constant (0.1 mM), whilst the samples varied in the molar equivalent of Cs⁺ added (eq = 0, 0.5, 1, 2, 4, 6 or 12).

S1.4 ¹H NMR titration

The 3.0 mM stock solution of the sumanene-ferrocene conjugate and 9 mM stock solution of Cs⁺ (in the form of CsCl) in the solvent system (CDCl₃:CD₃OD = 1/1 v/v) were prepared. The concentration of sumanene-ferrocene conjugate was kept constant (1.5 mM), whilst the samples varied in the molar equivalent of Cs⁺ added (eq = 0, 0.5, 1, 2, 3).

S1.5 Cyclic voltammetry

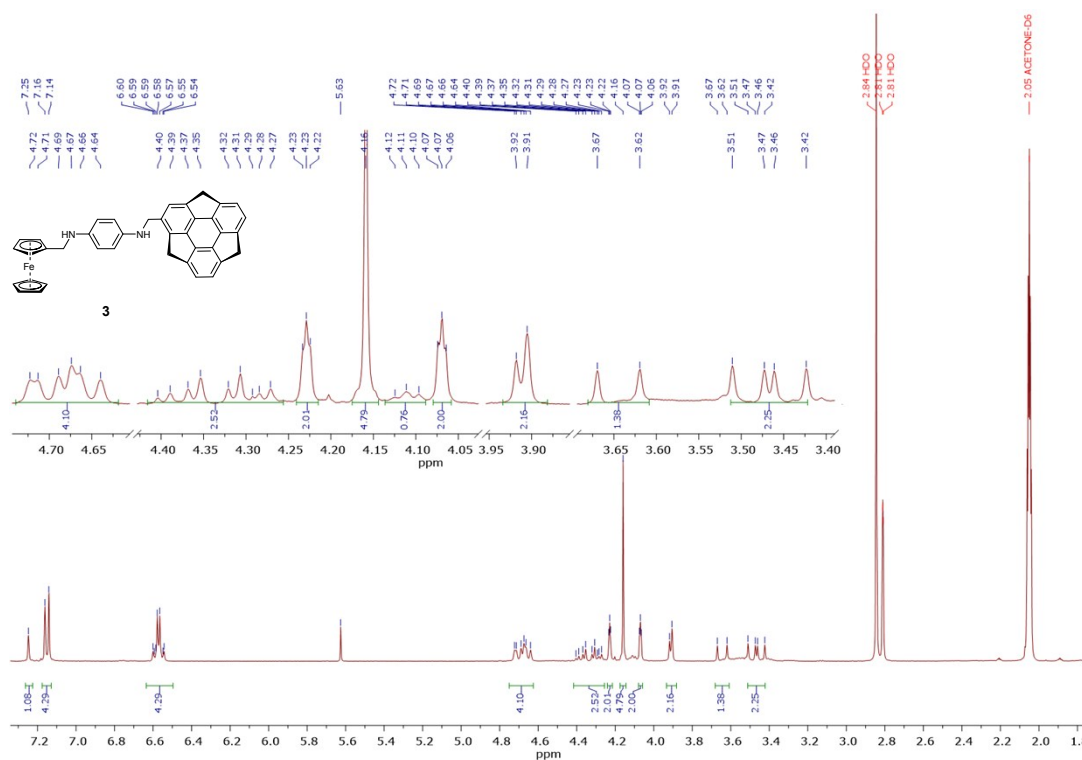
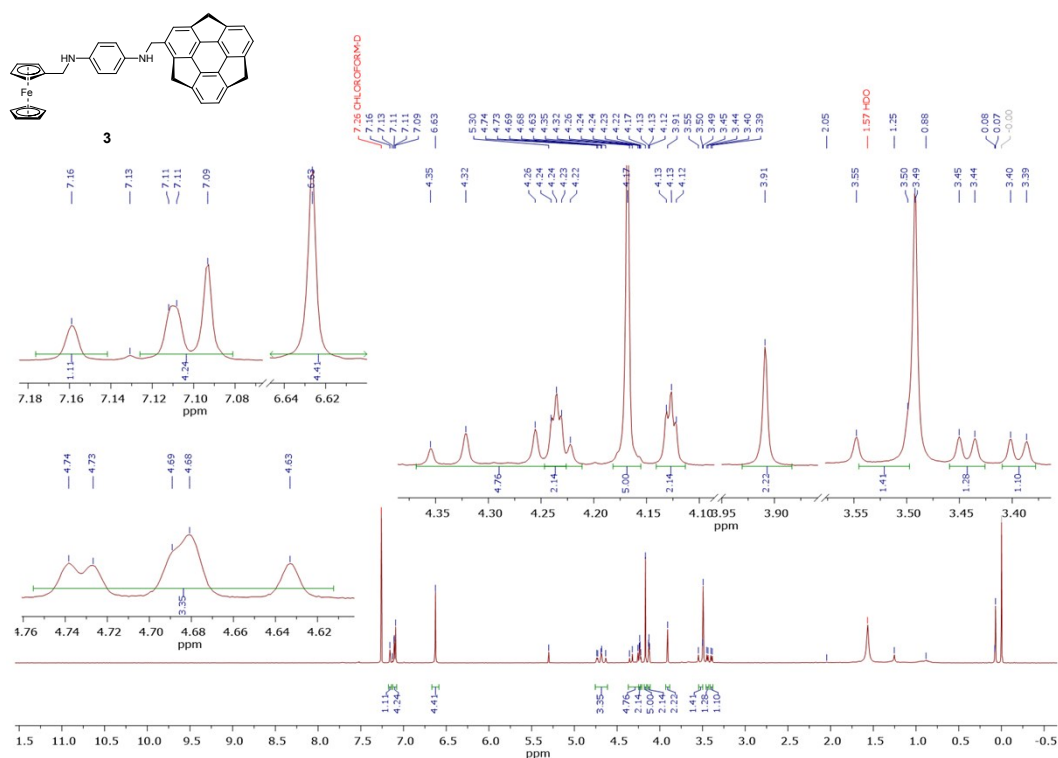
Measurements were conducted in CH_2Cl_2 with tetrabutylammonium perchlorate (TBAP; 0.1 M) as a supporting electrolyte, with a sumanene-ferrocene conjugate concentration of 0.5 mM and a scan rate of 0.05 V/s. The voltammograms were referenced against the ferrocene/ferrocenium couple (Fc/Fc^+). The glassy carbon electrode (GCE) played a role of the working electrode, Ag/AgCl electrode was used as the reference electrode and a platinum wire was used as the counter electrode. The working electrode was polished with Al_2O_3 slurry on a wet pad before the measurement. After the polishing step, the electrode was rinsed with the pure solvent.

For the Cs^+ recognition tests, cyclic voltammograms were measured in the solvent system ($\text{CHCl}_3:\text{MeOH} = 1/1 \text{ v/v}$) with TBAP as a supporting electrolyte (0.1 M). Two tests were run: (1) with the solution of pristine sumanene-ferrocene conjugate (0.5 mM), (2) with the solution of sumanene-ferrocene conjugate (0.5 mM) containing 12 molar equivalents of Cs^+ (in the form of its corresponding chloride).

Fc-5

¹H NMR (400 MHz, CDCl₃) peaks (ppm): 7.735, 7.733, 7.731, 7.729, 7.727, 7.725, 7.723, 7.721, 7.719, 7.717, 7.715, 7.713, 7.711, 7.709, 7.707, 7.705, 7.703, 7.701, 7.699, 7.697, 7.695, 7.693, 7.691, 7.689, 7.687, 7.685, 7.683, 7.681, 7.679, 7.677, 7.675, 7.673, 7.671, 7.669, 7.667, 7.665, 7.663, 7.661, 7.659, 7.657, 7.655, 7.653, 7.651, 7.649, 7.647, 7.645, 7.643, 7.641, 7.639, 7.637, 7.635, 7.633, 7.631, 7.629, 7.627, 7.625, 7.623, 7.621, 7.619, 7.617, 7.615, 7.613, 7.611, 7.609, 7.607, 7.605, 7.603, 7.601, 7.599, 7.597, 7.595, 7.593, 7.591, 7.589, 7.587, 7.585, 7.583, 7.581, 7.579, 7.577, 7.575, 7.573, 7.571, 7.569, 7.567, 7.565, 7.563, 7.561, 7.559, 7.557, 7.555, 7.553, 7.551, 7.549, 7.547, 7.545, 7.543, 7.541, 7.539, 7.537, 7.535, 7.533, 7.531, 7.529, 7.527, 7.525, 7.523, 7.521, 7.519, 7.517, 7.515, 7.513, 7.511, 7.509, 7.507, 7.505, 7.503, 7.501, 7.499, 7.497, 7.495, 7.493, 7.491, 7.489, 7.487, 7.485, 7.483, 7.481, 7.479, 7.477, 7.475, 7.473, 7.471, 7.469, 7.467, 7.465, 7.463, 7.461, 7.459, 7.457, 7.455, 7.453, 7.451, 7.449, 7.447, 7.445, 7.443, 7.441, 7.439, 7.437, 7.435, 7.433, 7.431, 7.429, 7.427, 7.425, 7.423, 7.421, 7.419, 7.417, 7.415, 7.413, 7.411, 7.409, 7.407, 7.405, 7.403, 7.401, 7.399, 7.397, 7.395, 7.393, 7.391, 7.389, 7.387, 7.385, 7.383, 7.381, 7.379, 7.377, 7.375, 7.373, 7.371, 7.369, 7.367, 7.365, 7.363, 7.361, 7.359, 7.357, 7.355, 7.353, 7.351, 7.349, 7.347, 7.345, 7.343, 7.341, 7.339, 7.337, 7.335, 7.333, 7.331, 7.329, 7.327, 7.325, 7.323, 7.321, 7.319, 7.317, 7.315, 7.313, 7.311, 7.309, 7.307, 7.305, 7.303, 7.301, 7.299, 7.297, 7.295, 7.293, 7.291, 7.289, 7.287, 7.285, 7.283, 7.281, 7.279, 7.277, 7.275, 7.273, 7.271, 7.269, 7.267, 7.265, 7.263, 7.261, 7.259, 7.257, 7.255, 7.253, 7.251, 7.249, 7.247, 7.245, 7.243, 7.241, 7.239, 7.237, 7.235, 7.233, 7.231, 7.229, 7.227, 7.225, 7.223, 7.221, 7.219, 7.217, 7.215, 7.213, 7.211, 7.209, 7.207, 7.205, 7.203, 7.201, 7.199, 7.197, 7.195, 7.193, 7.191, 7.189, 7.187, 7.185, 7.183, 7.181, 7.179, 7.177, 7.175, 7.173, 7.171, 7.169, 7.167, 7.165, 7.163, 7.161, 7.159, 7.157, 7.155, 7.153, 7.151, 7.149, 7.147, 7.145, 7.143, 7.141, 7.139, 7.137, 7.135, 7.133, 7.131, 7.129, 7.127, 7.125, 7.123, 7.121, 7.119, 7.117, 7.115, 7.113, 7.111, 7.109, 7.107, 7.105, 7.103, 7.101, 7.099, 7.097, 7.095, 7.093, 7.091, 7.089, 7.087, 7.085, 7.083, 7.081, 7.079, 7.077, 7.075, 7.073, 7.071, 7.069, 7.067, 7.065, 7.063, 7.061, 7.059, 7.057, 7.055, 7.053, 7.051, 7.049, 7.047, 7.045, 7.043, 7.041, 7.039, 7.037, 7.035, 7.033, 7.031, 7.029, 7.027, 7.025, 7.023, 7.021, 7.019, 7.017, 7.015, 7.013, 7.011, 7.009, 7.007, 7.005, 7.003, 7.001, 6.999, 6.997, 6.995, 6.993, 6.991, 6.989, 6.987, 6.985, 6.983, 6.981, 6.979, 6.977, 6.975, 6.973, 6.971, 6.969, 6.967, 6.965, 6.963, 6.961, 6.959, 6.957, 6.955, 6.953, 6.951, 6.949, 6.947, 6.945, 6.943, 6.941, 6.939, 6.937, 6.935, 6.933, 6.931, 6.929, 6.927, 6.925, 6.923, 6.921, 6.919, 6.917, 6.915, 6.913, 6.911, 6.909, 6.907, 6.905, 6.903, 6.901, 6.899, 6.897, 6.895, 6.893, 6.891, 6.889, 6.887, 6.885, 6.883, 6.881, 6.879, 6.877, 6.875, 6.873, 6.871, 6.869, 6.867, 6.865, 6.863, 6.861, 6.859, 6.857, 6.855, 6.853, 6.851, 6.849, 6.847, 6.845, 6.843, 6.841, 6.839, 6.837, 6.835, 6.833, 6.831, 6.829, 6.827, 6.825, 6.823, 6.821, 6.819, 6.817, 6.815, 6.813, 6.811, 6.809, 6.807, 6.805, 6.803, 6.801, 6.799, 6.797, 6.795, 6.793, 6.791, 6.789, 6.787, 6.785, 6.783, 6.781, 6.779, 6.777, 6.775, 6.773, 6.771, 6.769, 6.767, 6.765, 6.763, 6.761, 6.759, 6.757, 6.755, 6.753, 6.751, 6.749, 6.747, 6.745, 6.743, 6.741, 6.739, 6.737, 6.735, 6.733, 6.731, 6.729, 6.727, 6.725, 6.723, 6.721, 6.719, 6.717, 6.715, 6.713, 6.711, 6.709, 6.707, 6.705, 6.703, 6.701, 6.699, 6.697, 6.695, 6.693, 6.691, 6.689, 6.687, 6.685, 6.683, 6.681, 6.679, 6.677, 6.675, 6.673, 6.671, 6.669, 6.667, 6.665, 6.663, 6.661, 6.659, 6.657, 6.655, 6.653, 6.651, 6.649, 6.647, 6.645, 6.643, 6.641, 6.639, 6.637, 6.635, 6.633, 6.631, 6.629,

10



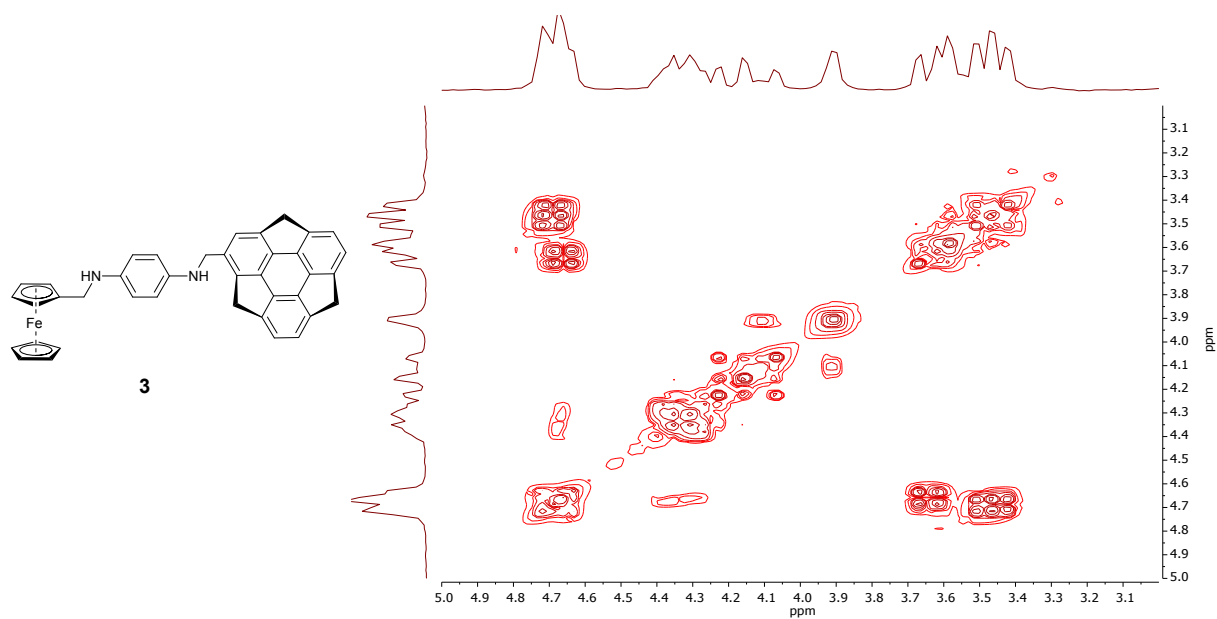


Fig. S5. Inset of ^1H - ^1H COSY NMR ($(\text{CD}_3)_2\text{CO}$, 400 MHz) spectrum of compound **3**.

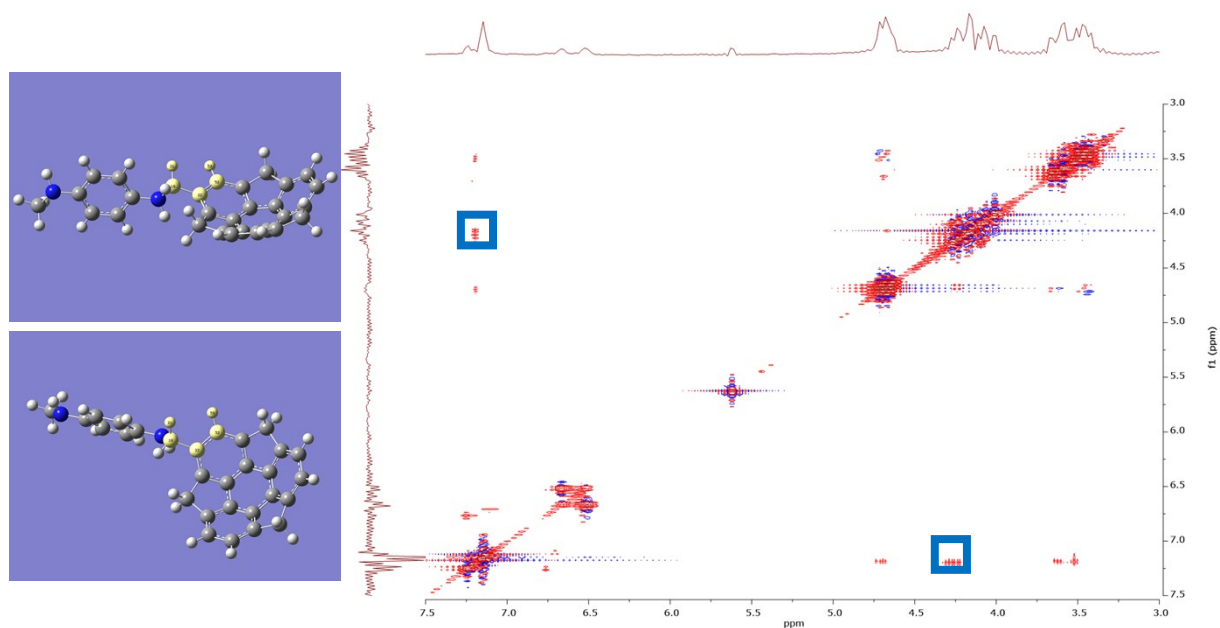
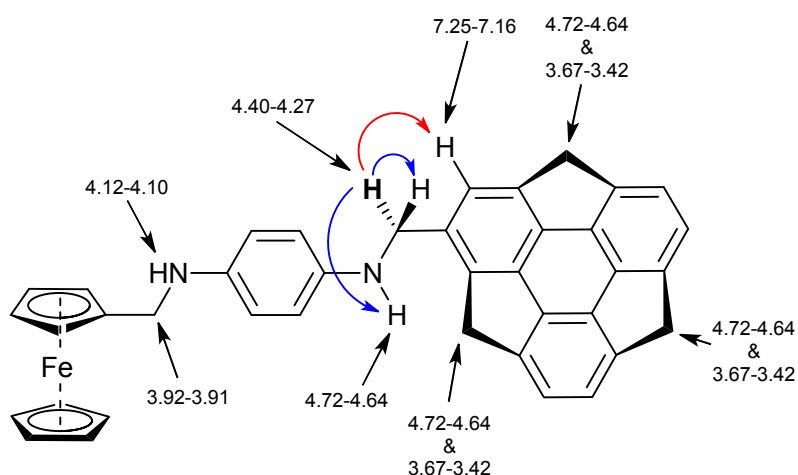


Fig. S6. ^1H - ^1H TOCSY NMR ($(\text{CD}_3)_2\text{CO}$, 400 MHz) spectrum of compound **3** together with the representation of the optimized partial structure of compound **3**.^[10] The crucial cross-correlations are marked in blue.

Table S1. Graphical representation and summary of the data on the crucial cross-correlations observed in the ^1H - ^1H COSY (marked blue) and ^1H - ^1H TOCSY (marked red) spectra of compound **3** (spectra recorded in $(\text{CD}_3)_2\text{CO}$). The chemical shifts for the respective protons are also presented. Cross-correlation between CH_2 -sumanene (4.40-4.27 ppm) and H-Ar of sumanene (7.25-7.16 ppm) observed in the ^1H - ^1H TOCSY experiment, confirmed that the CH_2 -sumanene diastereotopic protons and H-Ar of sumanene are included in the same spin system (U-shaped system, see the graphical representation in Fig. S6). This feature stands for the signal multiplicity of CH_2 -sumanene (multiplet, 4.40-4.27 ppm).



Chemical shift [ppm] and peak assignment		7.25-7.16 (m)	4.72-4.64 (m)	4.40-4.27 (m)	4.12-4.10 (t)	3.92-3.91 (d)	3.67-3.42 (3 x d)
		Ar (sumanene)	benzylic exo + NH-CH ₂ -sumanene	CH ₂ -sumanene	Fc-CH ₂ -NH	Fc-CH ₂	benzylic endo
7.25-7.16 (m)	Ar (sumanene)			X			
4.72-4.64 (m)	benzylic exo + NH-CH ₂ -sumanene			X			X
4.40-4.27 (m)	CH ₂ -sumanene	X	X				
4.12-4.10 (t)	Fc-CH ₂ -NH					X	
3.92-3.91 (d)	Fc-CH ₂				X		
3.67-3.42 (3 x d)	benzylic endo		X				

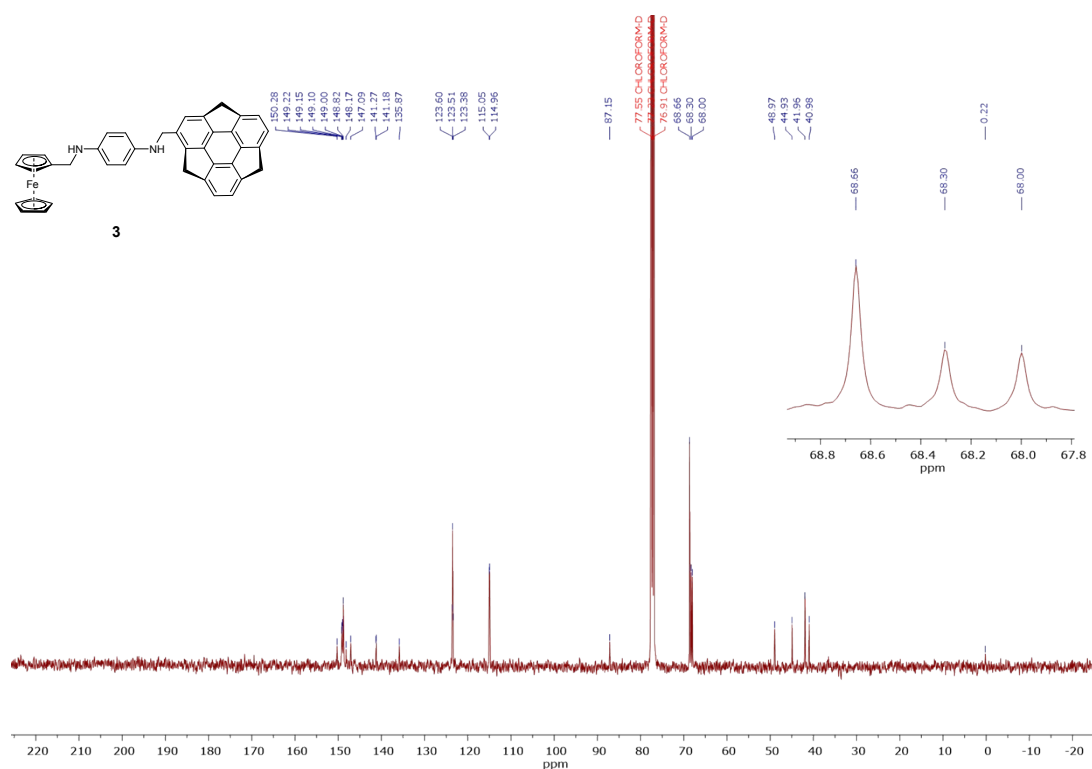


Fig. S7. ¹³C NMR (CDCl₃, 100 MHz) spectrum of compound **3**.

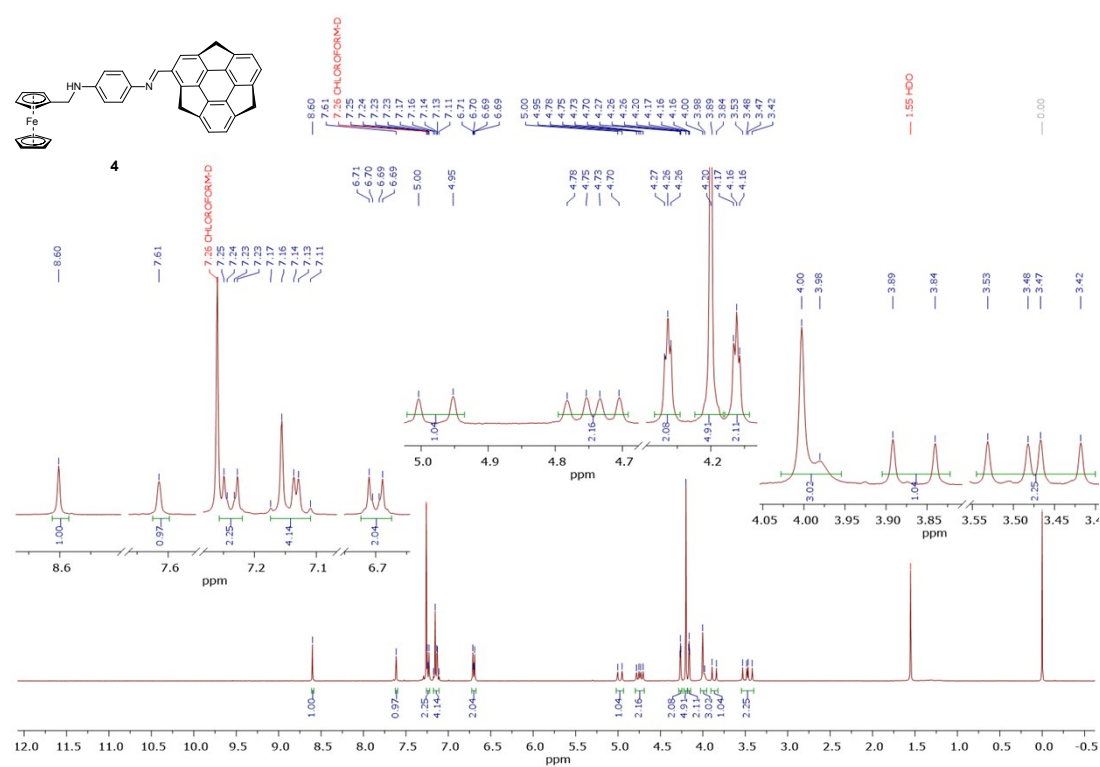


Fig. S8. ¹H NMR (CDCl₃, 400 MHz) spectrum of compound **4**.

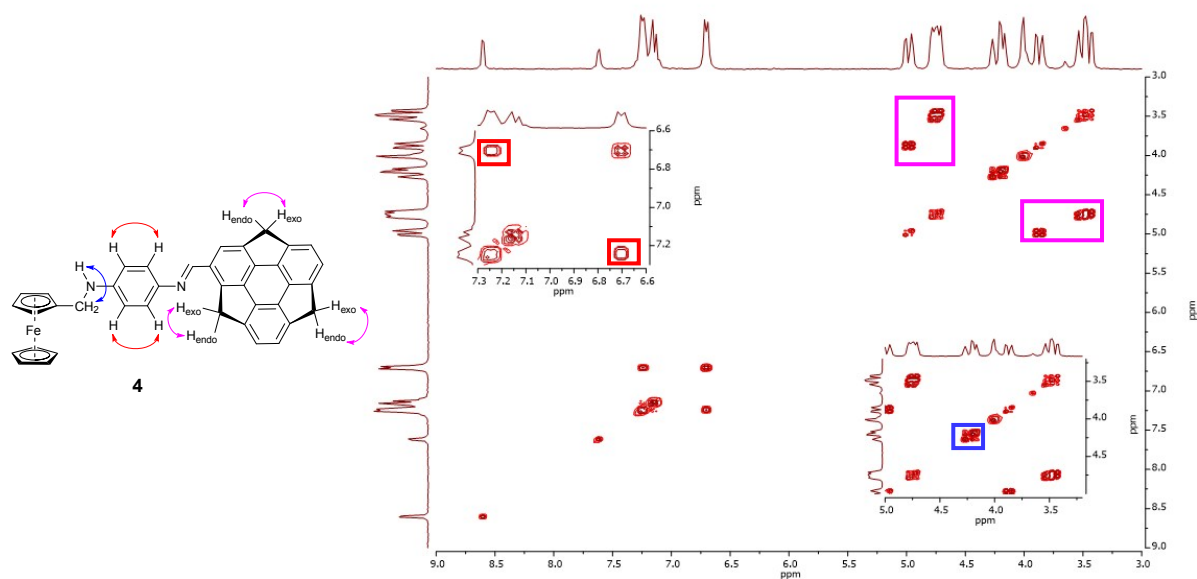


Fig. S9. ^1H - ^1H COSY NMR (CDCl₃, 400 MHz) spectrum of compound **4**. The crucial cross correlations are also marked.

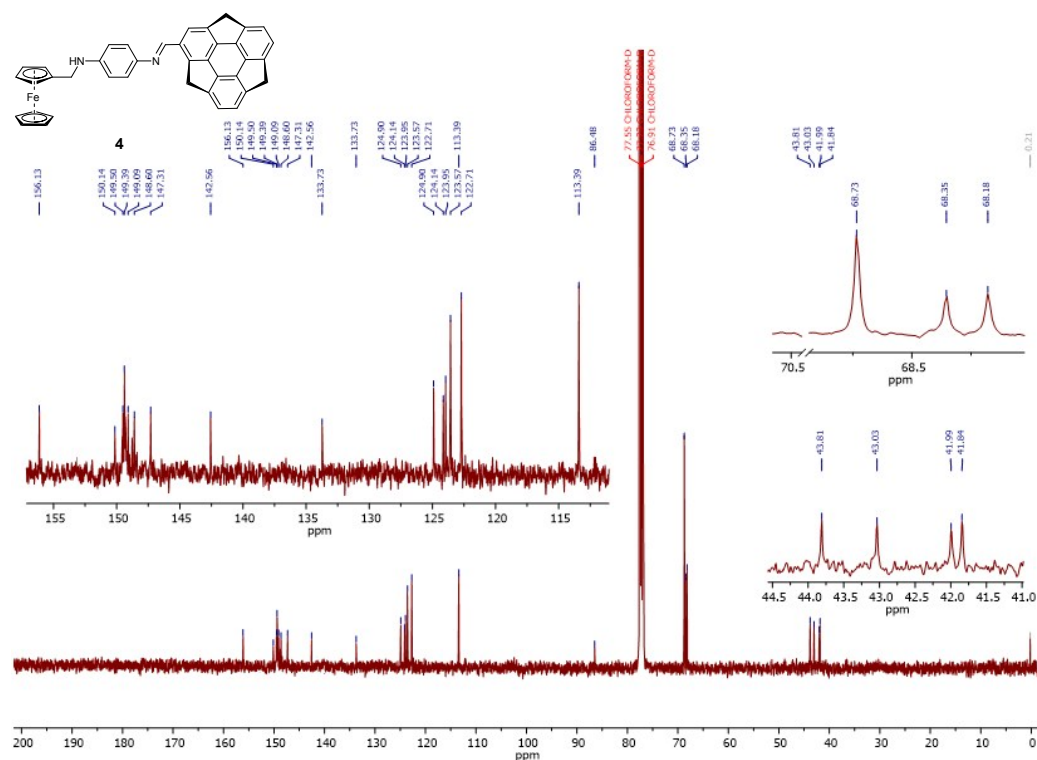


Fig. S10. ^{13}C NMR (CDCl₃, 100 MHz) spectrum of compound **4**.

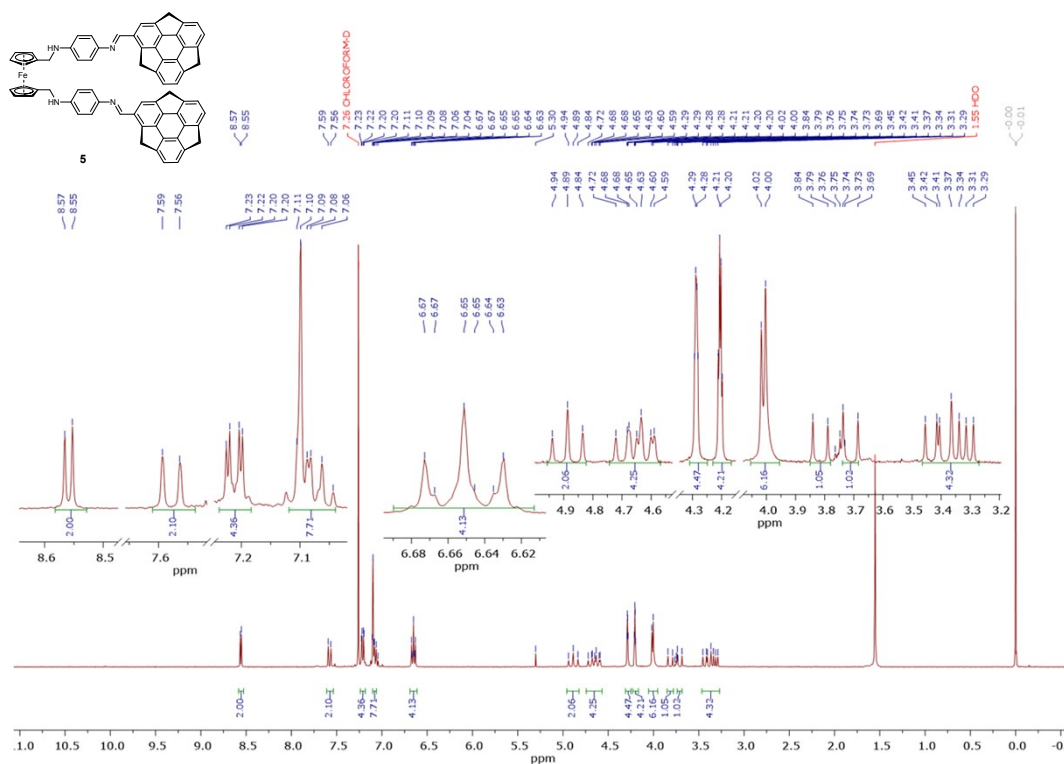


Fig. S11. ^1H NMR (CDCl_3 , 400 MHz) spectrum of compound **5**.

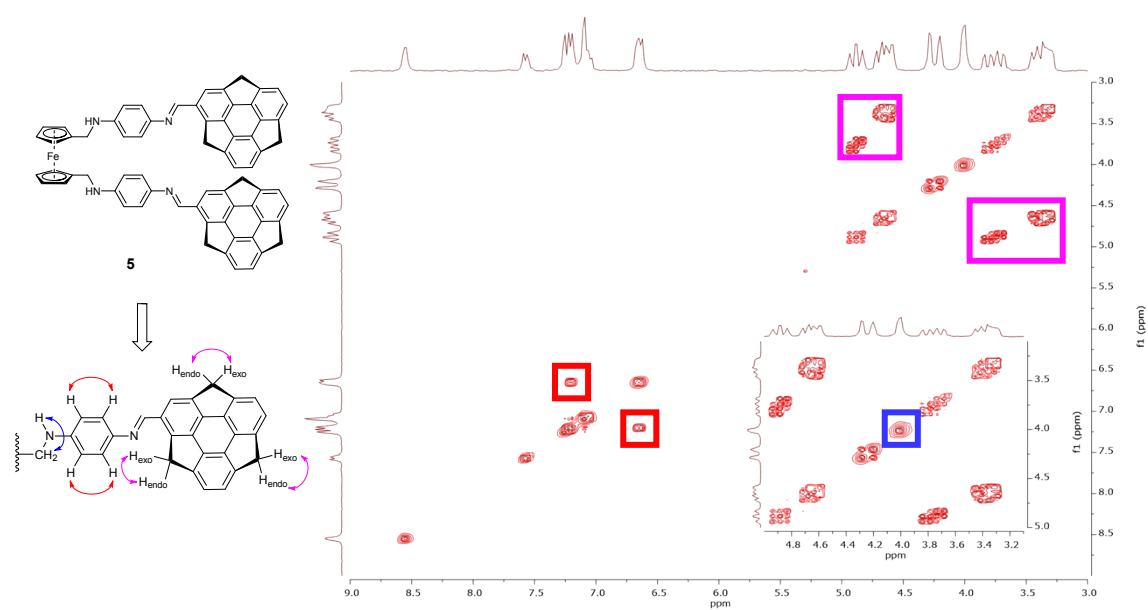


Fig. S12. ^1H - ^1H COSY NMR (CDCl_3 , 400 MHz) spectrum of compound **5**. The crucial cross correlations are also marked.

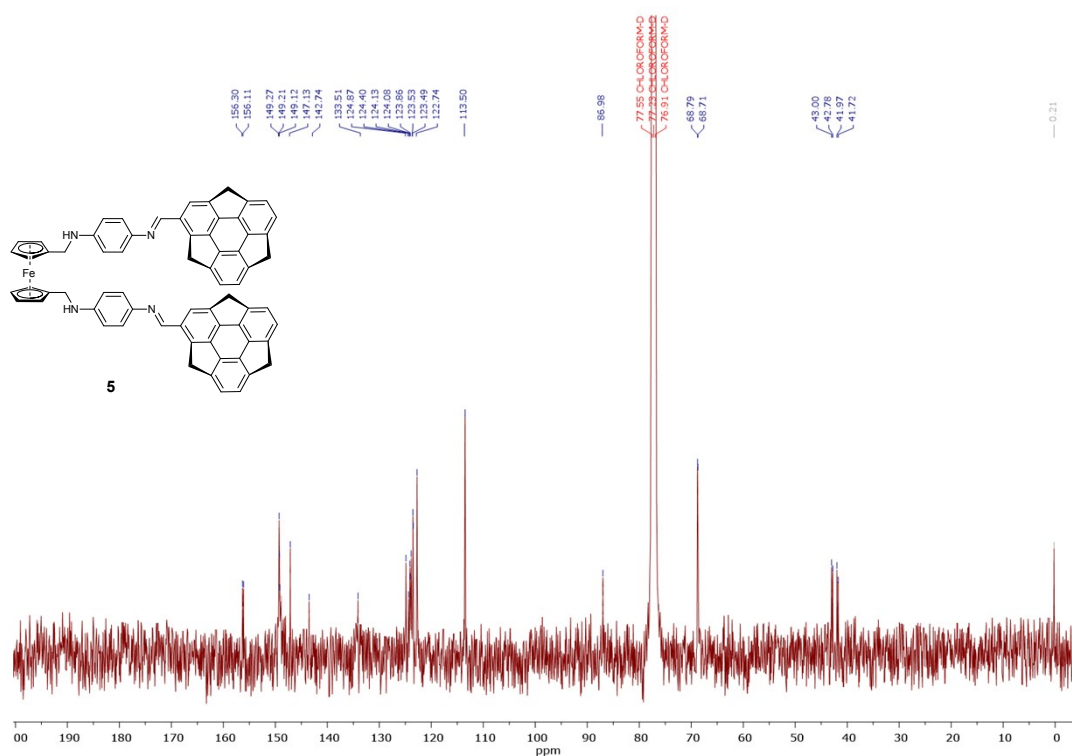


Fig. S13. ^{13}C NMR (CDCl₃, 100 MHz) spectrum of compound **5**.

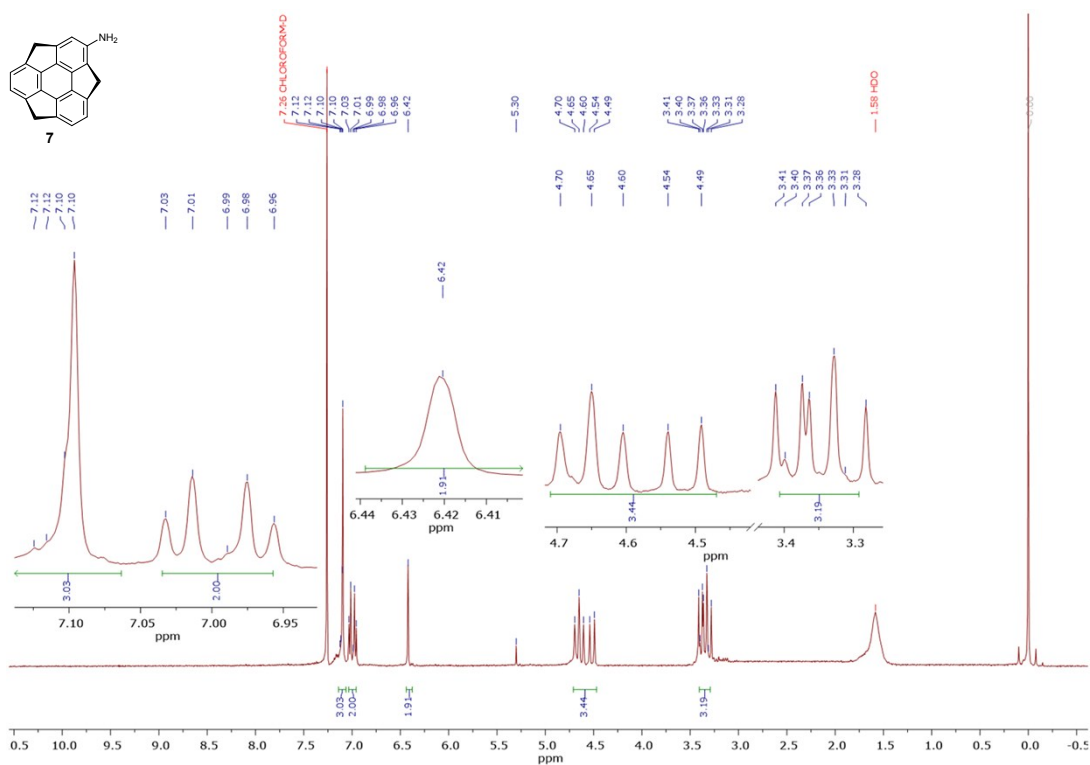


Fig. S14. ^1H NMR (CDCl₃, 400 MHz) spectrum of compound **7**.

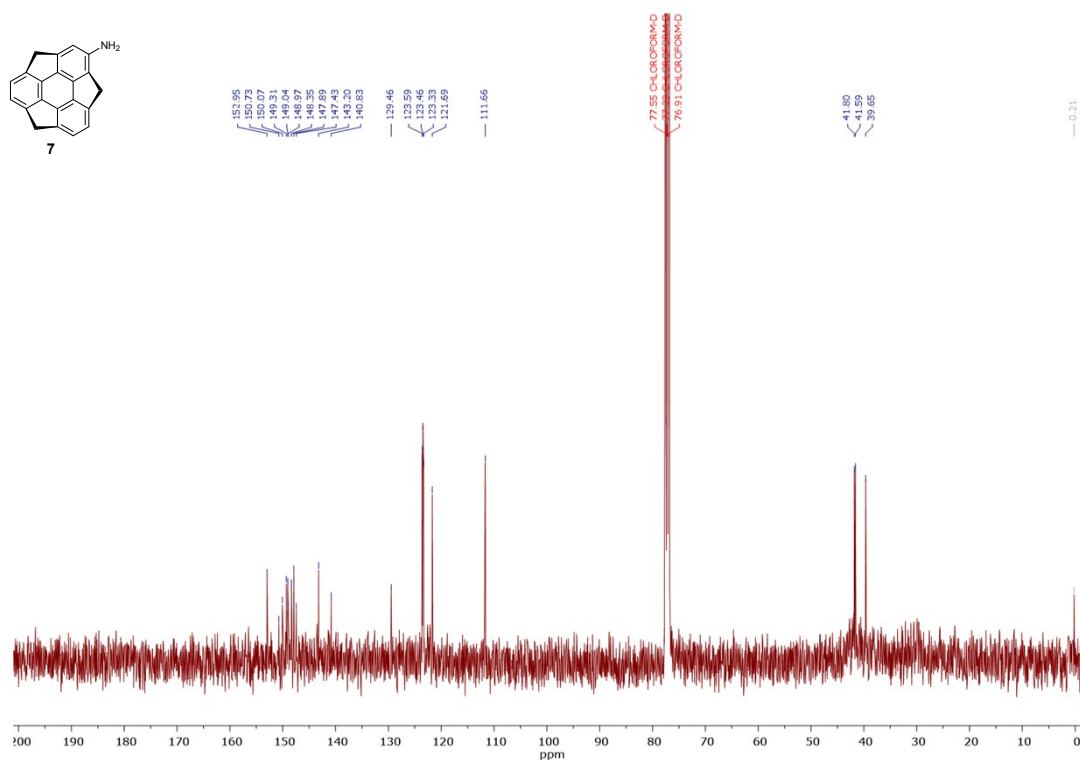


Fig. S15. ^{13}C NMR (CDCl_3 , 100 MHz) spectrum of compound **7**.

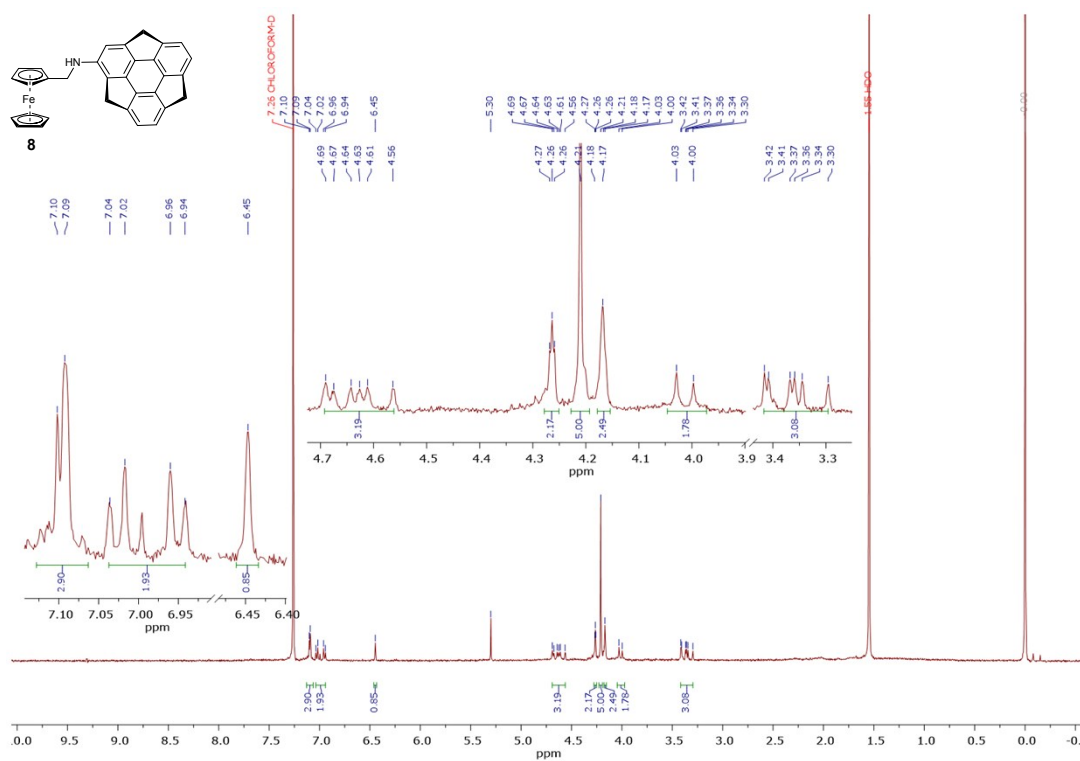


Fig. S16. ^1H NMR (CDCl_3 , 400 MHz) spectrum of compound **8**.

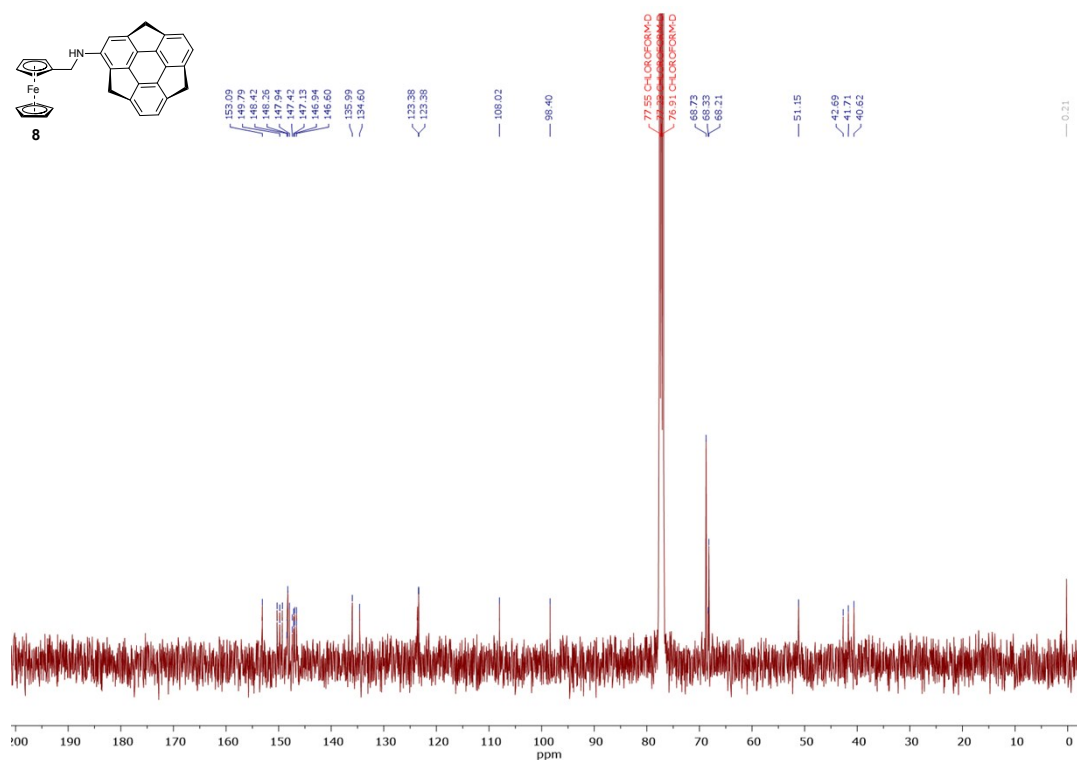


Fig. S17. ¹³C NMR (CDCl₃, 100 MHz) spectrum of compound **8**.

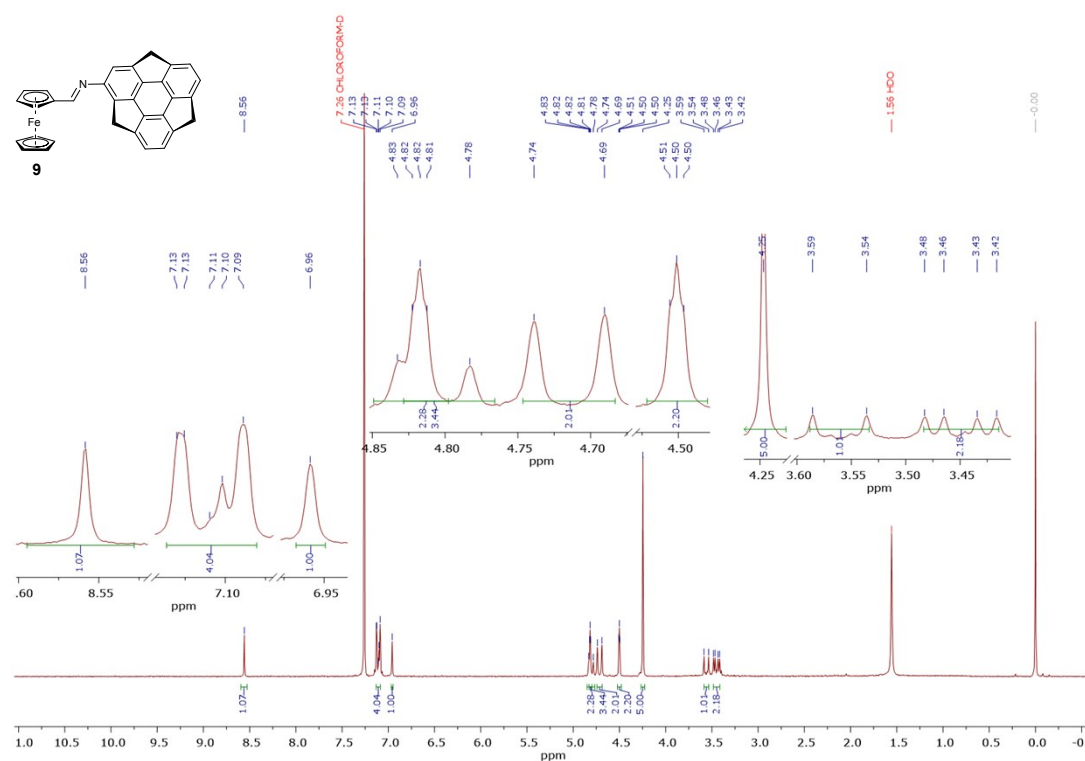


Fig. S18. ¹H NMR (CDCl₃, 400 MHz) spectrum of compound **9**.

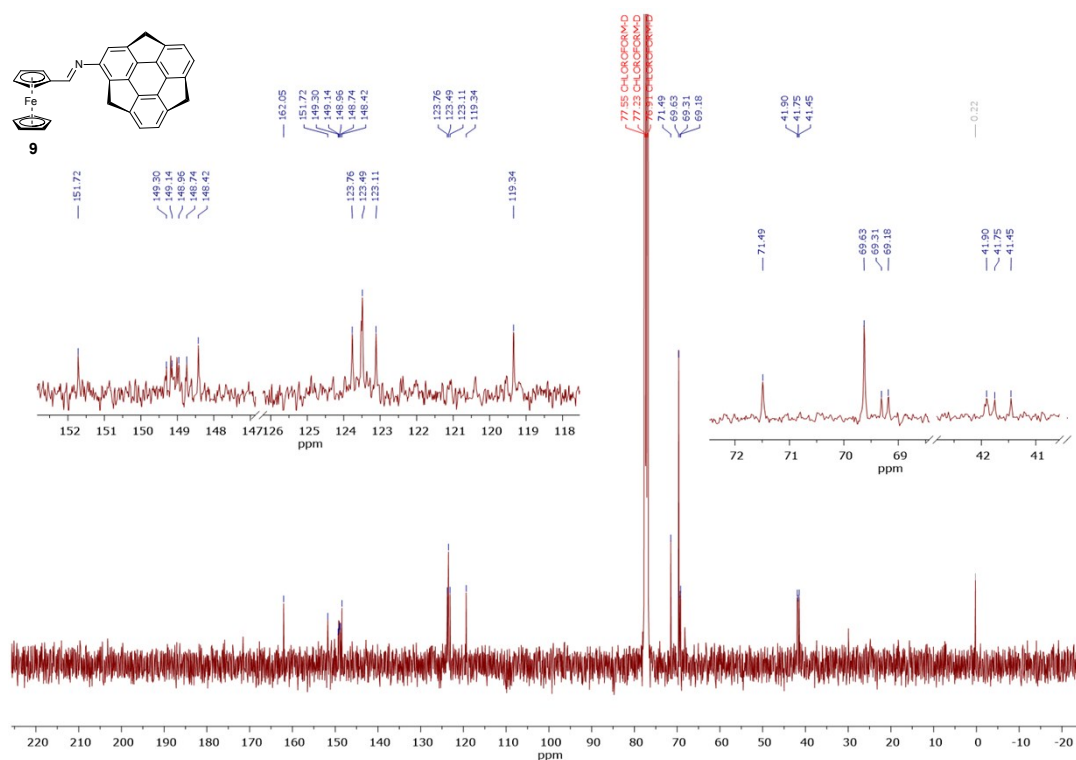


Fig. S19. ¹³C NMR (CDCl₃, 100 MHz) spectrum of compound **9**.

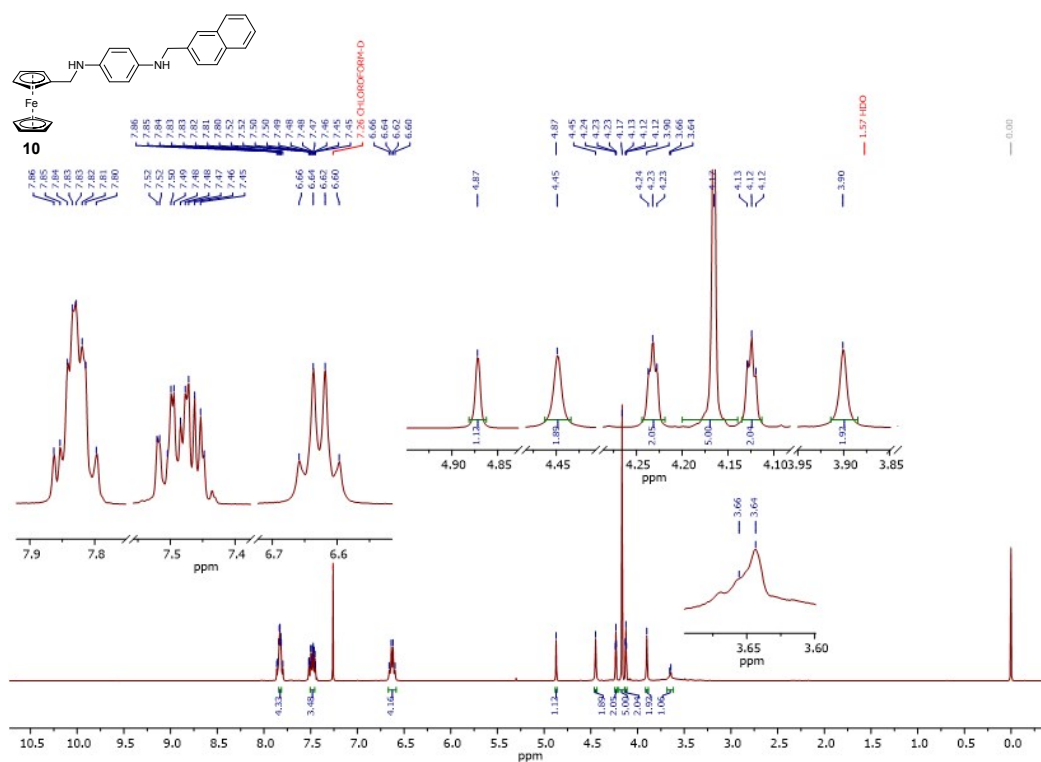


Fig. S20. ¹H NMR (CDCl₃, 400 MHz) spectrum of compound **10**.

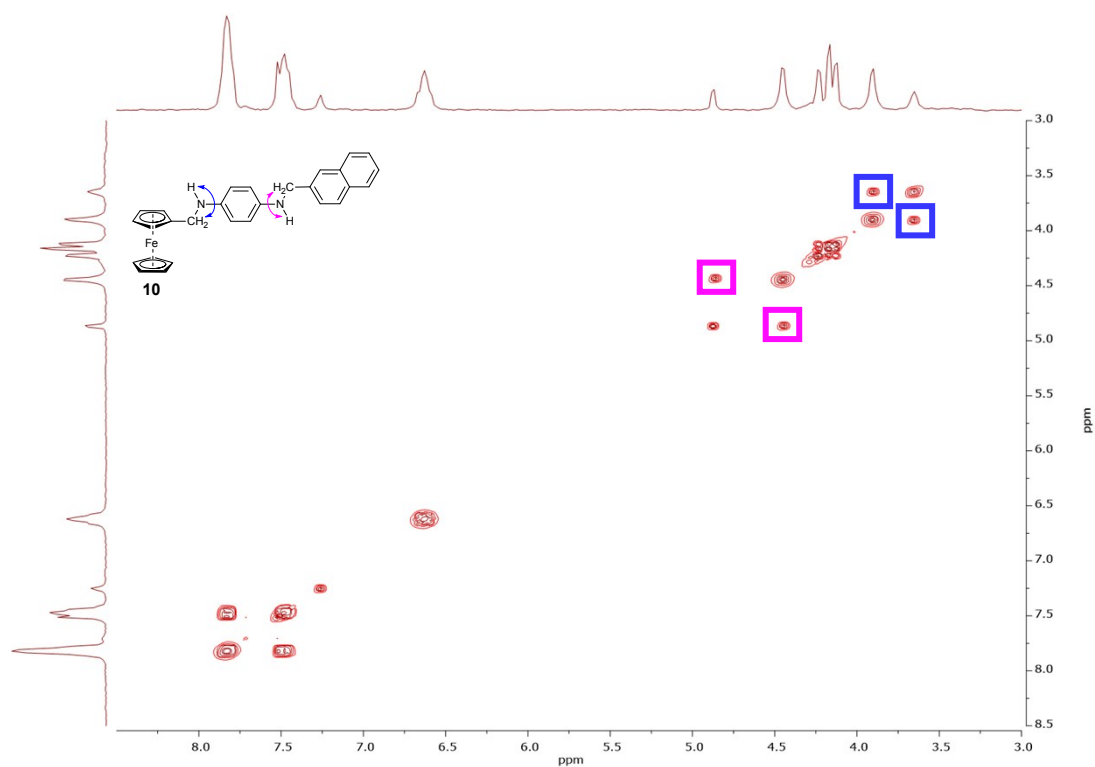


Fig. S21. ^1H - ^1H COSY NMR (CDCl_3 , 400 MHz) spectrum of compound **10**. The crucial cross correlations are also marked.

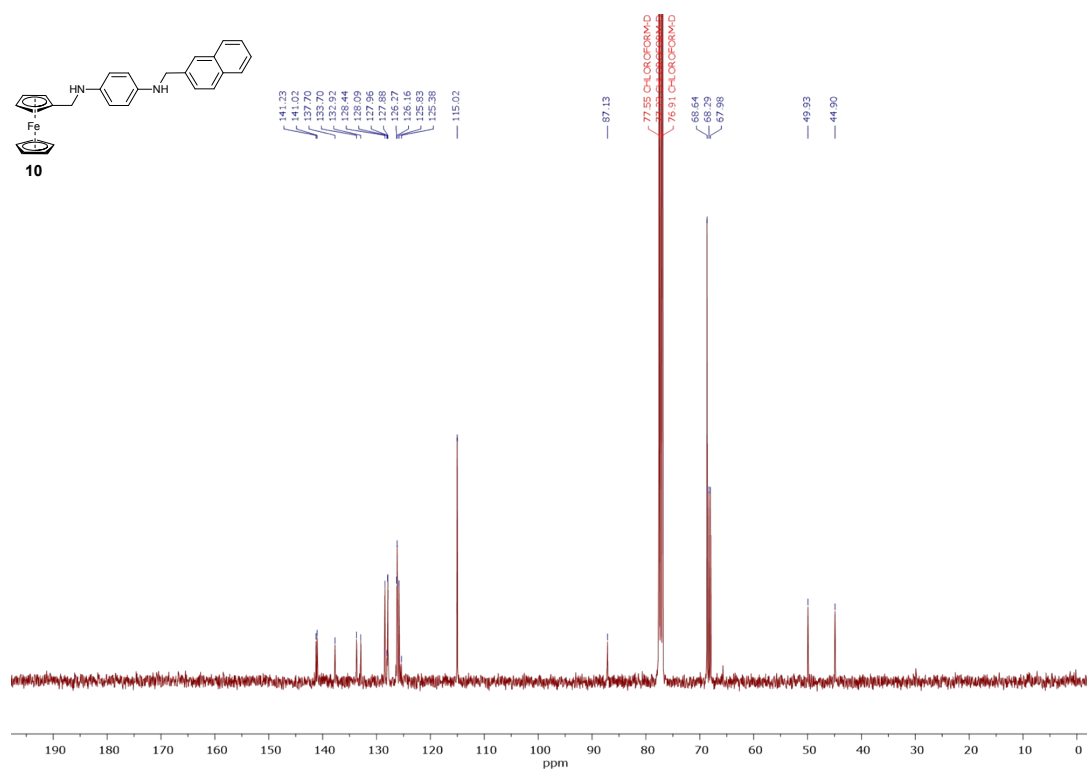


Fig. S22. ^{13}C NMR (CDCl_3 , 100 MHz) spectrum of compound **10**.

S3. IR spectra

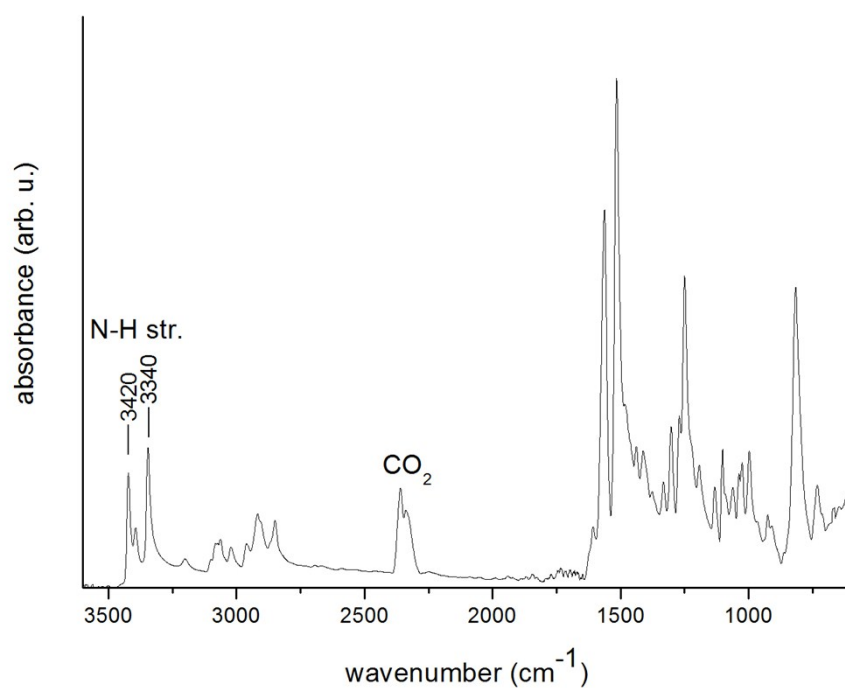
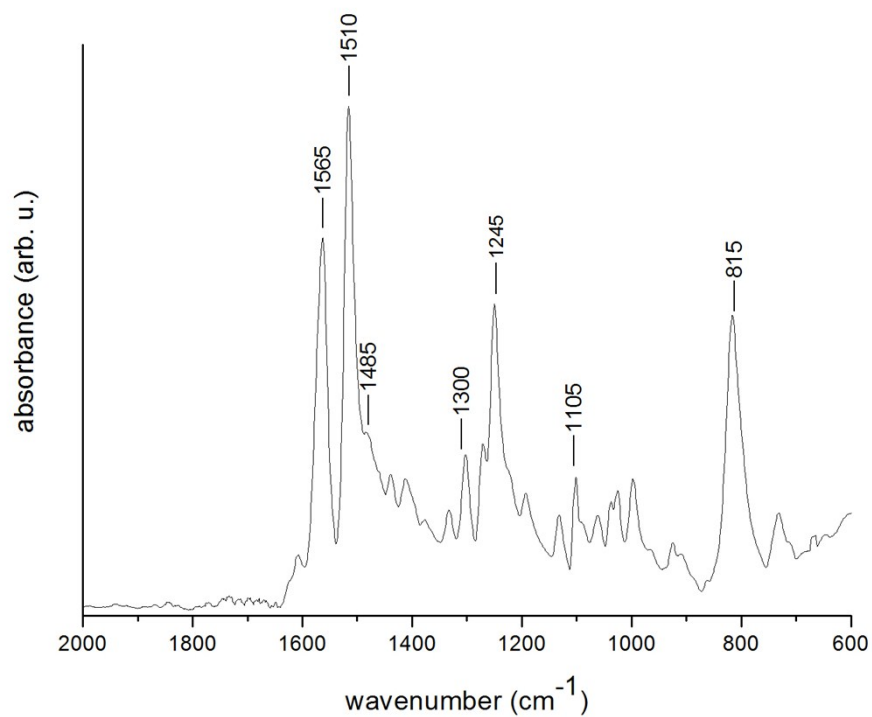


Fig. S23. IR (ATR) spectrum of compound **Fc-5** in the wavenumber range of 2000-600 cm^{-1} (**top**) and in the range of 3600-600 cm^{-1} showing NH stretching vibrations (**bottom**).

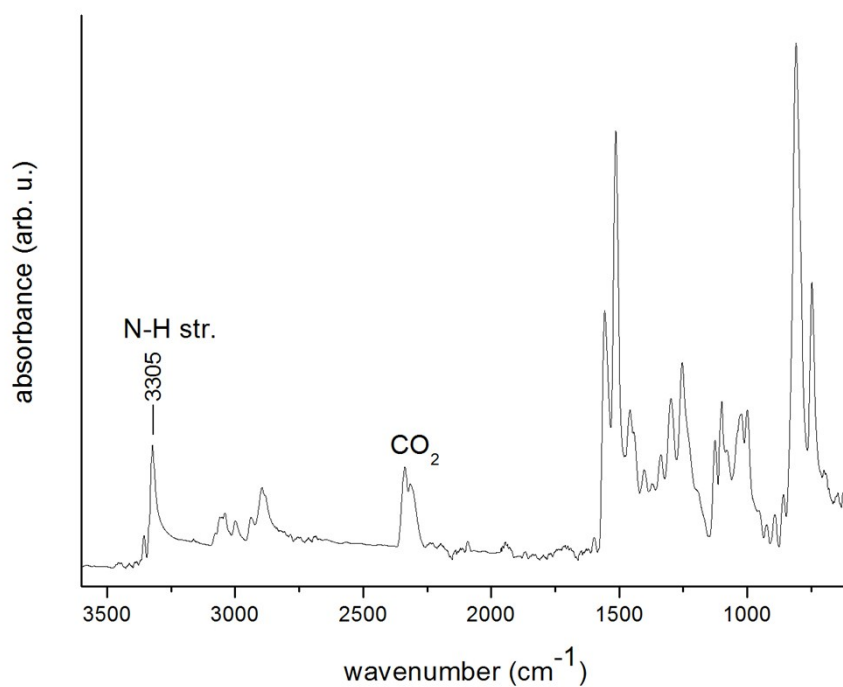
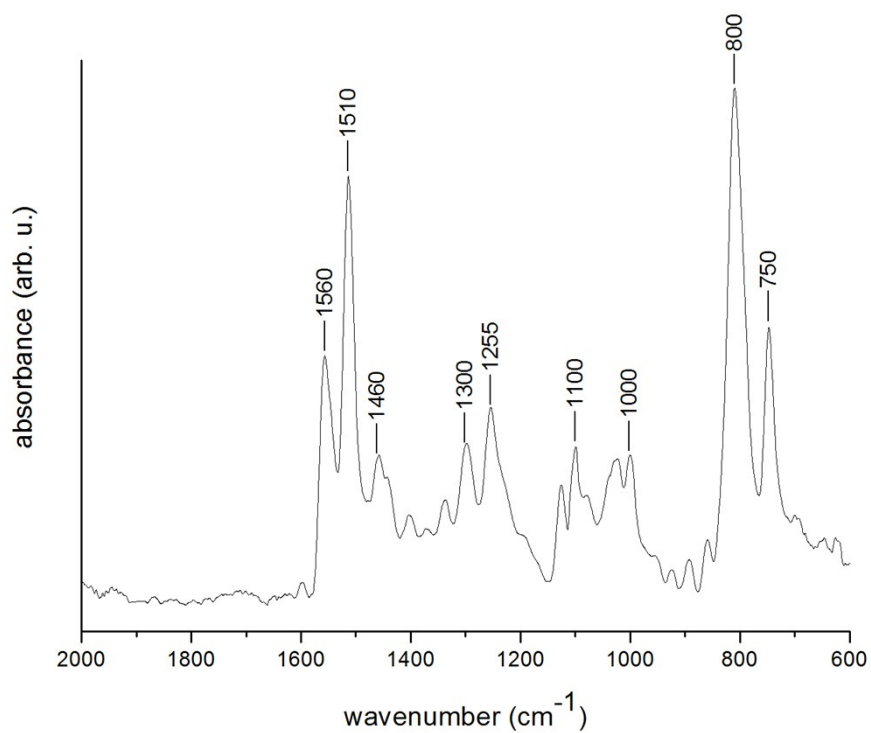


Fig. S24. IR (ATR) spectrum of compound **3** in the wavenumber range of 2000-600 cm⁻¹ (**top**) and in the range of 3600-600 cm⁻¹ showing NH stretching vibrations (**bottom**).

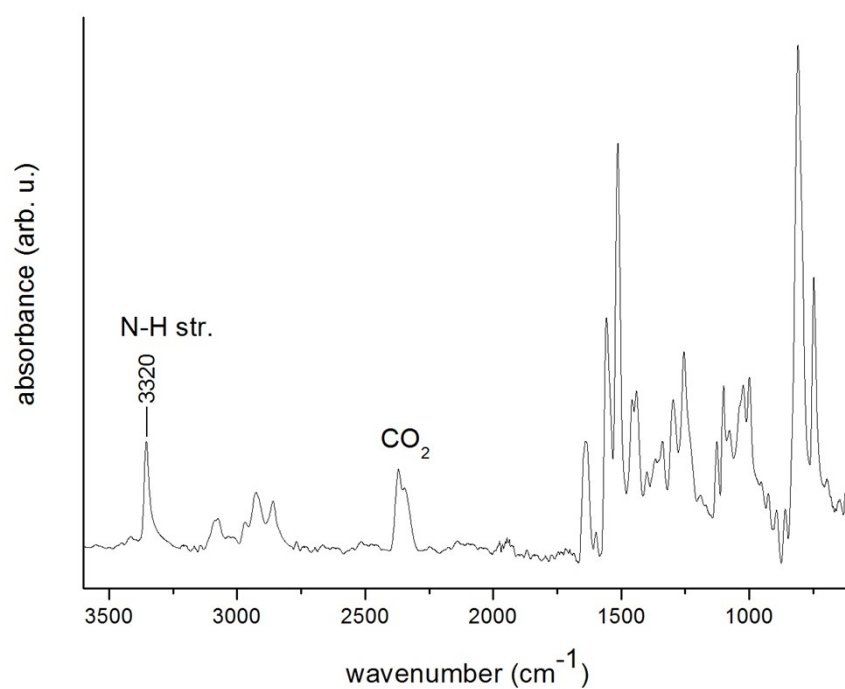
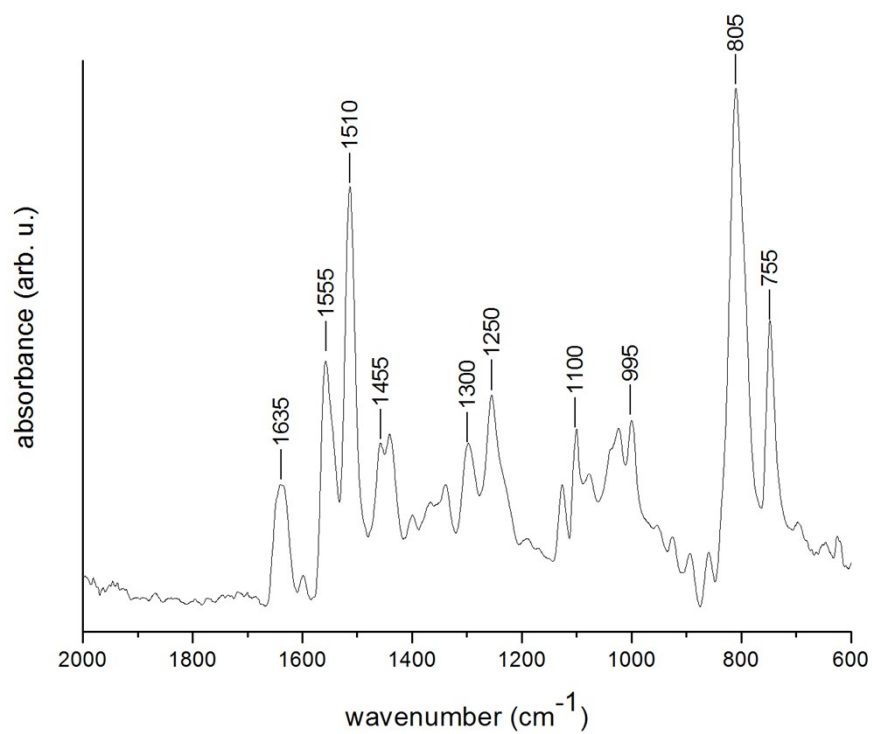


Fig. S25. IR (ATR) spectrum of compound **4** in the wavenumber range of 2000-600 cm⁻¹ (**top**) and in the range of 3600-600 cm⁻¹ showing NH stretching vibrations (**bottom**).

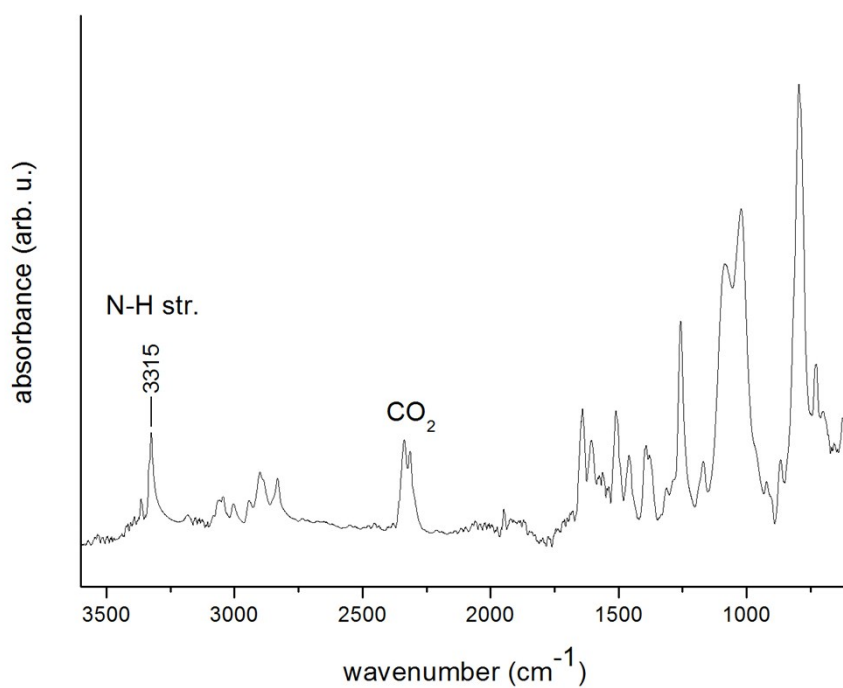
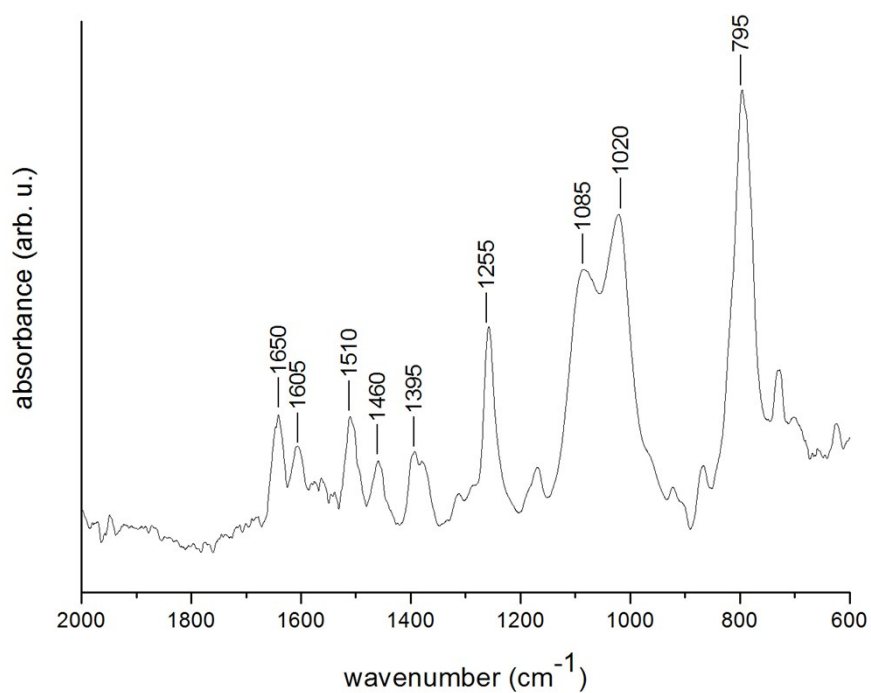


Fig. S26. IR (ATR) spectrum of compound **5** in the wavenumber range of 2000-600 cm⁻¹ (**top**) and in the range of 3600-600 cm⁻¹ showing NH stretching vibrations (**bottom**).

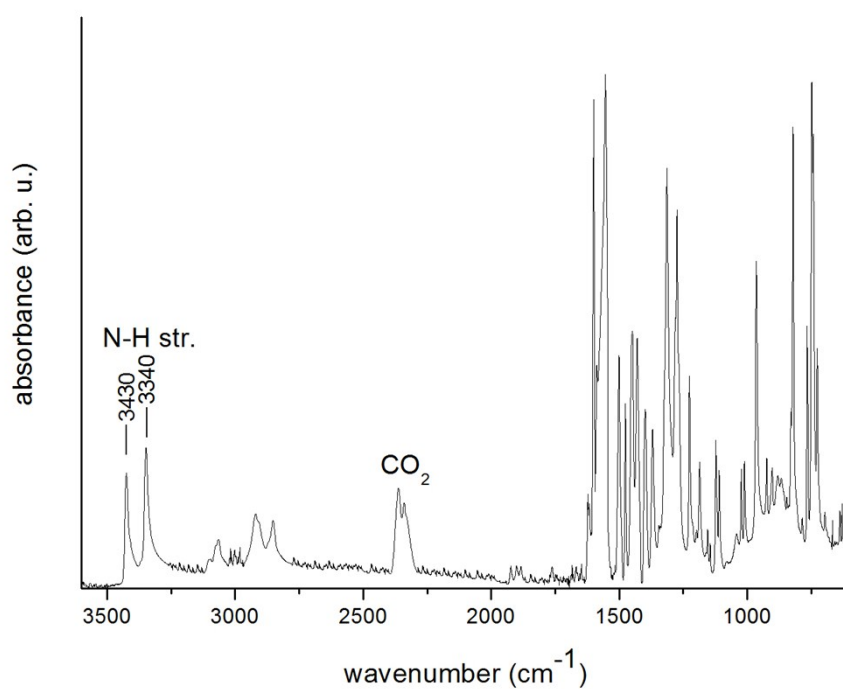
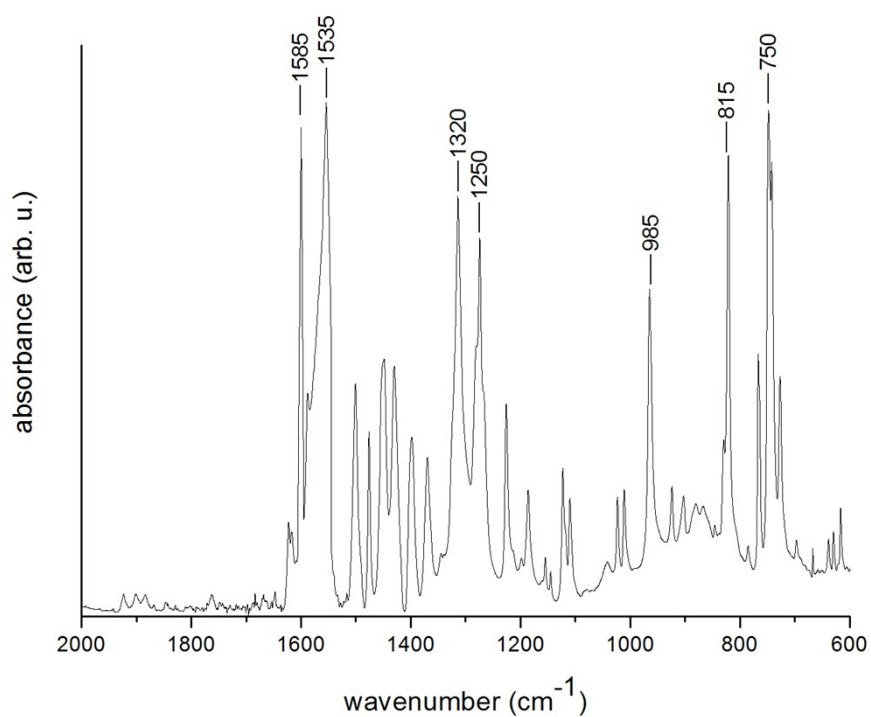


Fig. S27. IR (ATR) spectrum of aminosumanene (**7**) in the wavenumber range of 2000-600 cm⁻¹ (**top**) and in the range of 3600-600 cm⁻¹ showing NH stretching vibrations (**bottom**).

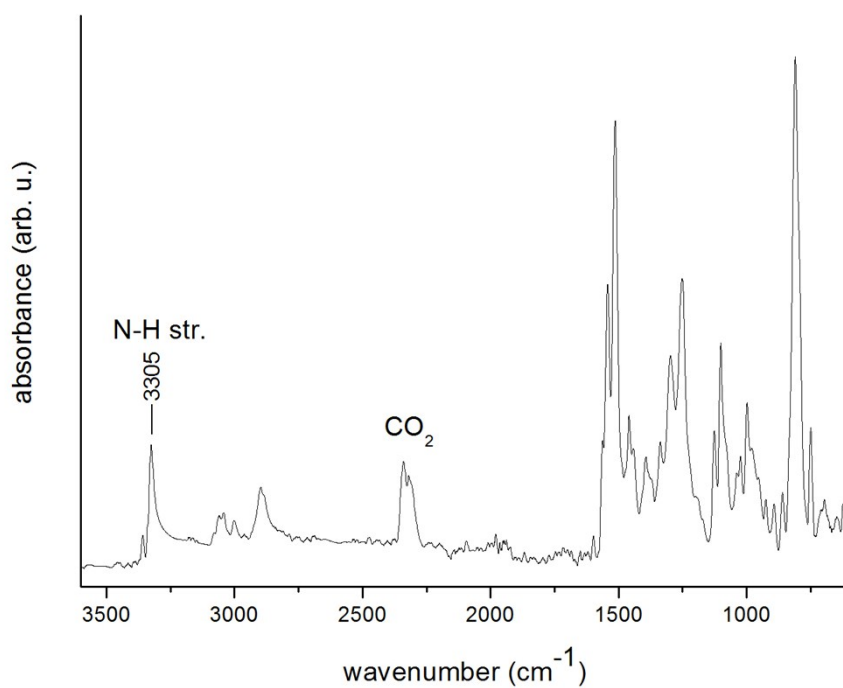
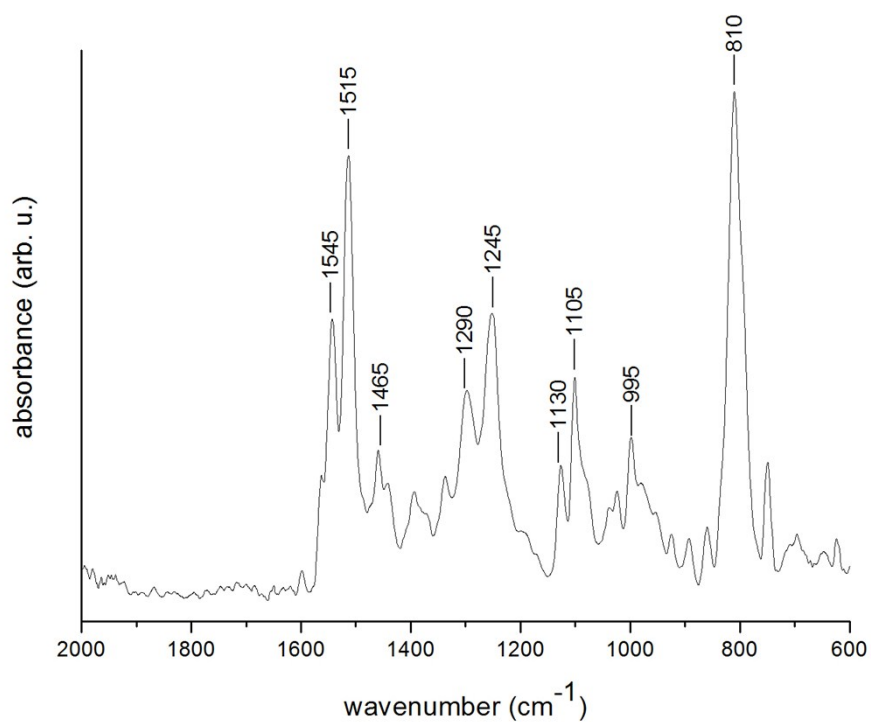


Fig. S28. IR (ATR) spectrum of compound **8** in the wavenumber range of 2000-600 cm⁻¹ (**top**) and in the range of 3600-600 cm⁻¹ showing NH stretching vibrations (**bottom**).

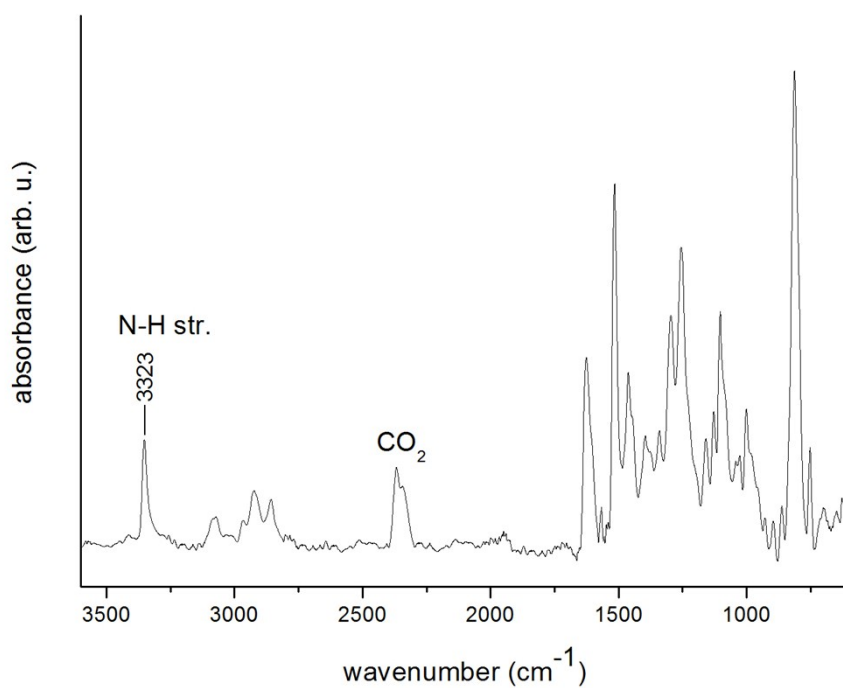
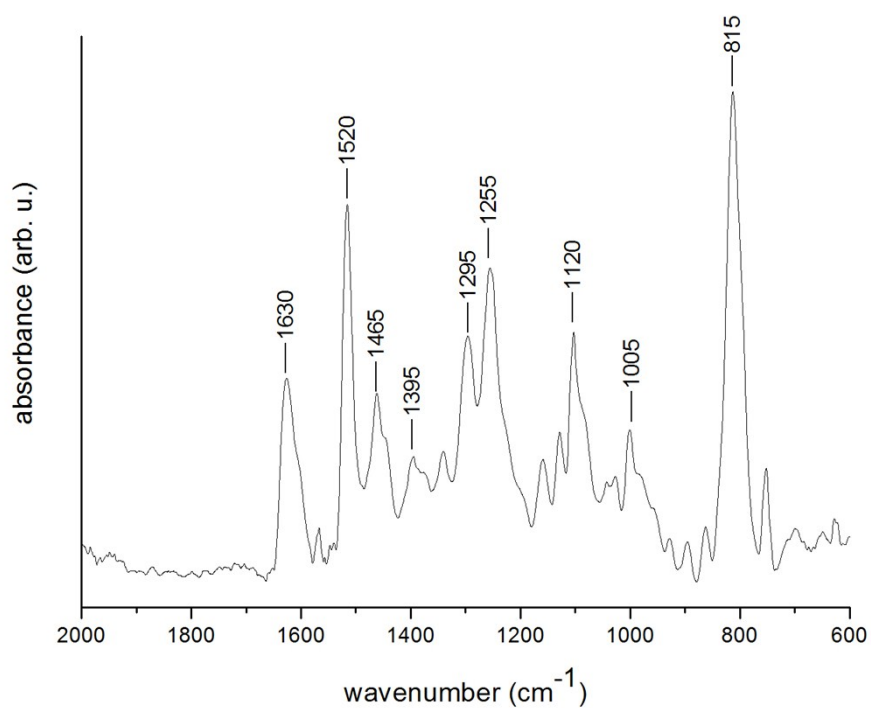


Fig. S29. IR (ATR) spectrum of compound **9** in the wavenumber range of 2000-600 cm⁻¹ (**top**) and in the range of 3600-600 cm⁻¹ showing NH stretching vibrations (**bottom**).

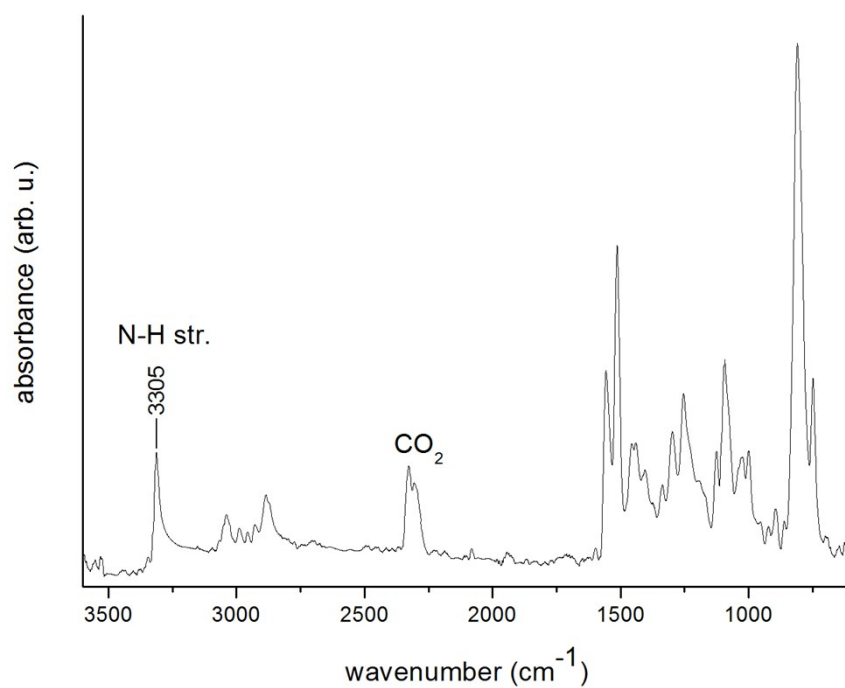
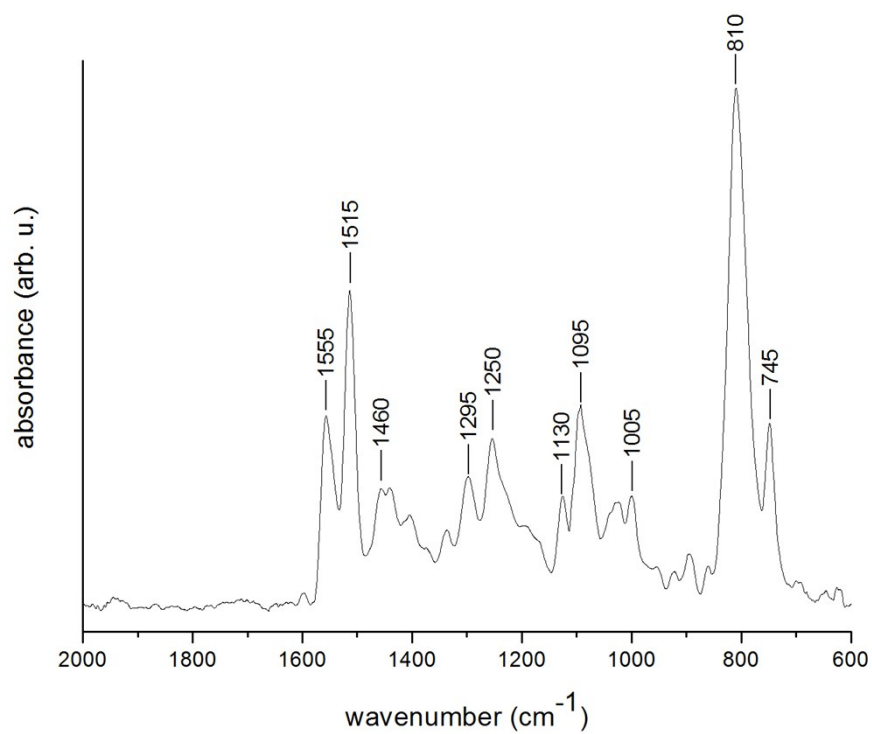


Fig. S30. IR (ATR) spectrum of compound **10** in the wavenumber range of 2000-600 cm^{-1} (**top**) and in the range of 3600-600 cm^{-1} showing NH stretching vibrations (**bottom**).

S4. UV-Vis spectra

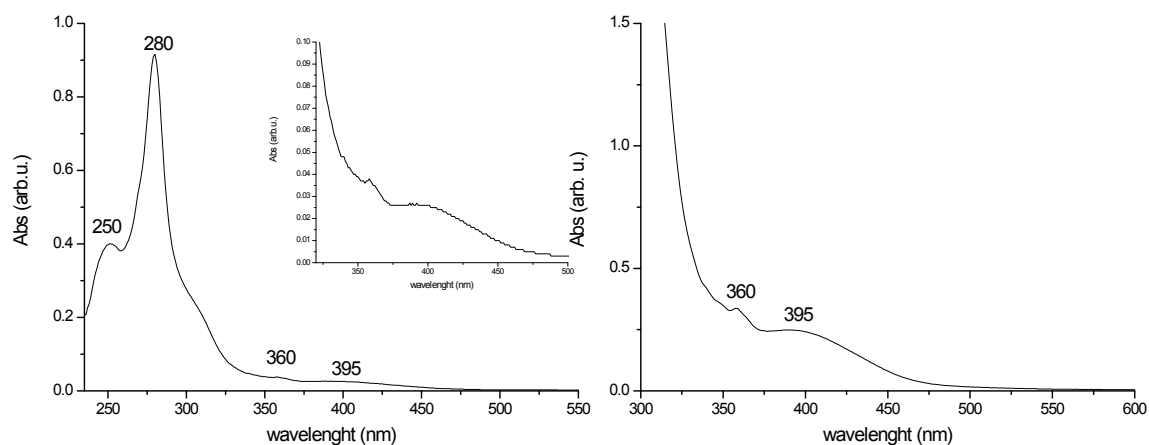


Fig. S31. UV-Vis spectra of compound **3** (solvent: CHCl₃:MeOH = 1:1 v/v; concentration: 1·10⁻⁵ M (left), 1·10⁻⁴ M (right)).

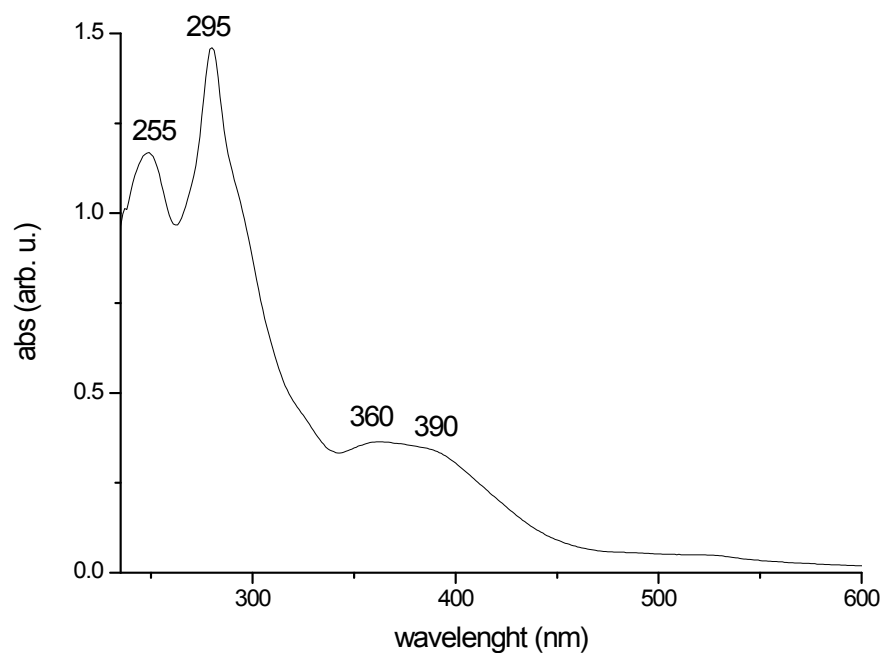


Fig. S32. UV-Vis spectrum of compound **4** (solvent: CHCl₃:MeOH = 1:1 v/v; concentration: 1·10⁻⁴ M).

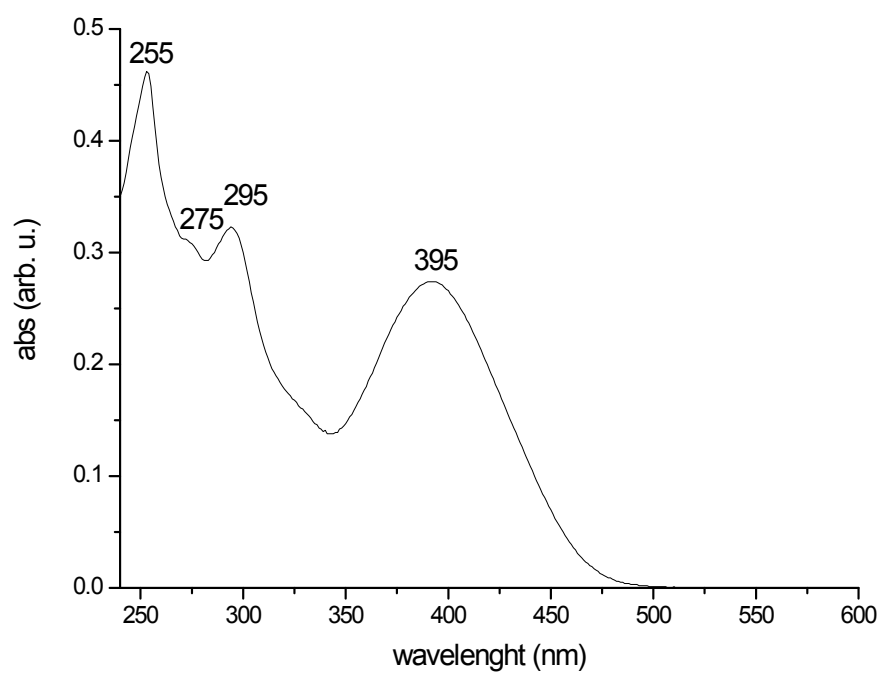


Fig. S33. UV-Vis spectrum of compound **5** (solvent: $\text{CHCl}_3\text{:MeOH} = 1\text{:}1$ v/v; concentration: $1 \cdot 10^{-5}$ M).

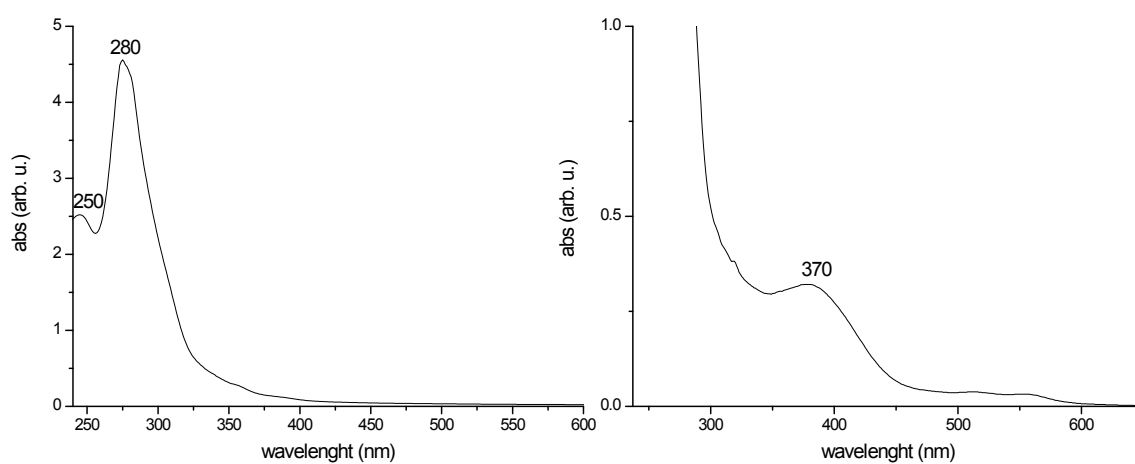


Fig. S34. UV-Vis spectra of compound **8** (solvent: $\text{CHCl}_3\text{:MeOH} = 1\text{:}1$ v/v; $1 \cdot 10^{-5}$ M (left), $1 \cdot 10^{-4}$ M (right)).

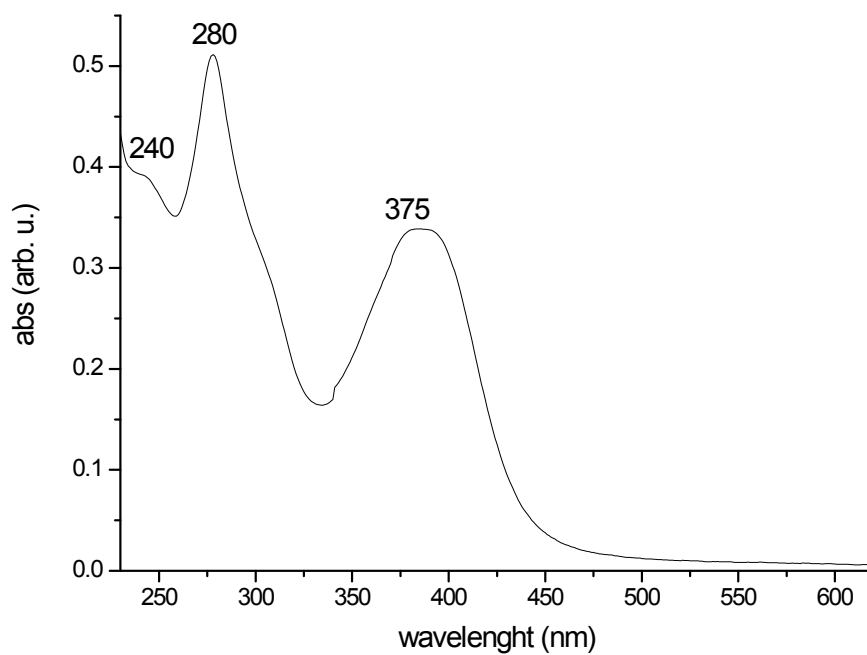


Fig. S35. UV-Vis spectrum of compound **9** (solvent: CHCl_3 :MeOH = 1:1 v/v; concentration: $1 \cdot 10^{-4}$ M).

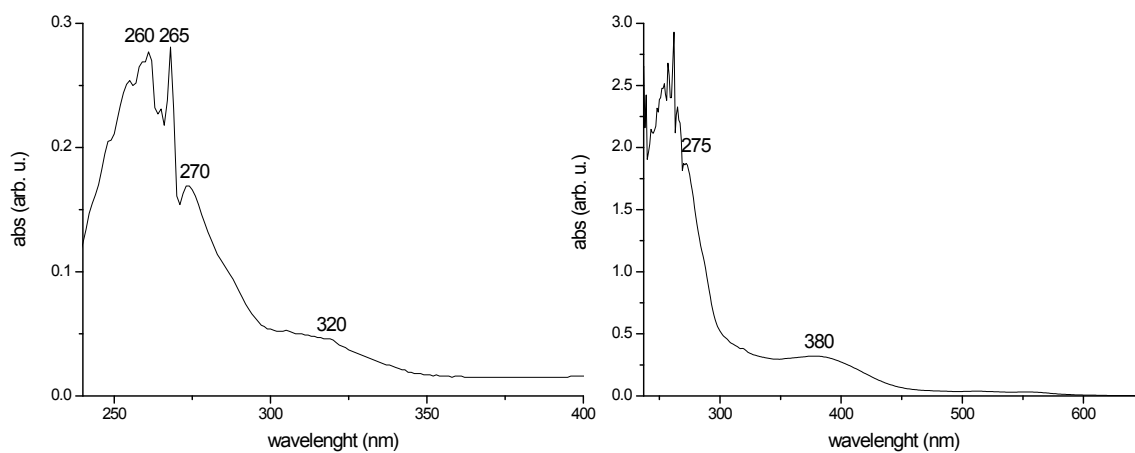


Fig. S36. UV-Vis spectra of compound **10** (solvent: CHCl_3 :MeOH = 1:1 v/v; concentration: $1 \cdot 10^{-5}$ M (left), $1 \cdot 10^{-4}$ M (right)).

S5. Fluorescence spectroscopy and titration experiments

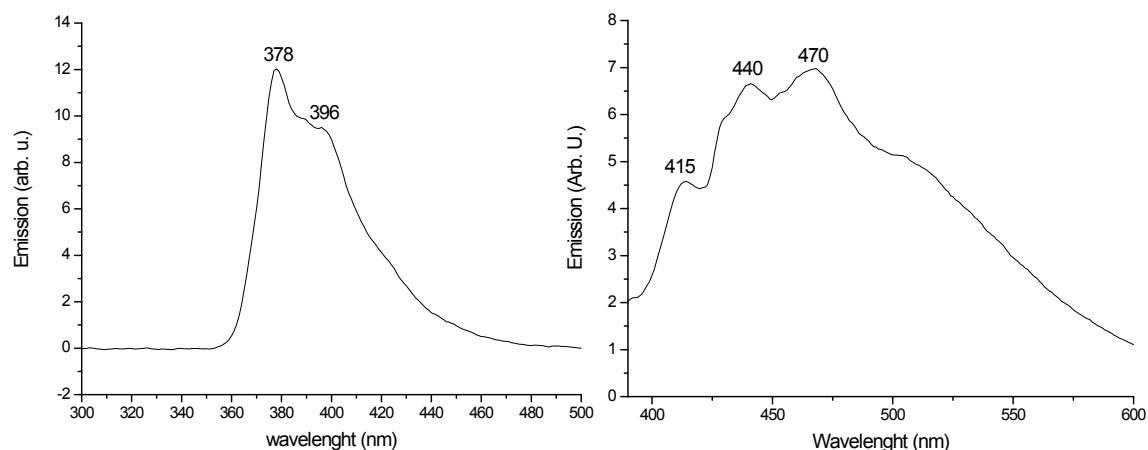


Fig. S37. Emission spectra of compound **3** (solvent: $\text{CHCl}_3:\text{MeOH} = 1:1$ v/v; concentration: $1 \cdot 10^{-4}$ M; excitation wavelength: 280 nm (left), 380 nm (right)).

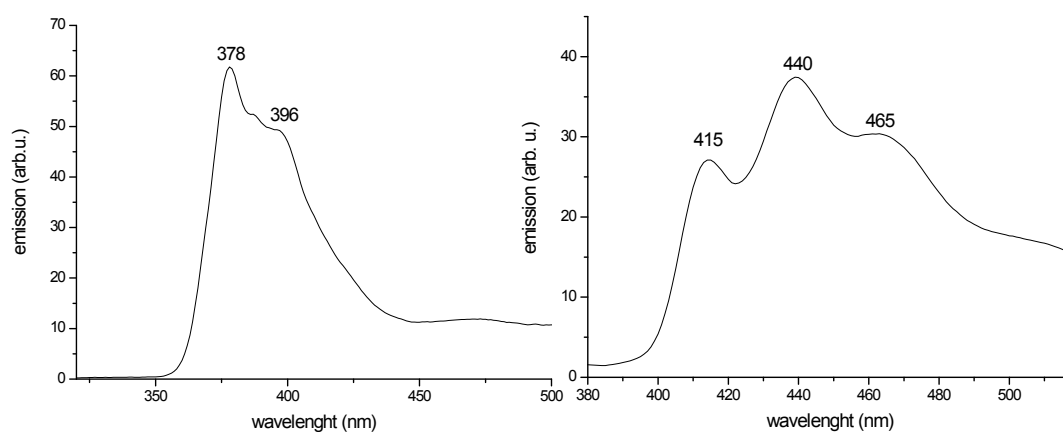


Fig. S38. Emission spectra of compound **4** (solvent: $\text{CHCl}_3:\text{MeOH} = 1:1$ v/v; concentration: $1 \cdot 10^{-4}$ M; excitation wavelength: 280 nm (left), 380 nm (right)).

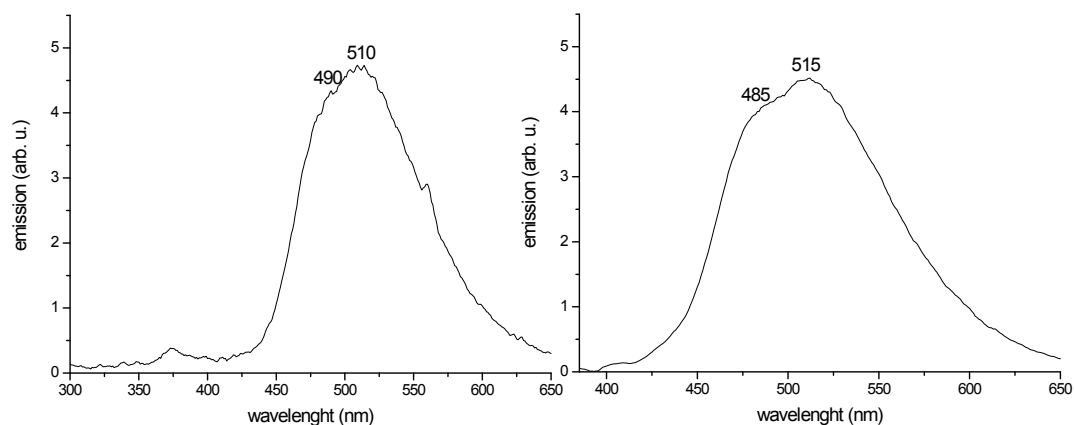


Fig. S39. Emission spectra of compound **5** (solvent: $\text{CHCl}_3\text{:MeOH} = 1\text{:}1$ v/v; concentration: $1 \cdot 10^{-4}$ M; excitation wavelength: 280 nm (left), 380 nm (right)).

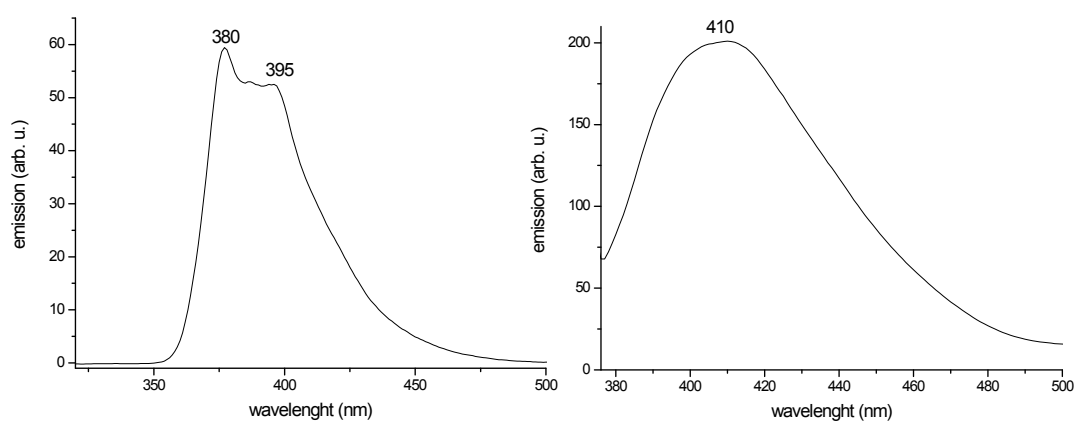


Fig. S40. Emission spectrum of compound **8** (solvent: $\text{CHCl}_3\text{:MeOH} = 1\text{:}1$ v/v; concentration: $1 \cdot 10^{-4}$ M; excitation wavelength: 280 nm (left), 370 nm (right)).

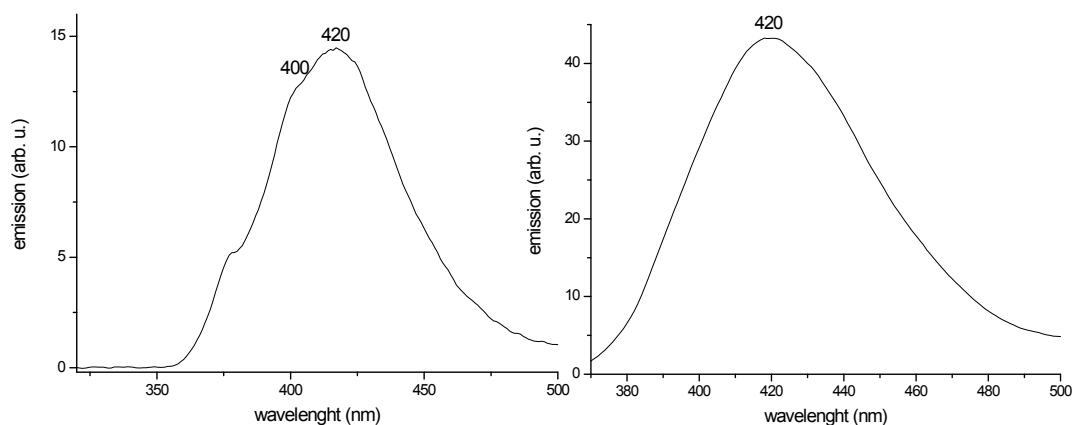


Fig. S41. Emission spectra of compound **9** (solvent: CHCl_3 :MeOH = 1:1 v/v; concentration: $1 \cdot 10^{-4}$ M; excitation wavelength: 280 nm (left), 380 nm (right)).

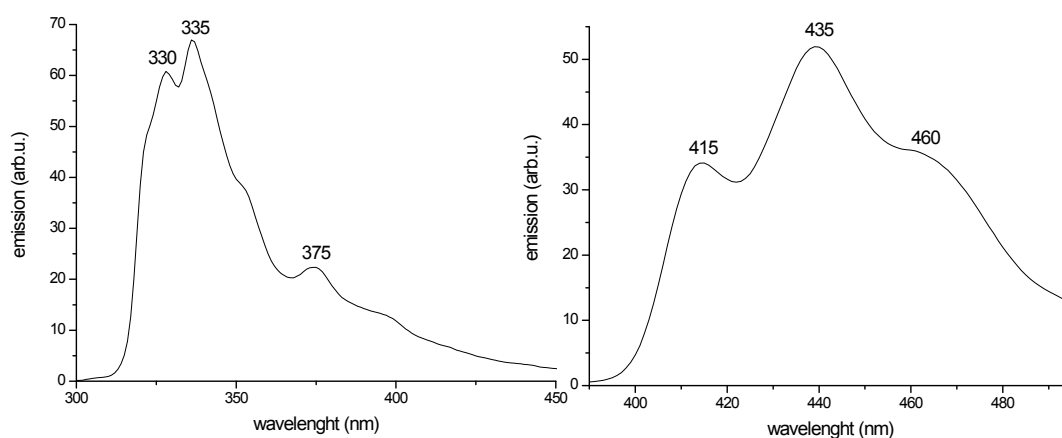


Fig. S42. Emission spectra of compound **10** (solvent: CHCl_3 :MeOH = 1:1 v/v; concentration: $1 \cdot 10^{-4}$ M; excitation wavelength: 280 nm (left), 380 nm (right)).

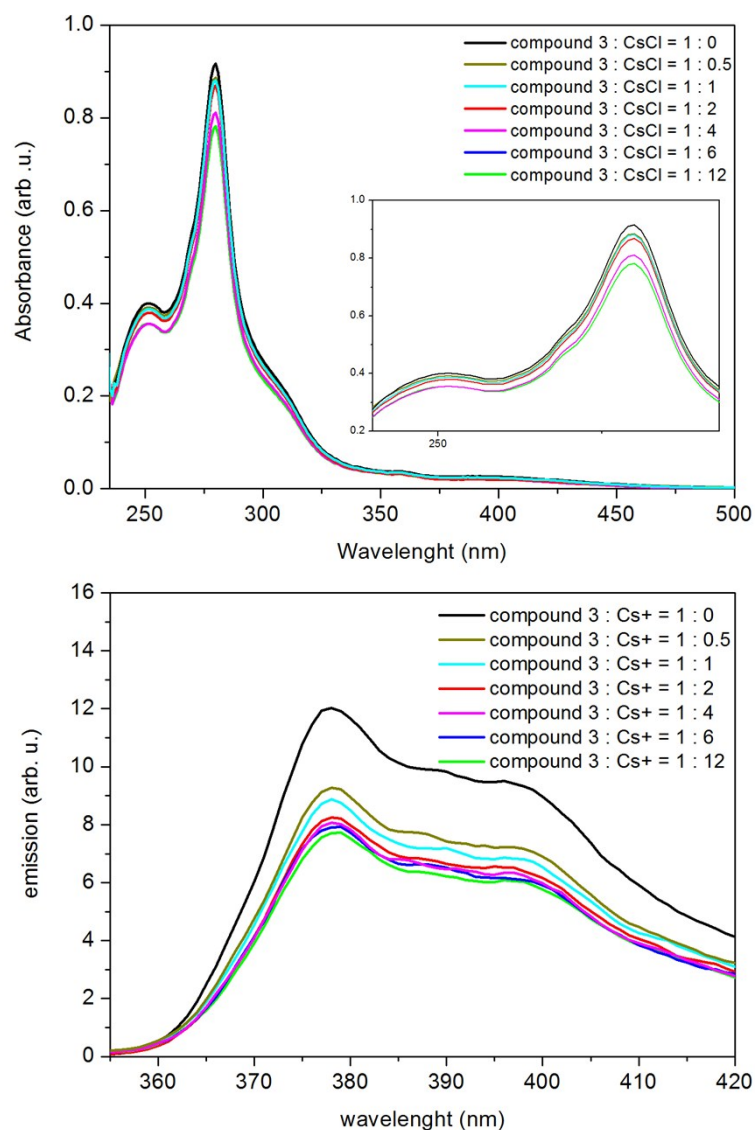


Fig. S43. Comparison between UV-Vis (**top**) or fluorescence (**bottom**) spectra titration methods for caesium cation (Cs^+ ; in the form of CsCl) binding studies with representative compound **3** (solvent: $\text{CHCl}_3\text{:MeOH} = 1\text{:}1$ v/v; compound **3** concentration: $1 \cdot 10^{-4}$ M; excitation wavelength for the fluorescence spectra: 280 nm).

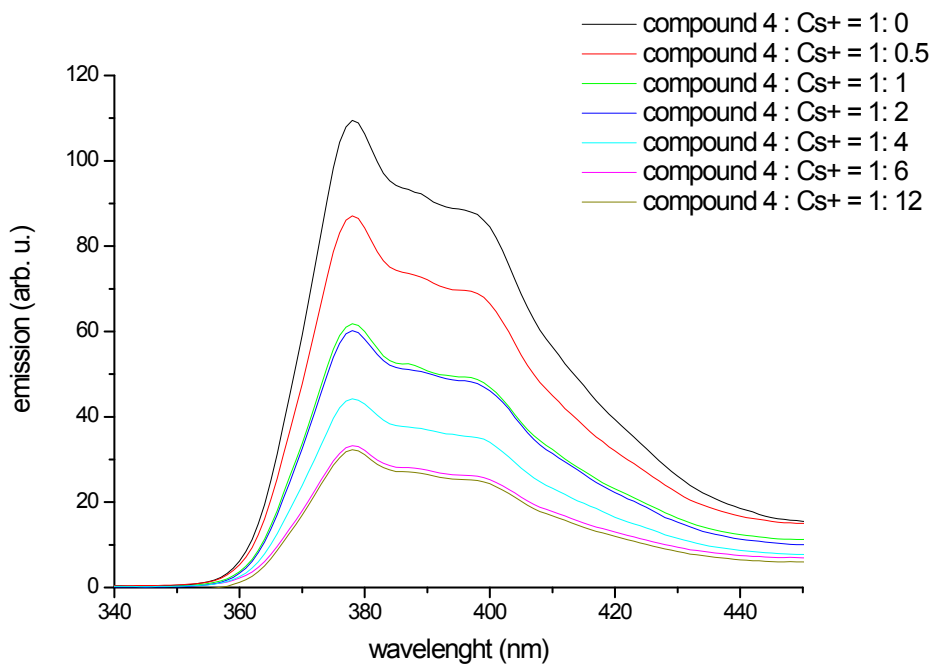


Fig. S44. Caesium cation (Cs⁺; in the form of CsCl) binding studies with compound **4** using the fluorescence spectra titration method (solvent: CHCl₃:MeOH = 1:1 v/v; compound **4** concentration: 1·10⁻⁴ M; excitation wavelength: 280 nm).

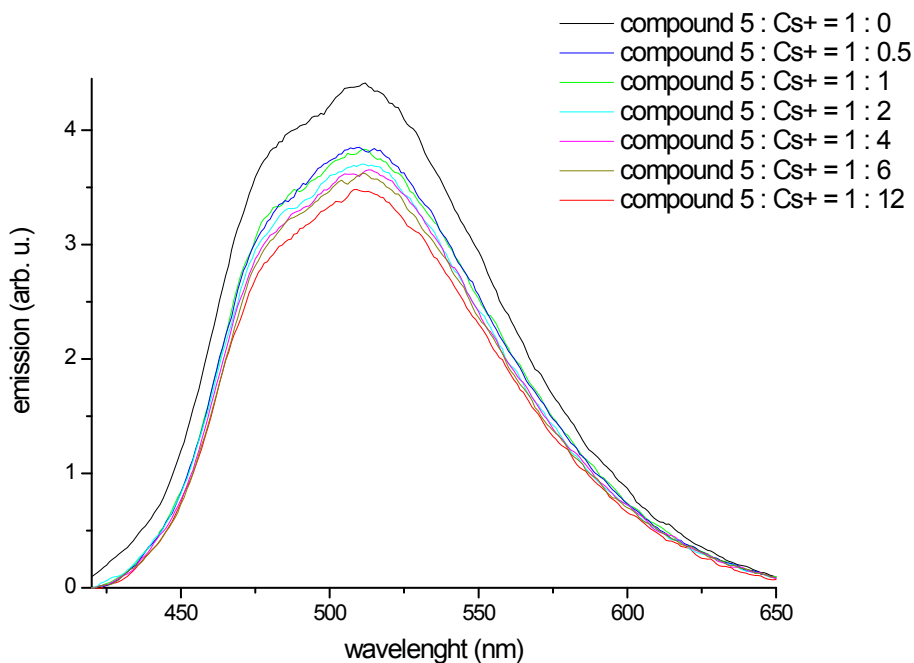


Fig. S45. Caesium cation (Cs⁺; in the form of CsCl) binding studies with compound **5** using the fluorescence spectra titration method (solvent: CHCl₃:MeOH = 1:1 v/v; compound **5** concentration: 1·10⁻⁴ M; excitation wavelength: 280 nm).

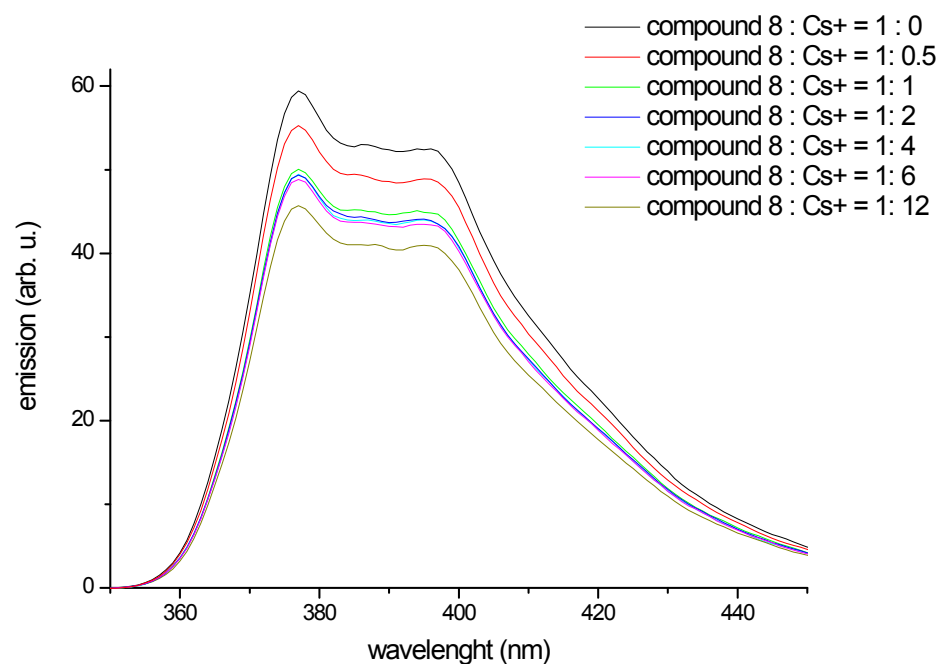


Fig. S46. Caesium cation (Cs⁺; in the form of CsCl) binding studies with compound **8** using the fluorescence spectra titration method (solvent: CHCl₃:MeOH = 1:1 v/v; compound **8** concentration: 1·10⁻⁴ M; excitation wavelength: 280 nm).

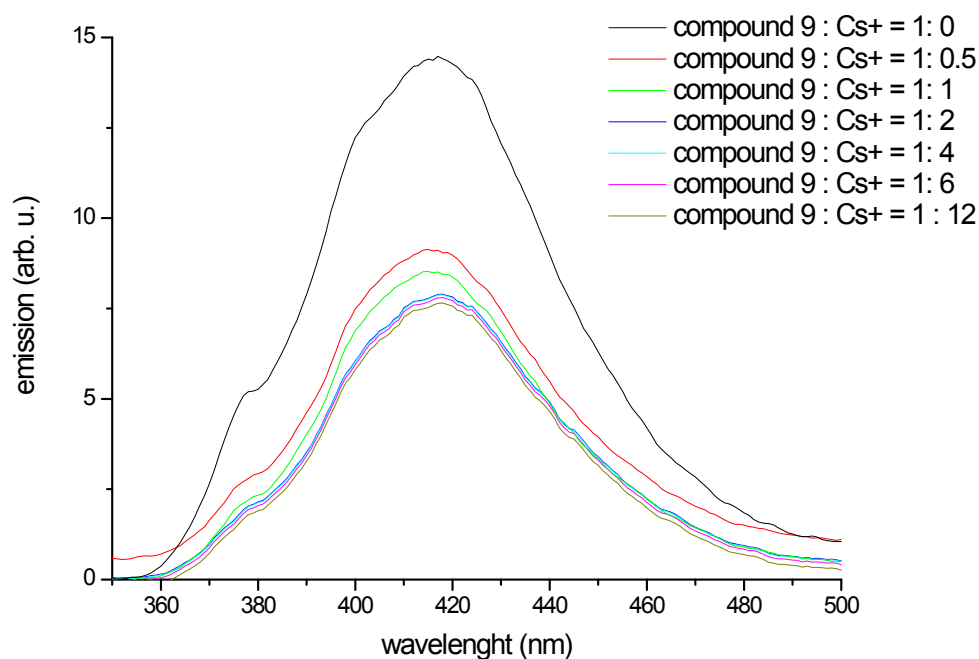


Fig. S47. Caesium cation (Cs⁺; in the form of CsCl) binding studies with compound **9** using the fluorescence spectra titration method (solvent: CHCl₃:MeOH = 1:1 v/v; compound **9** concentration: 1·10⁻⁴ M; excitation wavelength: 280 nm).

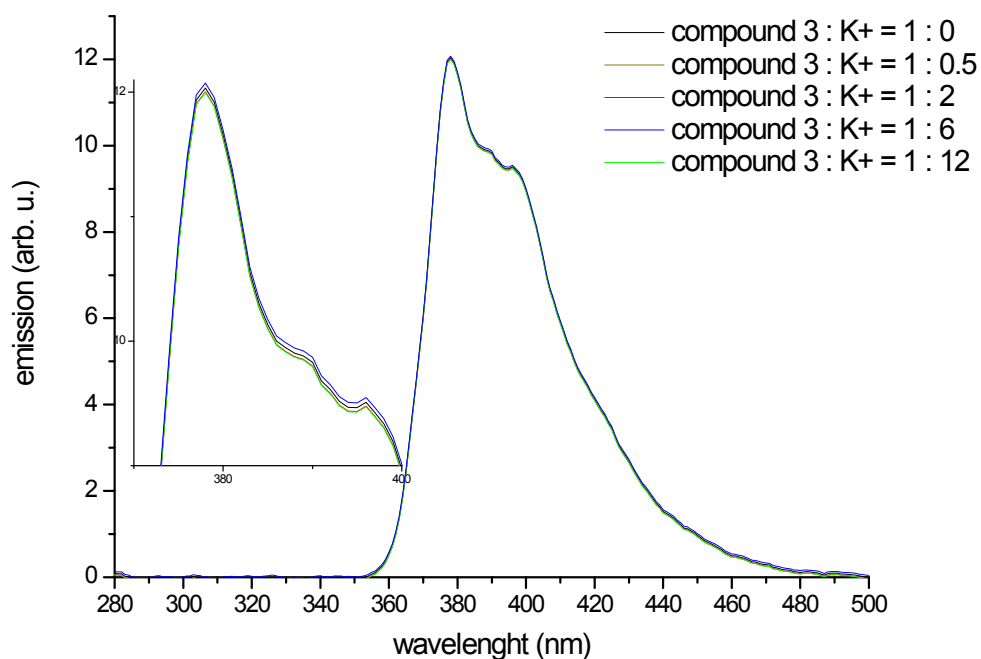


Fig. S48. Potassium cation (K⁺; in the form of KCl) binding studies with compound **3** using the fluorescence spectra titration method (solvent: CHCl₃:MeOH = 1:1 v/v; compound **3** concentration: 1·10⁻⁴ M; excitation wavelength: 280 nm).

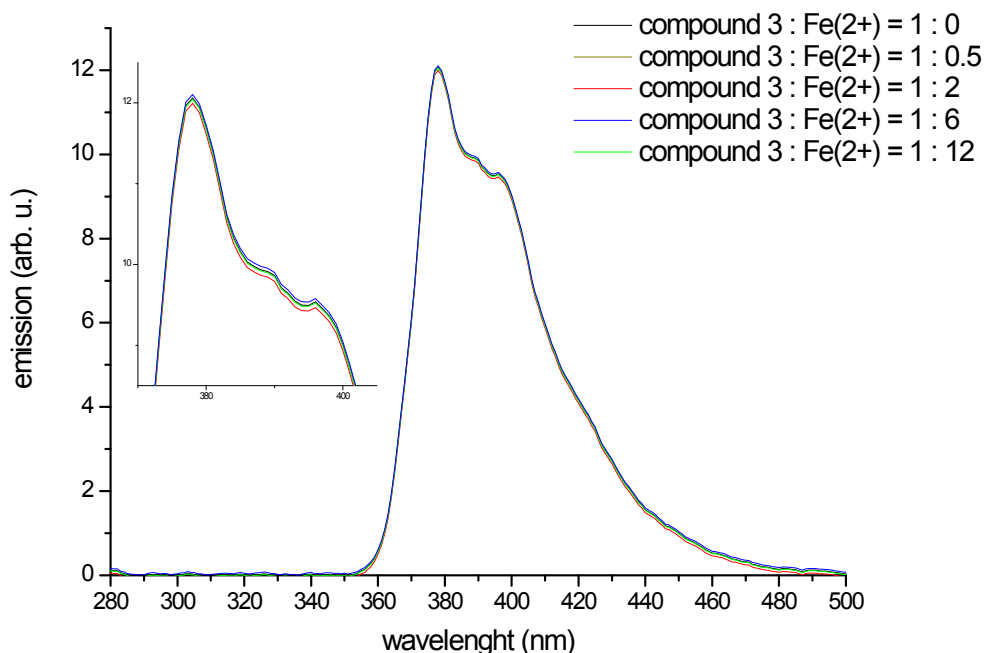


Fig. S49. Iron cation (Fe²⁺; in the form of FeCl₂) binding studies with compound **3** using the fluorescence spectra titration method (solvent: CHCl₃:MeOH = 1:1 v/v; compound **3** concentration: 1·10⁻⁴ M; excitation wavelength: 280 nm).

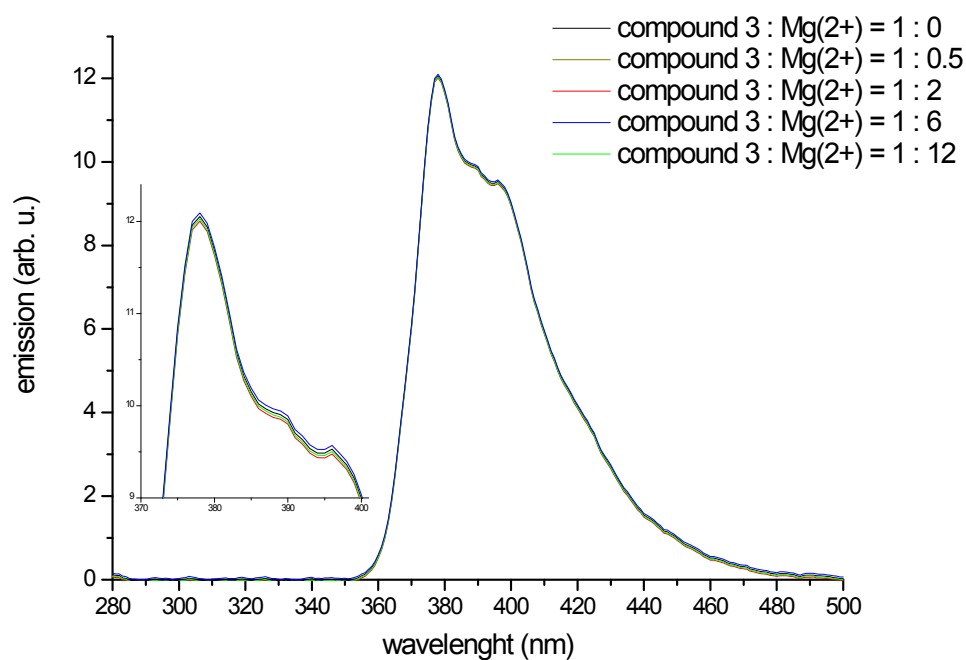


Fig. S50. Magnesium cation (Mg^{2+} ; in the form of $MgCl_2$) binding studies with compound **3** using the fluorescence spectra titration method (solvent: $CHCl_3$:MeOH = 1:1 v/v; compound **3** concentration: $1 \cdot 10^{-4}$ M; excitation wavelength: 280 nm).

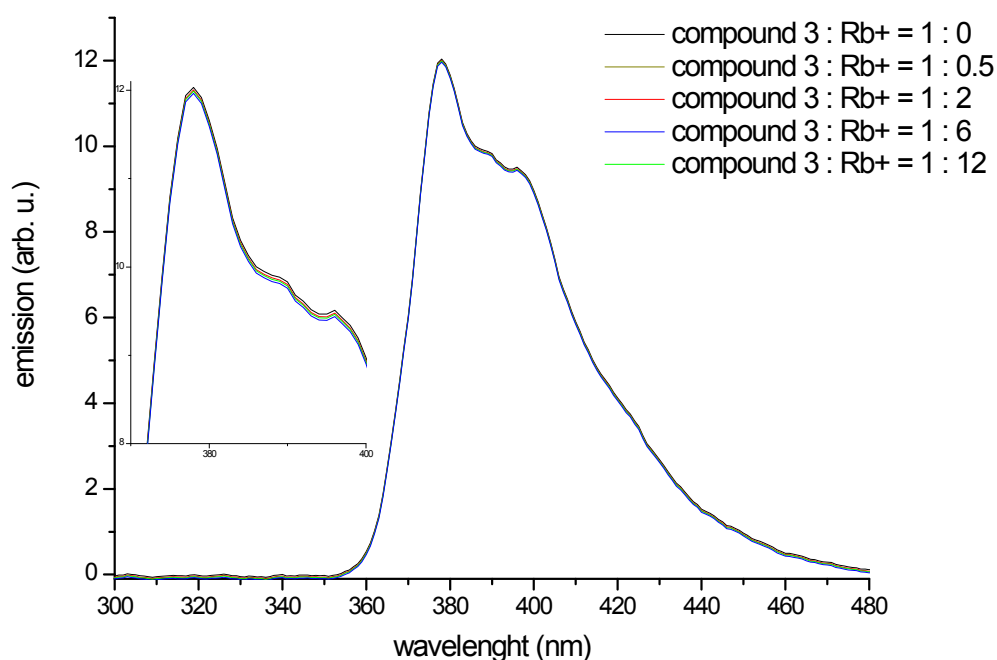


Fig. S51. Rubidium cation (Rb^{+} ; in the form of $RbCl$) binding studies with compound **3** using the fluorescence spectra titration method (solvent: $CHCl_3$:MeOH = 1:1 v/v; compound **3** concentration: $1 \cdot 10^{-4}$ M; excitation wavelength: 280 nm).

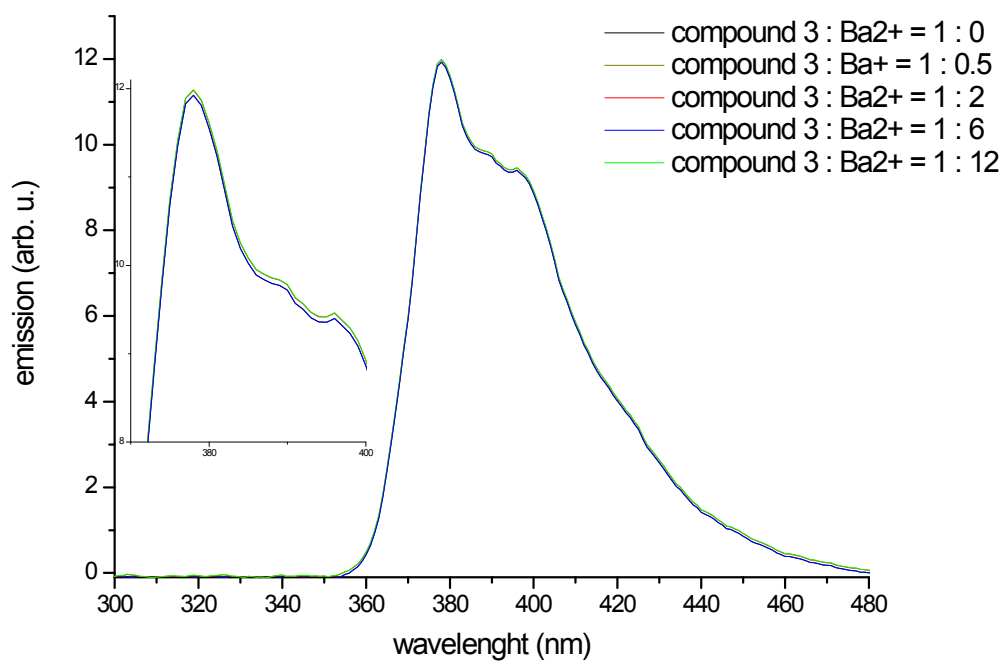


Fig. S52. Barium cation (Ba^+ ; in the form of BaCl_2) binding studies with compound **3** using the fluorescence spectra titration method (solvent: $\text{CHCl}_3\text{:MeOH} = 1\text{:}1$ v/v; compound **3** concentration: $1 \cdot 10^{-4}$ M; excitation wavelength: 280 nm).

S6. The Job's plots

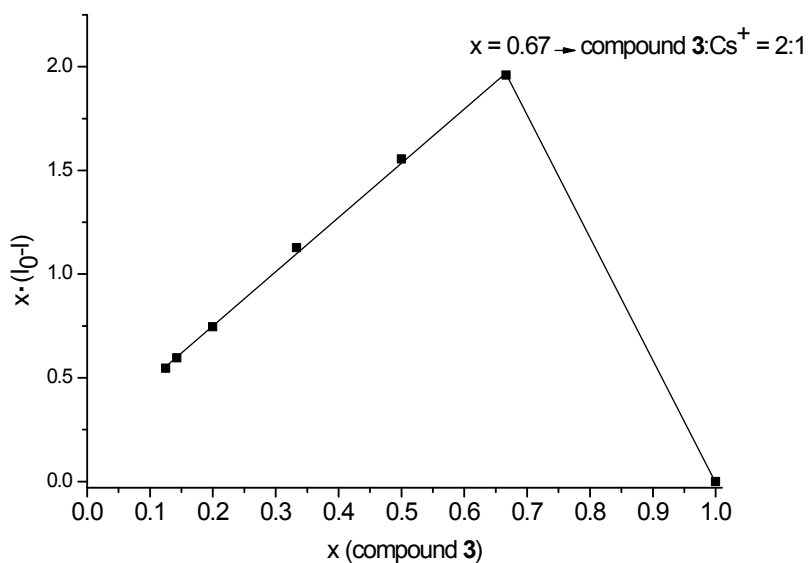


Fig. S53. The Job's plot related to the interactions of the compound **3** with Cs^+ (based on the data from the fluorescence spectra titration; x stands for the molar fraction of compound **3**, I_0 stands for the emission intensity of compound **3** without Cs^+ added, I stands for the emission intensity of compound with the given amount of Cs^+ added).

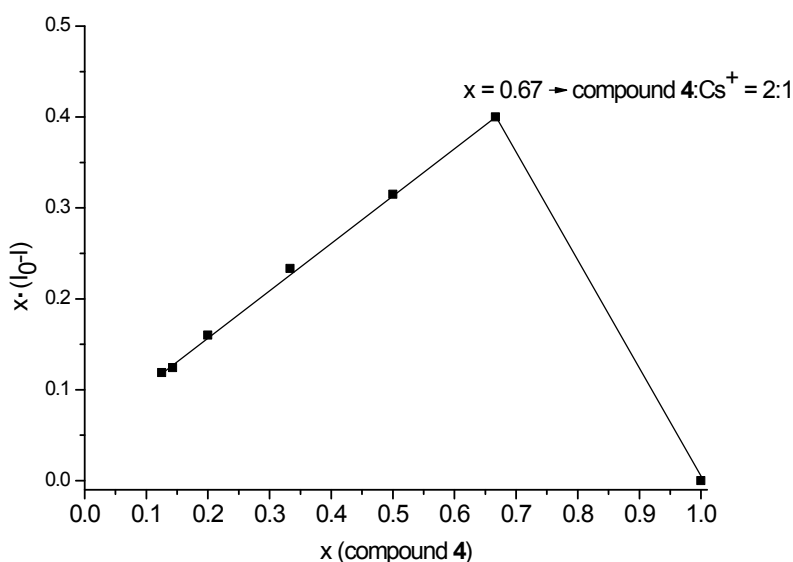


Fig. S54. The Job's plot related to the interactions of the compound **4** with Cs^+ (based on the data from the fluorescence spectra titration; x stands for the molar fraction of compound **4**, I_0 stands for the emission intensity of compound **4** without Cs^+ added, I stands for the emission intensity of compound with the given amount of Cs^+ added).

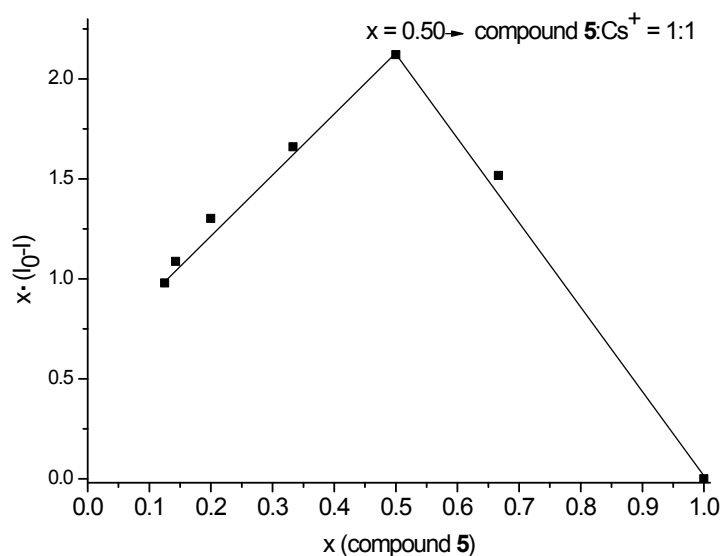


Fig. S55. The Job's plot related to the interactions of the compound **5** with Cs⁺ (based on the data from the fluorescence spectra titration; x stands for the molar fraction of compound **5**, I_0 stands for the emission intensity of compound **5** without Cs⁺ added, I stands for the emission intensity of compound with the given amount of Cs⁺ added).

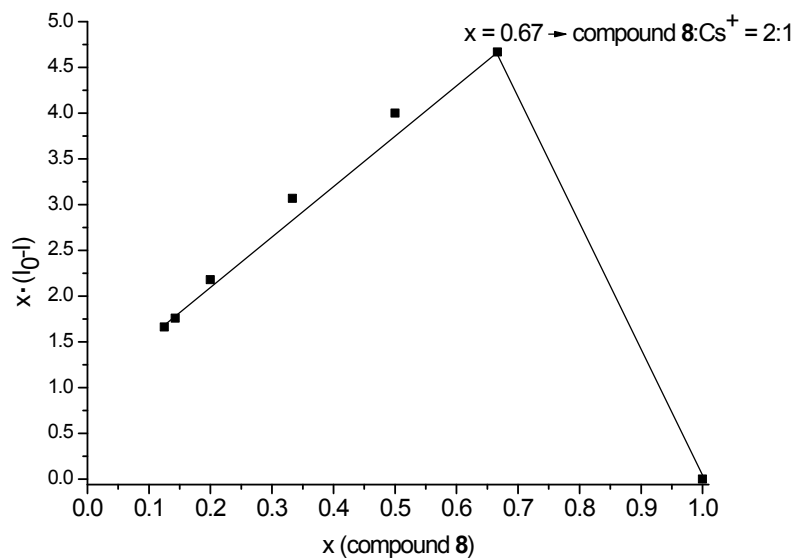


Fig. S56. The Job's plot related to the interactions of the compound **8** with Cs⁺ (based on the data from the fluorescence spectra titration; x stands for the molar fraction of compound **8**, I_0 stands for the emission intensity of compound **8** without Cs⁺ added, I stands for the emission intensity of compound with the given amount of Cs⁺ added).

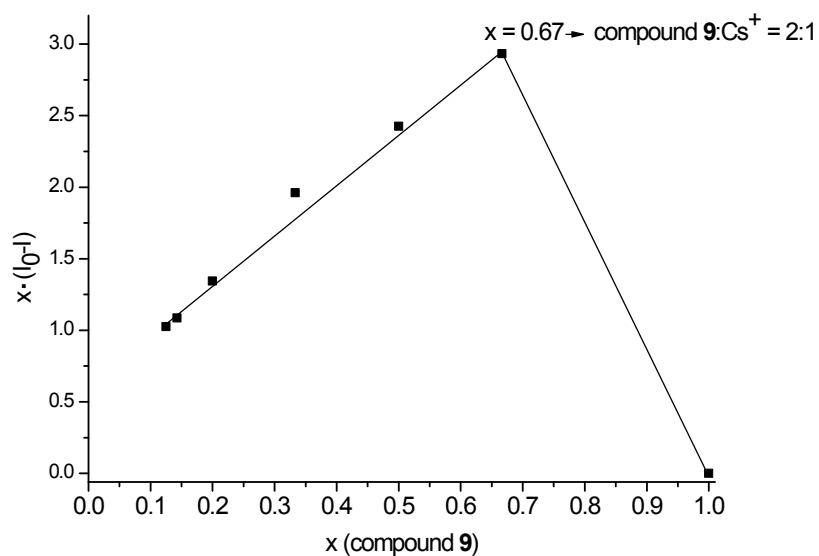


Fig. S57. The Job's plot related to the interactions of the compound **9** with Cs^+ (based on the data from the fluorescence spectra titration; x stands for the molar fraction of compound **9**, I_0 stands for the emission intensity of compound **9** without Cs^+ added, I stands for the emission intensity of compound with the given amount of Cs^+ added).

S7. ^1H NMR titration experiments

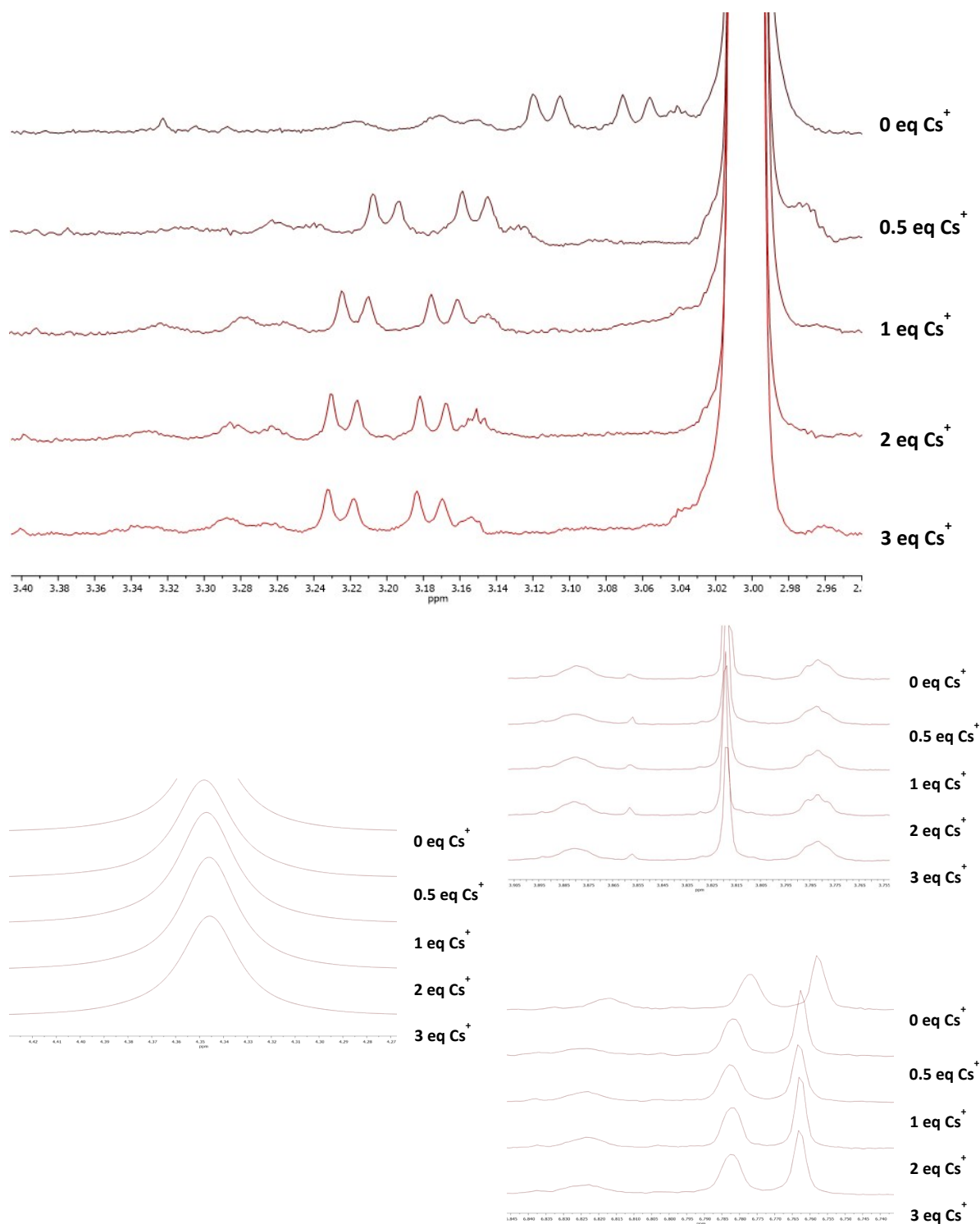


Fig. S58. Caesium cation (Cs^+ ; in the form of CsCl) binding studies with compound **3** using the ^1H NMR titration method (solvent: $\text{CDCl}_3:\text{CD}_3\text{OD} = 1:1$ v/v; compound **3** concentration: 1.5 mM). The insets of the spectra are presented.

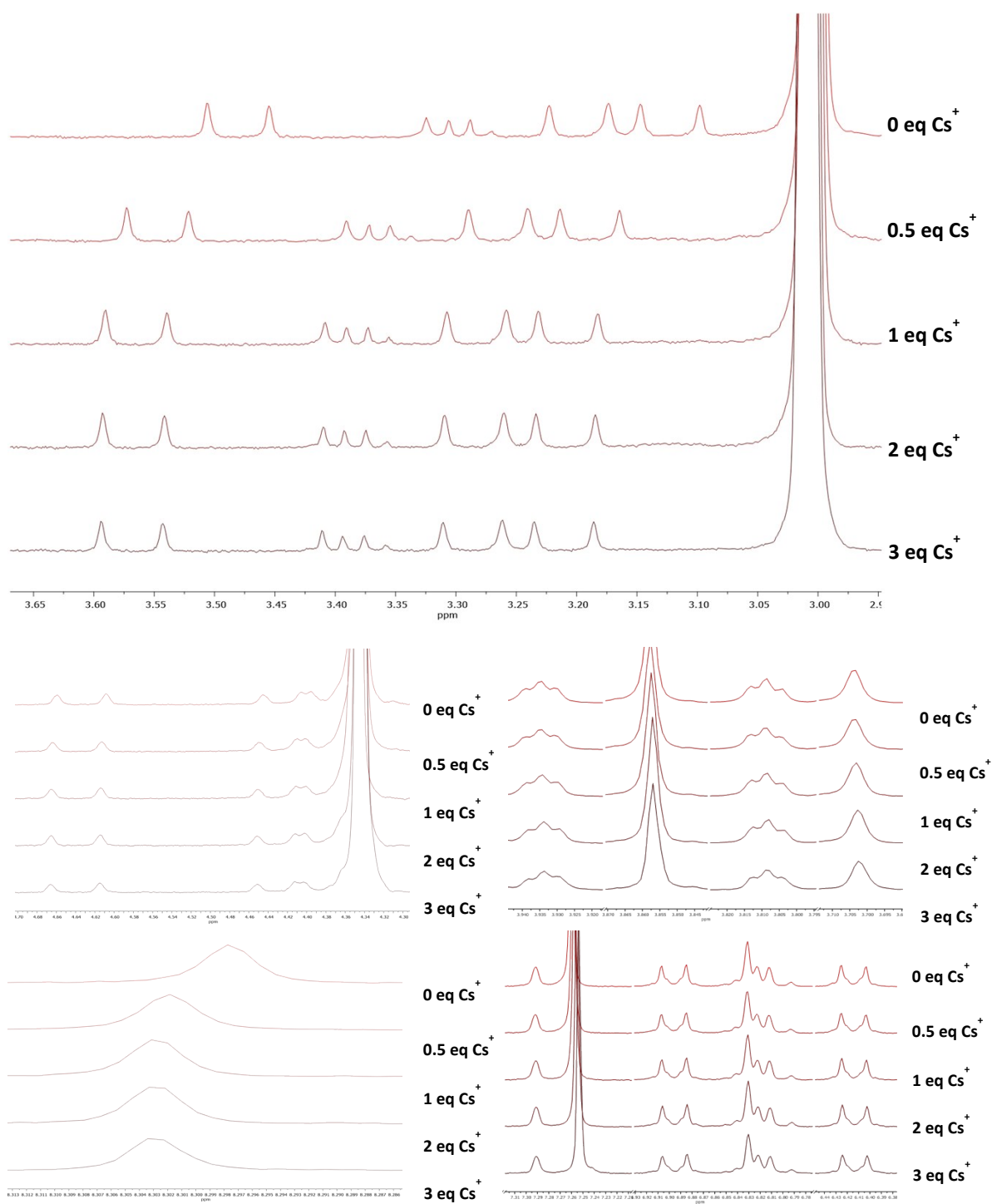


Fig. S59. Caesium cation (Cs^+ ; in the form of CsCl) binding studies with compound **4** using the ^1H NMR titration method (solvent: $\text{CDCl}_3:\text{CD}_3\text{OD} = 1:1$ v/v; compound **4** concentration: 1.5 mM). The insets of the spectra are presented.

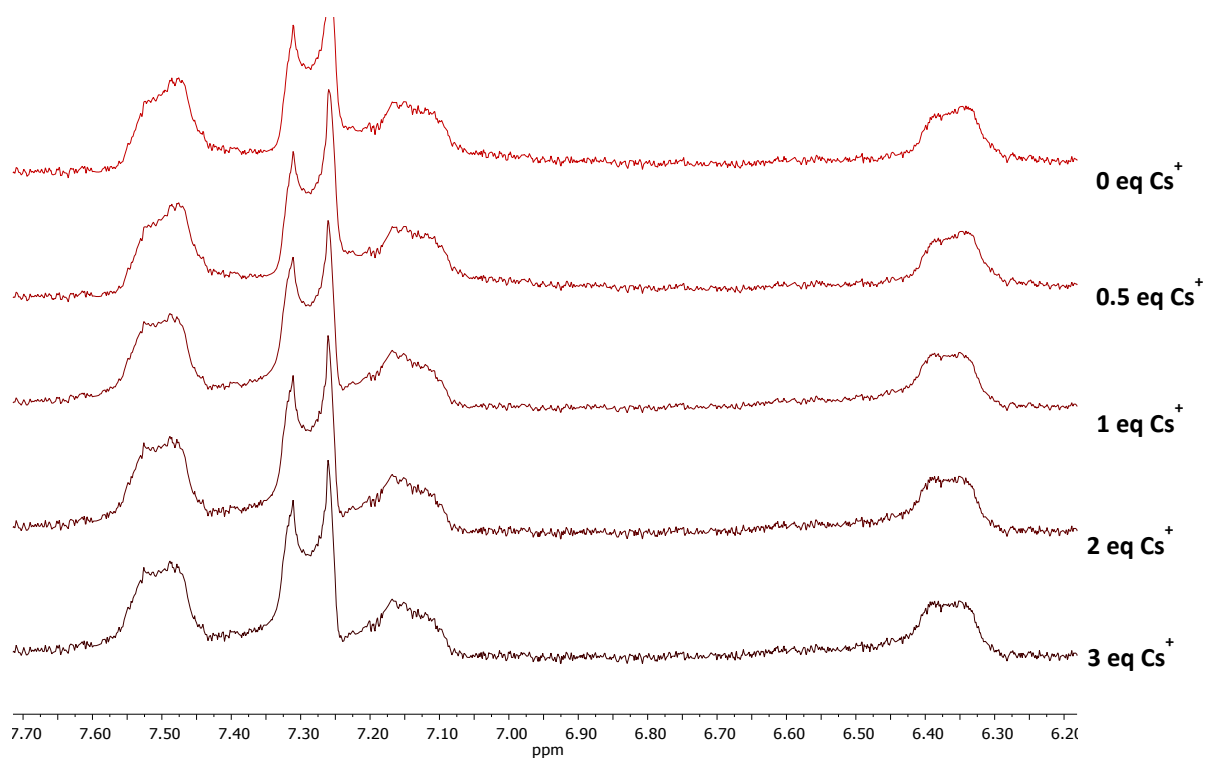


Fig. S60. Caesium cation (Cs^+ ; in the form of CsCl) binding studies with compound **10** using the ^1H NMR titration method (solvent: $\text{CDCl}_3:\text{CD}_3\text{OD} = 1:1$ v/v; compound **10** concentration: 1.5 mM).

S8. Cyclic voltammograms

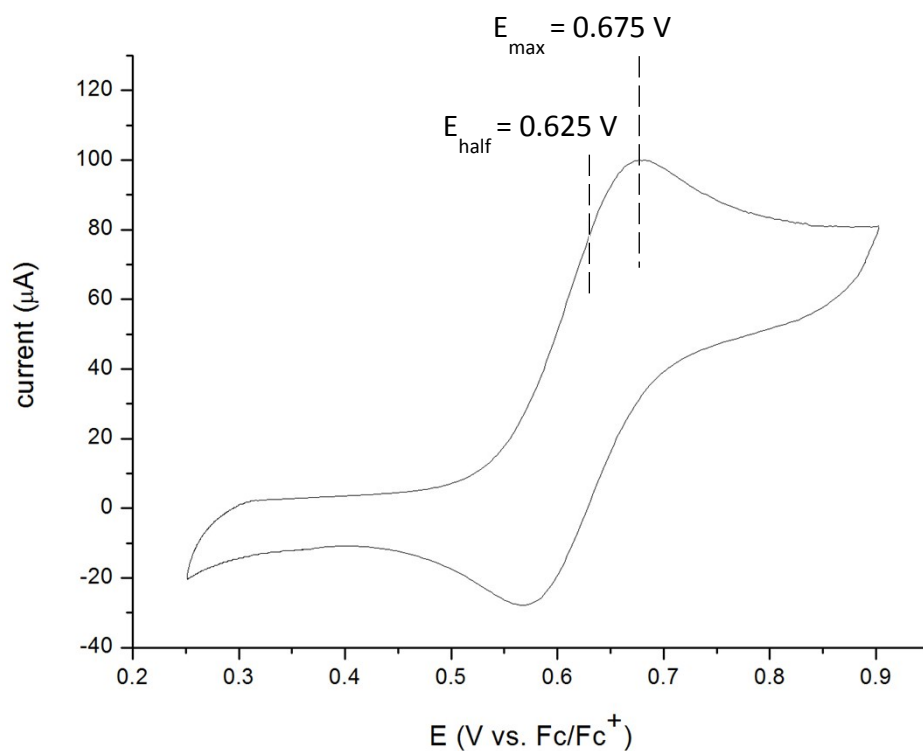


Fig. S61. Cyclic voltammogram of compound **3** in CH₂Cl₂.

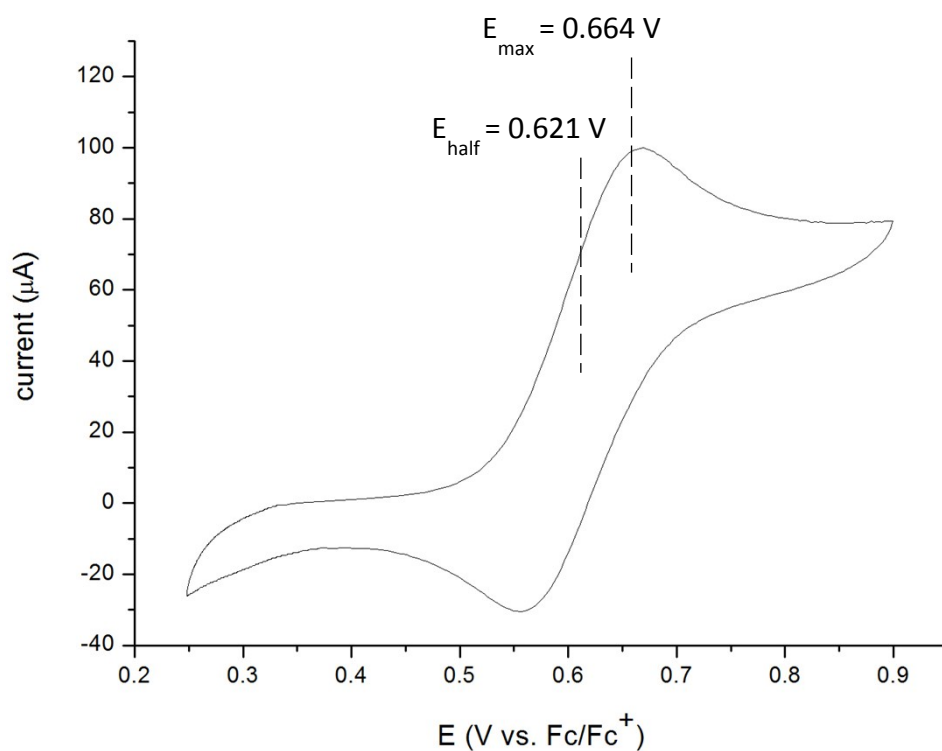


Fig. S62. Cyclic voltammogram of compound **4** in CH₂Cl₂.

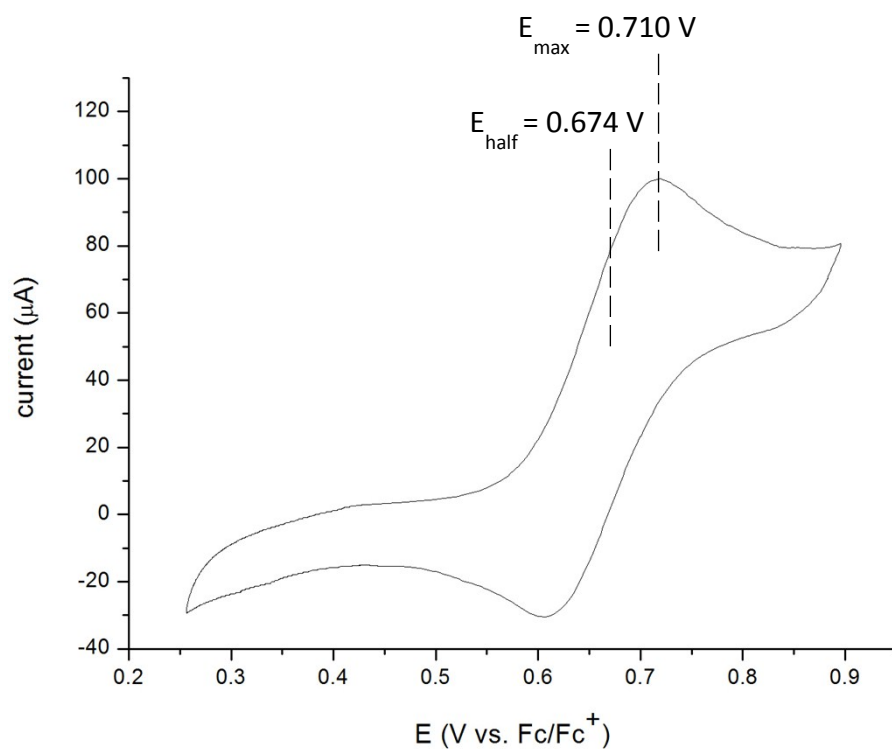


Fig. S63. Cyclic voltammogram of compound **5** in CH_2Cl_2 .

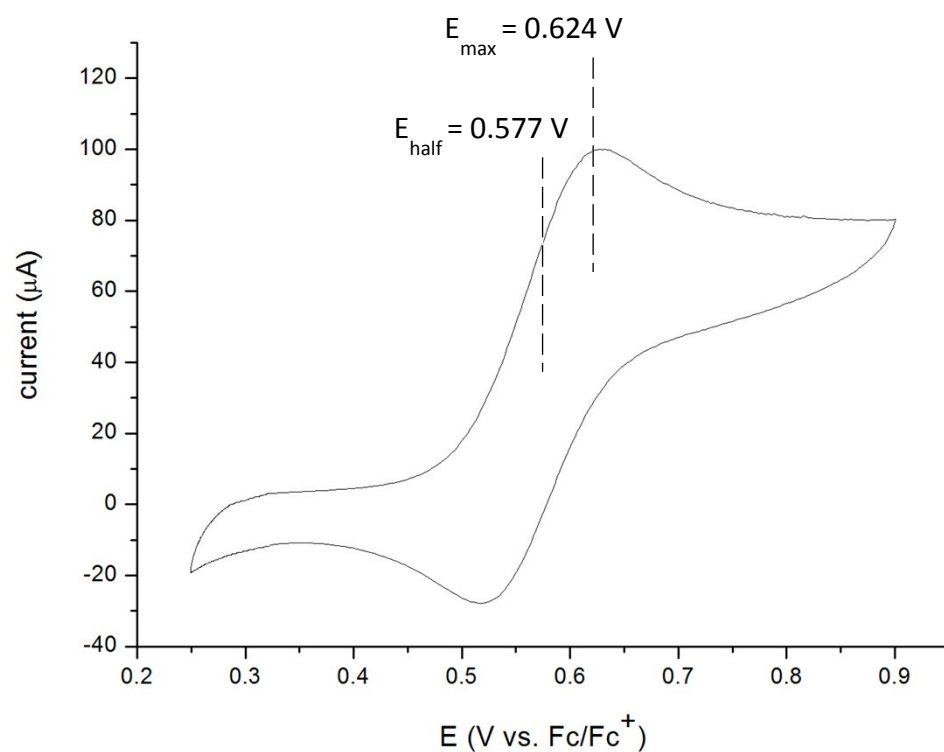


Fig. S64. Cyclic voltammogram of compound **8** in CH_2Cl_2 .

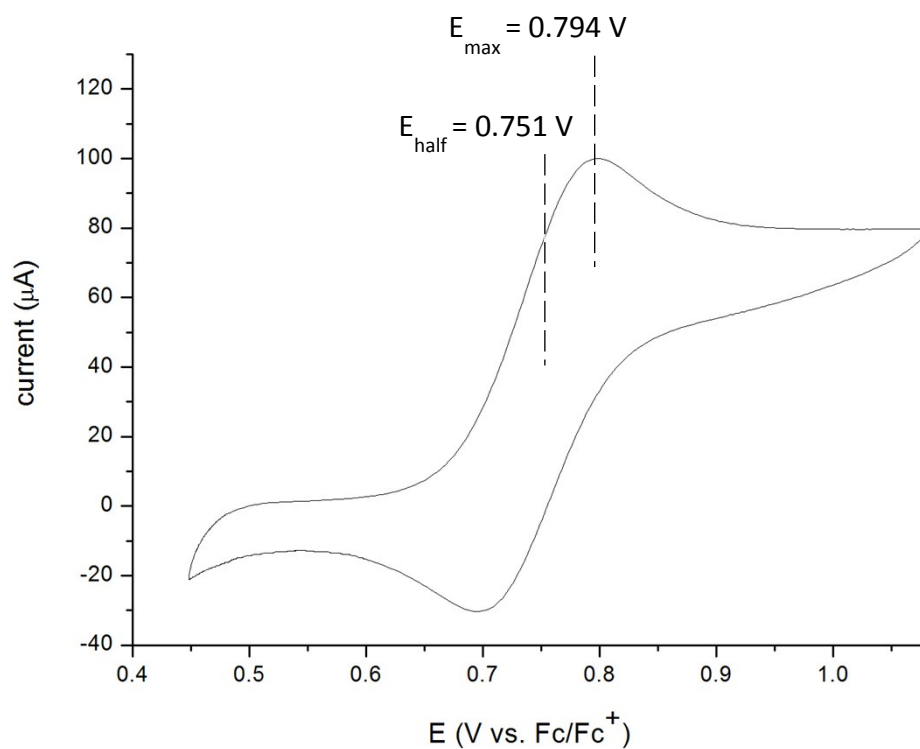


Fig. S65. Cyclic voltammogram of compound **9** in CH_2Cl_2 .

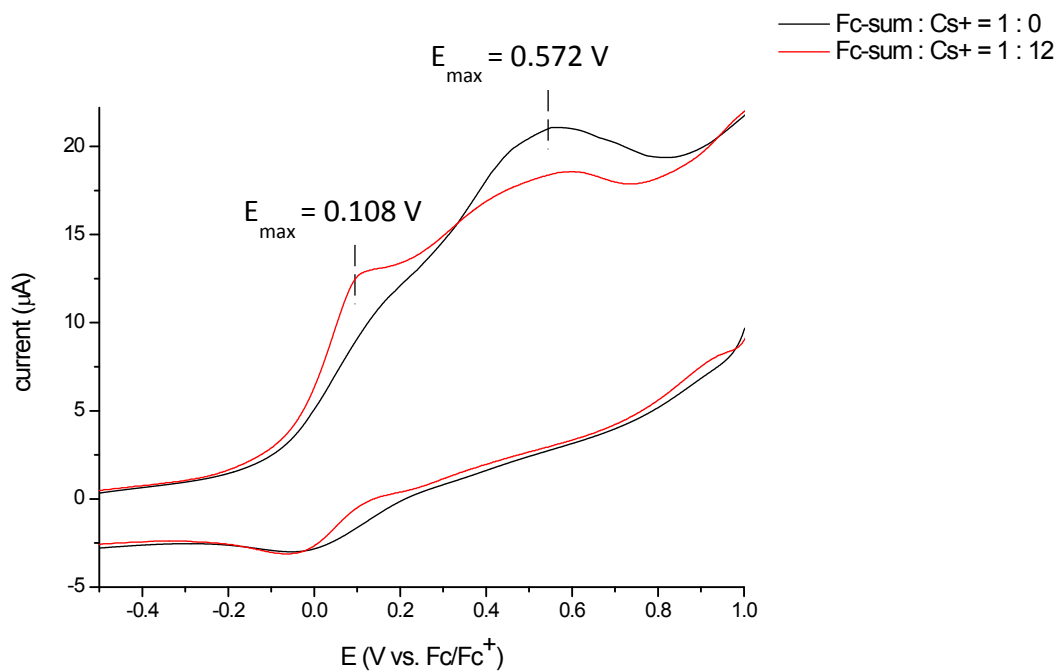


Fig. S66. Cyclic voltammogram of compound **3** in $\text{CHCl}_3:\text{MeOH} = 1:1$ v/v, with (black curve) and without (red curve) Cs^+ added (12 eq).

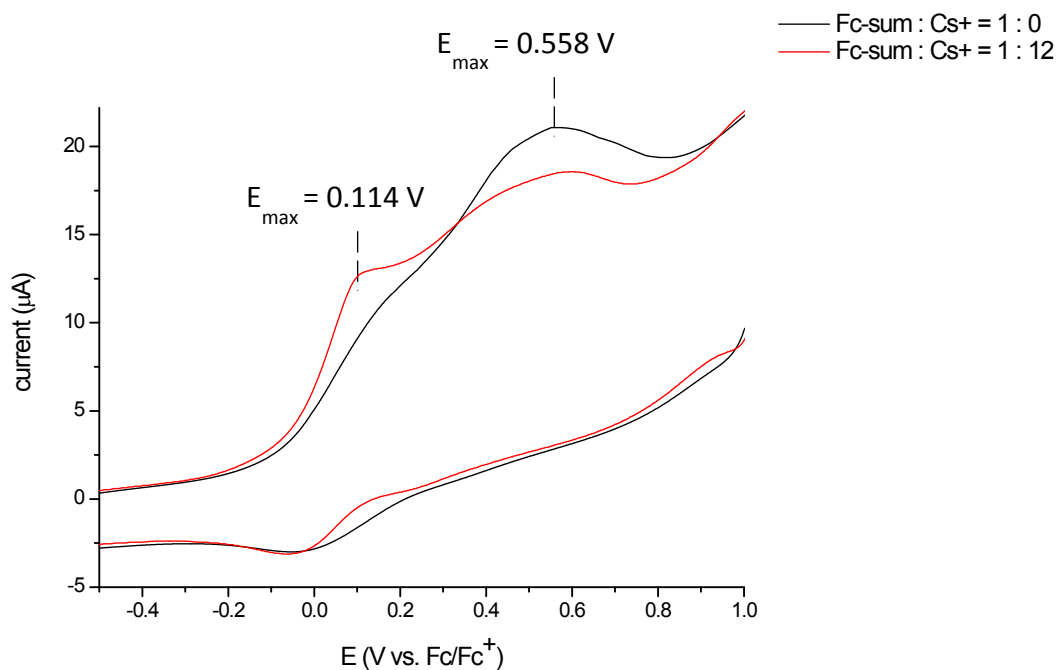


Fig. S67. Cyclic voltammogram of compound **4** in $\text{CHCl}_3:\text{MeOH} = 1:1$ v/v, with (black curve) and without (red curve) Cs^+ added (12 eq).

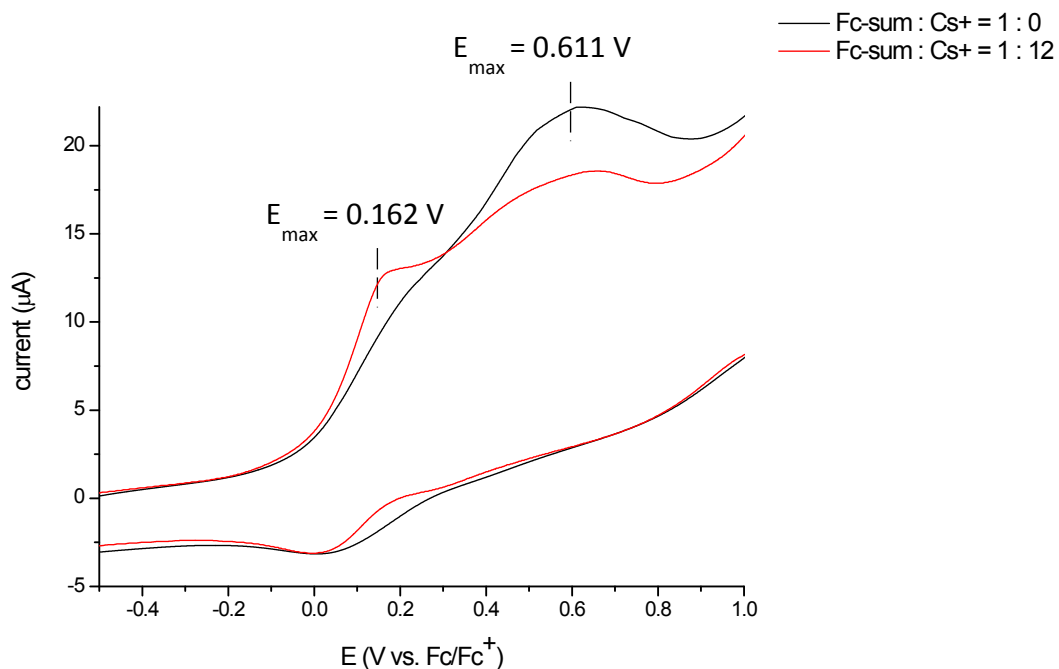


Fig. S68. Cyclic voltammogram of compound **5** in $\text{CHCl}_3:\text{MeOH} = 1:1$ v/v, with (black curve) and without (red curve) Cs^+ added (12 eq).

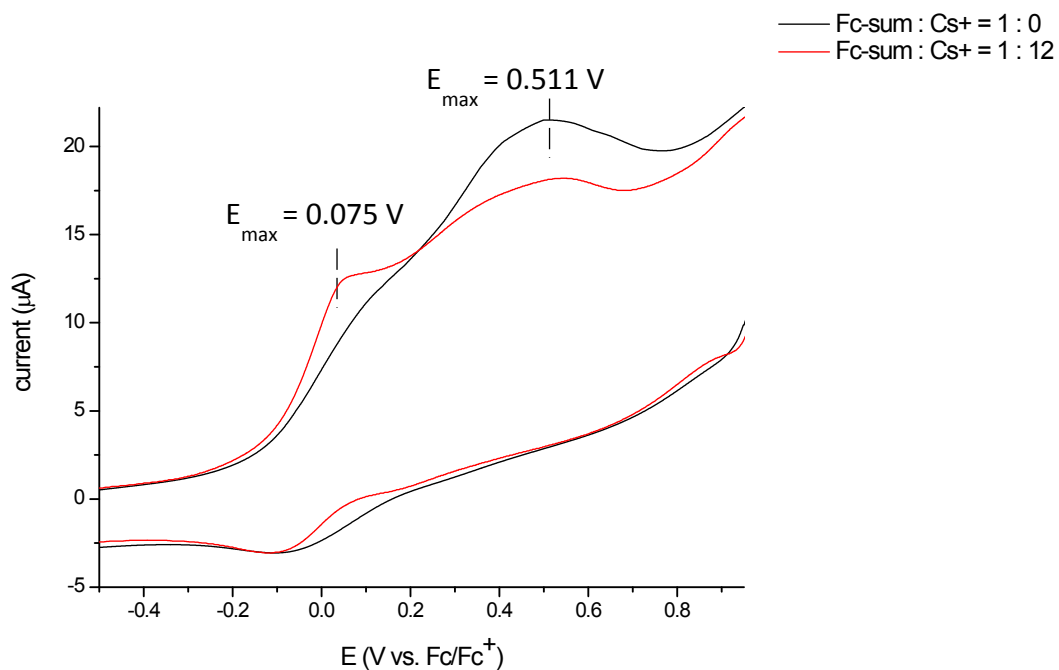


Fig. S69. Cyclic voltammogram of compound **8** in $\text{CHCl}_3:\text{MeOH} = 1:1$ v/v, with (black curve) and without (red curve) Cs^+ added (12 eq).

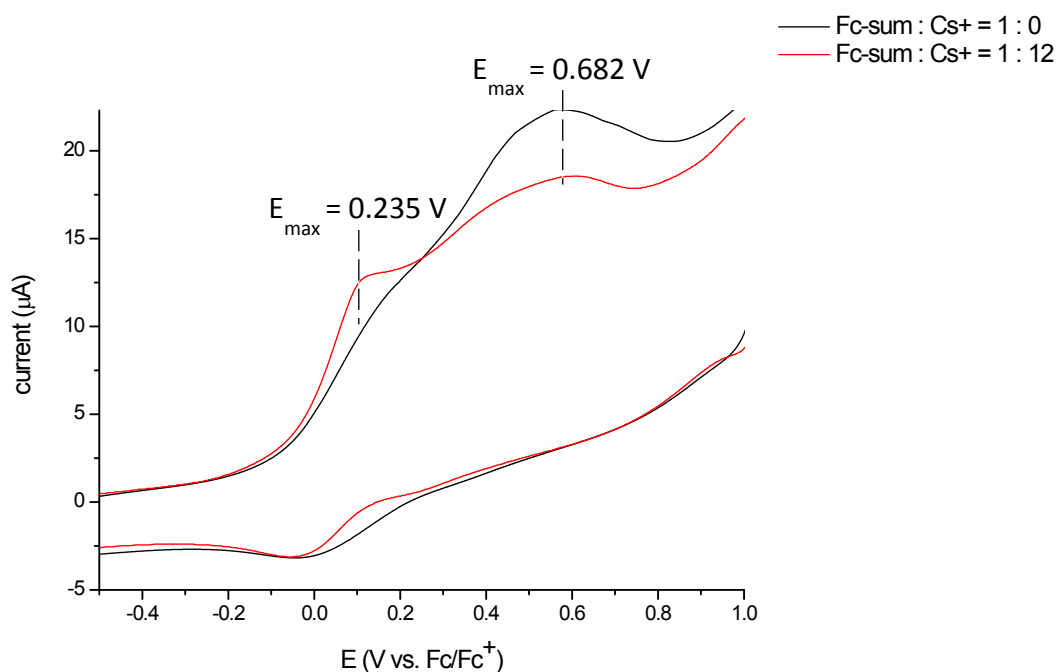


Fig. S70. Cyclic voltammogram of compound **9** in $\text{CHCl}_3:\text{MeOH} = 1:1$ v/v, with (black curve) and without (red curve) Cs^+ added (12 eq).

S9. Details on calculation of K_a and LOD

Calculations were based on the Stern-Volmer equation:

$$\frac{I_0}{I} = 1 + K_a \cdot C_{cation}$$

, where C_{cation} is the molar concentration of the cation, I_0 and I are the fluorescence intensity of Fc-sumanene derivative in the absence and in the presence of cation, respectively (reference no. 26 in the manuscript). K_a and LOD were calculated as follows:

- K_a value for compound **5** was calculated accordingly on the basis of the $I_0/I = f(C_{cation})$ linear dependency (Fig. S71). K_a values for compounds **3**, **4**, **8**, **9** were calculated accordingly on the basis of the $I_0/I = f(C_{cation}^2)$ linear dependences (Fig. S72). $I_0/I = f(C_{cation})$ linear plots for compounds **3**, **4**, **8**, **9** are also presented in Fig. S71. Despite the fact that the Stern-Volmer method fits best for 1:1 interaction model, both $I_0/I = f(C_{cation})$ and $I_0/I = f(C_{cation}^2)$ plots for compounds **3**, **4**, **8** were linear, thus enabling calculation of K_a . However, the calculated K_a numbers for compounds **3**, **4**, **8**, **9** should be treated as the approximate ones.
- LOD values were calculated accordingly on the basis of the $I_0 - I/I_0 = f(C_{cation})$ linear dependences (Fig. S73).

The plots are given below. The results of calculations are summarized in **Table 2** in the main article file.

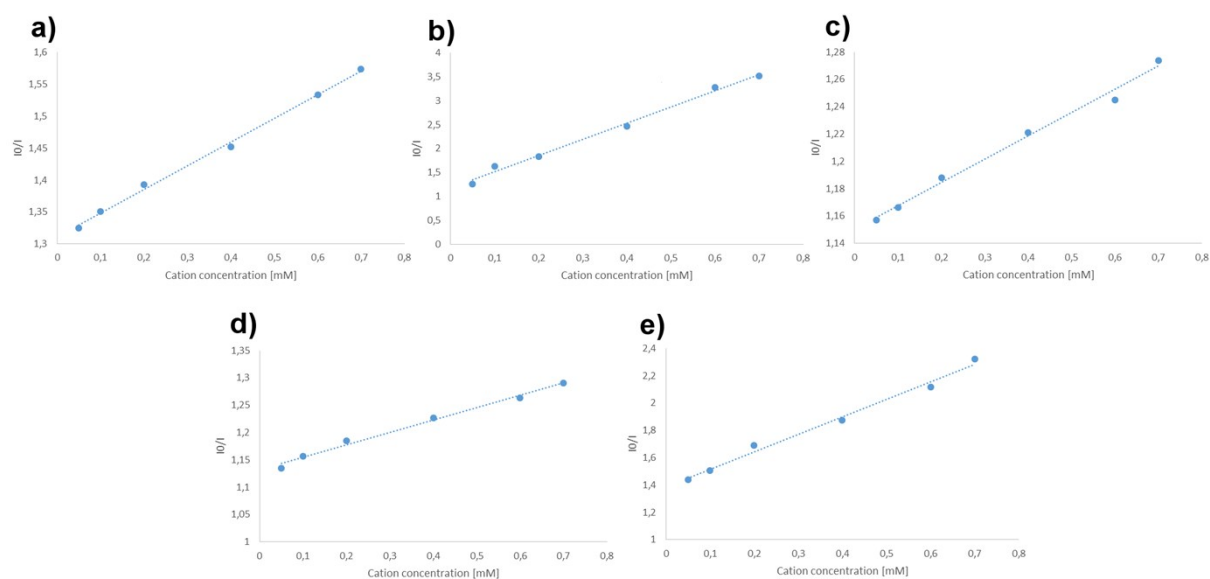


Fig. S71. $I_0/I = f(C_{cation})$ plot for: (a) compound 3, (b) compound 4, (c) compound (5), (d) compound (8), (e) compound 9.

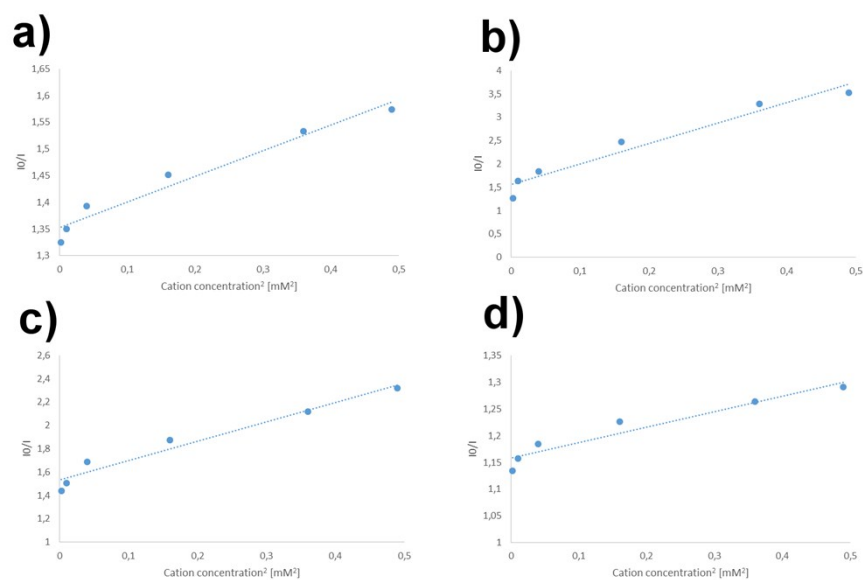


Fig. S72. $I_0/I = f(C_{cation}^2)$ plot for: (a) compound 3, (b) compound 4, (c) compound (8), (d) compound 9.

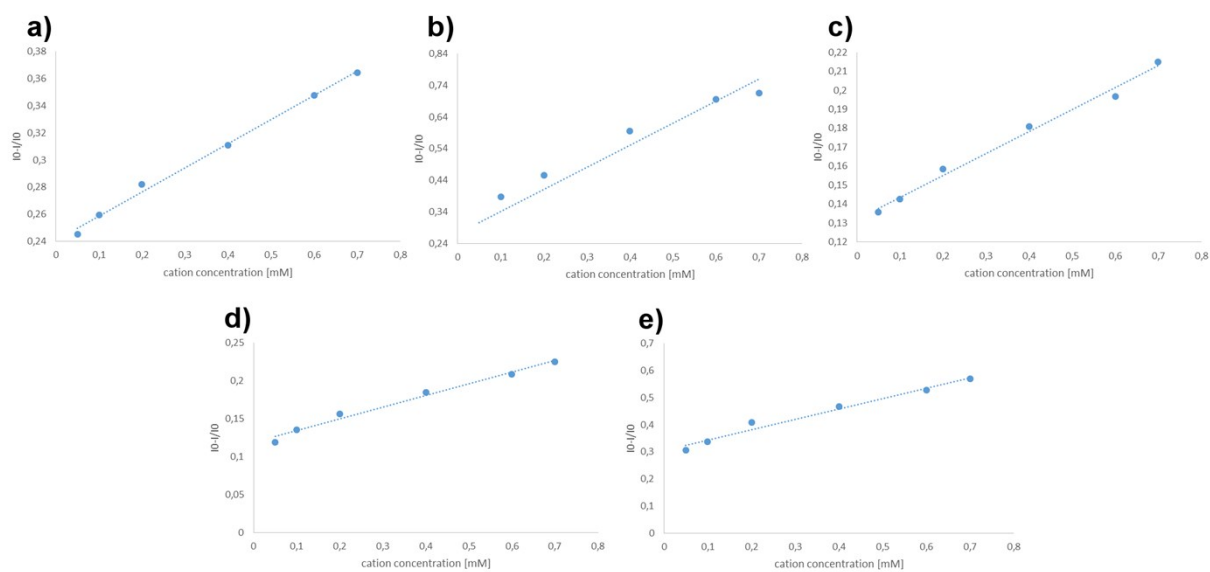


Fig. S73. $I_0 - I/I = f(C_{cation})$ plot for: (a) compound **3**, (b) compound **4**, (c) compound (**5**), (d) compound (**8**), (e) compound **9**.

S10. References

- [1] H. Sakurai, T. Daiko, T. Hirao. *Science*, **2003**, 301, 1878.
- [2] B. B. Shrestha, S. Karanjit, G. Panda, S. Higashibayashi, H. Sakurai. *Chem. Lett.*, **2013**, 42, 386-388.
- [3] P. Chen, C. Liu, J. Hu, H. Zhang, R. Sun. *J. Organomet. Chem.*, **2018**, 854, 113-121.
- [4] N. Dwadnia, F. Allouch, N. Pirio, J. Roger, H. Cattey, S. Fournier, M.-J. Penouilh, C. H. Devillers, D. Lucas, D. Naoufal, R. B. Salem, J.-C. Hierso. *Organometallics*, **2013**, 32, 5784–5797.
- [5] R. Arancibia, A. H. Klahn, G. E. Buono-Core, E. Gutierrez-Puebla, A. Monge, M. E. Medina, C. Olea-Azar, J. D. Maya, F. Godoy. *J. Organomet. Chem.*, **2011**, 696, 3238-3244.
- [6] MeOH was dried over molecular sieves 3Å and bubbled with N₂ before the reaction.
- [7] The compound **5** can be also isolated by means of filtration (67% yield). After filtration of the reaction mixture, the crude product is washed with cold (-30°C) methanol (5 mL), cold (-30°C) THF (1.5 mL) and dried under vacuum.
- [8] The solvent was bubbled with N₂ before the reaction.
- [9] The compound **8** and be also purified with PTLC (SiO₂; CH₂Cl₂/MeOH = 95:5 v/v; R_f (**8**) = 0.9; 63% yield).
- [10] The optimized partial structure of compound **3** was obtained with Gaussian09 software (M. J. Frisch, et al. *Gaussian 09, Revision B.01*, Gaussian Inc., Wallingford, CT, **2010**).